The Hong Kong Polytechnic University
Department of Building Services Engineering

An Experimental and Numerical Study on the Thermal Environment in an Air-conditioned Sleeping Space

Pan Dongmei

A thesis submitted in partial fulfillment of the requirements

for the Degree of Doctor of Philosophy

December 2011

Certificate of Originality

I hereby declare that this thesis is my own work and that, to the best of my knowledge and belief, it reproduces no material previously published or written, nor material that has been accepted for the award of any other degree or diploma, except where due acknowledgement has been made in the text.

Pan Dongmei

Department of Building Services Engineering

The Hong Kong Polytechnic University

Hong Kong SAR, China

December, 2011

Abstract

A human being spends approximately one-third of his / her life in sleep. Sleep can help people overcome tiredness and is very important to one's memory. The influence of thermal parameters in a sleeping environment on the quality of sleep has been gradually understood. Therefore, air conditioning shall serve to maintain an appropriate indoor thermal environment not only in workplaces during daytime, but also in bedrooms in residences or guestrooms in hotels at nighttime for sleeping. However, the current practices in air conditioning are mainly concerned with the situations in which people are awake in workplaces or other leisure places. These may however not be directly applicable to air conditioning for sleeping environments. Therefore, it becomes highly necessary to study the thermal environment in an air conditioned sleeping space in order to provide people with a thermally comfortable sleeping environment at a low energy consumption.

The thesis reports, first of all, two numerical studies on the micro-climate around, and the thermal neutrality of, a sleeping person placed in a space with a displacement ventilation system. A sleeping computational thermal manikin (SCTM) was developed and used to investigate the micro-climate around a naked SCTM, including air temperature and velocity distributions, and heat transfer characteristics. Then, the results of the numerical study on the thermal neutrality for a sleeping person are presented, including the thermal neutrality for a naked sleeping person and the effects of the total insulation value of a bedding system on the thermal neutrality of a sleeping person. The results of the two numerical studies were validated by the experimental data from earlier related studies. The results showed that the thermal resistance of a bedding could significantly affect the thermal neutral

temperature of a sleeping person, i.e., the higher the thermal resistance of the bedding, the lower the thermal neutral temperature. It was further suggested that the supply air velocity did not significantly affect the thermal neutral temperature when people were covered with different beddings at 100% percentage coverage of body surface area by bedding and bed.

Secondly, a study on developing a four-node thermoregulation model for predicting the thermal physiological responses of a sleeping person is presented. The four-node thermoregulation model for a sleeping person was developed by modifying Gagge's two-node model. The four-node thermoregulation model was validated by comparing the predicted thermal physiological responses, including skin and core temperatures, using the model developed with the experimental data previously obtained by others. The comparison results demonstrated that the four-node thermoregulation model developed could be used to predict the thermoregulatory responses of a sleeping person with an acceptable accuracy. Therefore, the validated four-node thermoregulation model can be used as a useful tool to predict the influences of different indoor thermal parameters, such as air temperature and humidity, in a sleeping environment and different bedding systems on the thermoregulatory responses of a sleeping person.

Thirdly, a study on evaluating the operational and energy saving performance of a novel bed-based task/ambient conditioning (TAC) system is presented. Both experimental and numerical approaches were employed in the study, and are separately reported. In the experimental part, the development of a novel bed-based TAC system placed in an experimental bedroom and the related experimental performance evaluations are presented. The experimental results demonstrated that

the use of the novel bed-based TAC system can help achieve energy saving, compared to the use of a full air conditioning (FAC) system. The experimental results also suggested that the operational and energy saving performance of the novel bed-based TAC system would be affected by a number of factors, such as supply air flow rate and temperature, and supply vane angle. Given the limitations of the current experimental bedroom, where simulated space cooling load was only generated indoors, the energy saving potential when using the novel bed-based TAC system in an actual bedroom where there can be space cooling load from outdoors was studied through a theoretical analysis. The results of theoretical analysis demonstrated that the energy saving potential when using the novel bed-based TAC system in an actual bedroom can be significantly larger than that in the experimental bedroom. On the other hand, in the numerical part, a numerical model for the bed-based TAC system placed in the experimental bedroom was established, and validated using the experimental data obtained. The validated numerical model was further used to analyze the performances of the bed-based TAC system developed at the operating conditions other than the experimental conditions. The numerical results showed that the supply air flow rate of 75 L/s might be regarded as an optimum one for the novel bed-based TAC system because of the largest energy saving potential without the risk of cold draft inside the occupied zone. At a supply vane angle of +60°, the predicted value of EUC was even smaller than 1. When the supply vane angle was set at +30°, the predicted EUC value was larger than 1. The predicted EUC values increased when the supply vane angle was altered from -30° to 0°, and then to -60°. Therefore, it was shown that by suitably controlling its supply air flow velocity and temperature, supply vane angles, the bed-based TAC system can be operated to maintain an acceptable level of thermal comfort without cold draft in an occupied zone at a low energy consumption.

Publications Arising from the Thesis

Journal Papers

- **Pan Dongmei**, Chan Mingyin, Deng Shiming, Xia Liang and Xu Xiangguo. Numerical studies on the microclimate around a sleeping person and the related thermal neutrality. *Ergonomics*, 54 (2011) 1088-1100 (Based on Chapter 4).

- **Pan Dongmei**, Chan Mingyin, Xia Liang, Xu Xiangguo and Deng Shiming. Performance evaluation of a novel bed-based task/ambient conditioning (TAC). *Energy and Buildings*, 44(2012) 54-62 (Based on Chapter 6).

- **Pan Dongmei**, Chan Mingyin, Deng Shiming and Qu Minglu. A four-node thermoregulation model for predicting the thermal physiological responses of a sleeping person. *Building and Environment*, in press (Based on Chapter 5).

Manuscripts

- **Pan Dongmei**, Chan Mingyin, Deng Shiming. Numerical study on the operating performances of the novel bed-based task/ambient conditioning (TAC) system (Based on Chapter 7 and under preparation).

Acknowledgements

I must express my grateful thanks to my Chief Supervisor, Dr. Chan Mingyin, Assistant Professor, and my Co-Supervisor, Prof. Deng Shiming, Professor and Associate Head, of the Department of Building Services Engineering (BSE), The Hong Kong Polytechnic University, for their readily available supervision, valuable suggestions, patient guidance, continuous help and encouragement throughout the course of the work.

My special thanks go to The Hong Kong Polytechnic University for financially supporting my study. I would like to also thank Dr. Xu Xiangguo, Dr. Xia Liang, Miss Qu Minglu, Miss Pan Yan and Miss Li Ning for their assistance in my simulation and experimental work. Furthermore, I am grateful to Dr. Lin Zhongping of Tongji University China, for the inspirations I got from his work. In addition, I wish to express my gratitude to the technicians in the Heating, Ventilation and Air Conditioning Laboratory of the BSE Department for their supports during my experimental work.

Finally, I would like to express my deepest appreciation to my family members: my husband, Pan Qinyi, my mother, my elder sister and her husband. I could not have finished my work without their on-going loves, supports, patience and understandings.

Table of Contents

List of Figures

Chapter 6

Chapter 7

List of Tables

Chapter 7

Nomenclature

Variable	Description	Unit
A_a	Equivalent area between the unoccupied zone and the occupied zone	m^2
A_C	Percentage coverage of body surface area by bedding and bed	100%
A_D	Nude body surface area	m^2
A_{en}	Area of the envelope	m^2
C_p	Specific heat of air	kJ/(kg·°C)
$C_{p,b}$	Specific heat of body, 3.490	kJ/(kg·°C)
$C_{p,bl}$	Specific heat of blood, 4.187	kJ/(kg·°C)
CFD	Computational Fluid Dynamics	ND
CTM	Computational Thermal Manikin	ND
D	Hydraulic diameter	m
E_{max}	Maximum evaporative potential from skin	W/m^2
$E_{max,i}$	Maximum evaporative potential from the i^{th} skin part, i = 1 - 3	W/m^2
E_{rsw}	Evaporative heat transfer by regulatory sweating from skin	W/m^2
$E_{rsw,i}$	Evaporative heat transfer by regulatory sweating from the i^{th} skin part, i = 1 - 3	W/m^2
E_{sk}	Total evaporative heat transfer from skin	W/m^2

$E_{sk,i}$	Total evaporative heat transfer from the i^{th} skin part, i = 1 - 3	W/m^2
EUC	Energy utilization coefficient	ND
f_{cl}	Clothing area factor	ND
$F_{p\rightarrow i}$	Angle factor from SCTM to the i^{th} internal surface	ND
h_c	Convective heat transfer coefficient	W/(m^2·K)
h_{fg}	Heat of vaporization of water, 2430	kJ/kg
h_r	Radiative heat transfer coefficient	W/(m^2·K)
H_{fab}	Bedding thickness	mm
i_m	Total vapor permeation efficiency, 0.38	ND
I	Turbulence Intensity	%
K	Effective conductance between the core layer and the skin layer, 5.28	W/(m^2·K)
l	Height	m
L_R	Lewis ratio,16.5	K/kPa
m	Whole mass of human body	kg
m_{bl}	Blood flow rate	kg/(m^{2}s)
$m_{bl,NREM}$	Blood flow rate from the core to the skin layer, in NREM stages	kg/(m^{2}s)
$m_{bl,REM}$	Blood flow rate from the core to the skin layer, in REM stages	kg/(m^{2}s)
m_i	Mass corresponding to the i^{th} skin part, i = 1 - 3	kg
m_{rsw}	Regulatory sweat rate from skin	kg/(m^{2}s)
$m_{rsw,i}$	Regulatory sweat rate from the i^{th} skin node part, i = 1 - 3	kg/(m^{2}s)

$m_{rsw,NREM,i}$	Regulatory sweat rate from the i^{th} skin node part, i = 1 - 3, in NREM stages	kg/(m^{2}s)
$m_{rsw,REM,i}$	Regulatory sweat rate from the i^{th} skin node part, i = 1 - 3, in REM stages	kg/(m^{2}s)
m_{sk}	Skin mass	kg
M	Metabolic heat production	W/m^2
M_{shiv}	Heat production from shivering	W/m^2
$M_{shiv,NREM,i}$	Heat production from shivering corresponding to the i^{th} skin node part, i = 1 - 3, in NREM stages	W/m^2
$M_{shiv,REM,i}$	Heat production from shivering corresponding to the i^{th} skin node part, i = 1 - 3, in REM stages	W/m^2
NREM	Non Rapid Eye Moment	ND
P_a	Water vapor partial pressure	kPa
P_{oz}	Water vapor partial pressure in the occupied zone	kPa
$P_{sk,a}$	Saturated water vapor pressure at skin temperature	kPa
$P_{sk,a,i}$	Saturated water vapor pressure at the i^{th} skin part, i = 1 - 3	kPa
PMV	Predicted Mean Vote	ND
Q_c	Convective heat loss from skin	W/m^2
$Q_{c,i}$	Convective heat loss from the i^{th} skin part, i = 1 - 3	W/m^2
Q_{co}	Cooling load	W
$Q_{co,1}$	Cooling load when using the FAC system	W
$Q_{co,2}$	Cooling load when using the novel bed-based TAC system	W

$Q_{cr\text{-}sk}$	Heat from the core layer to the skin layer by mass transfer	W/m^2
$Q_{cr\text{-}sk,i}$	Heat from the core layer to the i^{th} skin part by mass transfer, i = 1 - 3	W/m^2
Q_{load}	Thermal load on body	W/m^2
Q_r	Radiative heat loss from skin	W/m^2
$Q_{r,i}$	Radiative heat loss from the i^{th} skin part, i = 1 - 3	W/m^2
Q_{res}	Heat loss from respiration	W/m^2
Q_s	Supply cooling capacity	W
Q_t	Sensible heat loss from skin	W/m^2
r_b	Thermal resistance of a bedding	$m^2 \cdot K/W$
r_m	Thermal resistance of bed with mattress	$m^2 \cdot K/W$
R_a	Equivalent thermal resistance between the unoccupied zone and the occupied zone	$m^2 \cdot K/W$
R_{cl}	Thermal resistance of clothing	$m^2 \cdot kPa/W$
R_{en}	Combined thermal resistance of the envelope	$m^2 \cdot K/W$
$R_{e,i}$	Total evaporative resistance corresponding to the i^{th} skin part, i = 1 - 3	$m^2 \cdot kPa/W$
$R_{e,t}$	Total evaporative resistance	$m^2 \cdot kPa/W$
R_i	Thermal resistance corresponding to the i^{th} skin part, i = 1 - 3	$m^2 \cdot kPa/W$
R_t	Total insulation value of a bedding system	$m^2 \cdot K/W$
REM	Rapid Eye Moment	ND
S_{cr}	Rate of heat storage in core layer	W/m^2
S_{sk}	Rate of heat storage in skin layer	W/m^2

$S_{sk,i}$	Rate of heat storage in the i^{th} skin part, i = 1 - 3	W/m^2
SCTM	Sleeping Computational Thermal Maninkin	ND
t	Time	s
t_a	Ambient air temperature	°C
t_i	Mean internal surface temperature on the i^{th} internal surface	°C
t_o	Operative temperature	°C
t_{ou}	Outdoor air temperature	°C
t_{oz}	Average air temperature in the occupied zone	°C
t_r	Mean radiant temperature	°C
t_{re}	Return air temperature	°C
t_s	Supply air temperature	°C
t_{uz}	Average air temperature in the unoccupied zone	°C
T_b	Body temperature	°C
$T_{b,n}$	Set point for body temperature	°C
T_{cl}	Clothing surface temperature	°C
T_{cr}	Core temperature	°C
$T_{cr,n}$	Set point for core temperature	°C
T_{ex}	Experimental temperature values	°C
T_{pre}	Predicted temperature values	°C
T_{sk}	Skin temperature	°C
$T_{sk,av}$	Average skin temperature	°C
$T_{sk,i}$	Skin temperature corresponding to the i^{th} skin part, i = 1 – 3	°C
$T_{sk,n}$	Set point for skin temperature	°C

$T_{sk,n,i}$	Set point for skin temperature corresponding to the i^{th} skin part, i = 1 - 3	°C
TAC	Task/ambient air conditioning	ND
v	Supply air velocity	m/s
V	Supply air flow rate	m^3/s
w	Skin wettedness	ND
w_i	Skin wettedness corresponding to the i^{th} skin part, i = 1 - 3	ND
w_{rsw}	Skin wettedness due to regulatory sweat	ND
$w_{rsw,i}$	Skin wettedness due to regulatory sweat, corresponding to the i^{th} skin part, i = 1 - 3	ND
W	External work done	W/m^2
ΔT	Temperature difference between skin and its surrounding air	°C

Greek symbols

α_i	Ratio of the i^{th} skin node surface area to body surface area, i = 1 - 3	ND
δ	Relative error	ND
ε	Emissivity	ND
η	Sweating evaporative efficiency	ND
η_c	Percentage reduction in cooling load	ND
μ_i	Ratio between the i^{th} skin node mass to body mass, i = 1 - 3	ND

ξ	Actual ratio of skin mass to whole mass of human body	ND
ξ_n	Ratio of skin mass to whole body mass at neutrality, 0.1	ND
ρ	Air density	m3/s

Note: ND = No Dimensions

Subscripts

a	Air
b	Bedding
c	Convective
cr	Core
en	Envelope
i	Number of the i^{th} internal surface (i= 1 – 6) or the i^{th} skin part *(*i= 1 – 3)
n	Neutral
oz	Occupied zone
ou	Outdoor
r	Radiative
re	Return
res	Respiration
s	Supply
sk	Skin
uz	Unoccupied zone
w	Wall

Chapter 1

Introduction

A human being spends approximately one-third of his / her life in sleep. Sleep can help people overcome tiredness and is very important to one's memory. The influence of thermal parameters in a sleeping environment on the quality of sleep has been gradually understood. Therefore, air conditioning shall serve to maintain an appropriate indoor thermal environment not only in workplaces during daytime, but also in bedrooms in residences or guestrooms in hotels at nighttime for sleeping in the tropics or subtropics.

However, the current practices in air conditioning are mainly concerned with the situations in which people are awake in workplaces or other leisure places. These may however not be directly applicable to air conditioning for sleeping environments in the tropics or subtropics. Therefore, it becomes highly necessary to study the thermal environment in an air conditioned sleeping space in order to provide people with a thermally comfortable sleeping environment at a low energy consumption.

Human thermal comfort has been one of focal points when developing air conditioning technology, for a workplace at daytime or a sleeping environment at nighttime. Currently, although there have been extensive research efforts in numerically studying human thermal comfort in workplaces at daytime, there has been a lack of numerical studies on human thermal comfort in sleeping environments at nighttime. In addition, thermoregulation of a sleeping person to maintain a small oscillation of core temperature at nighttime is different from that of a waking person

at daytime. Furthermore, the current applications of task/ambient air conditioning (TAC) systems are mainly for daytime activities, such as in work stations, but not for bedrooms in residences or other sleeping environments.

The thesis begins with an extensive literature review on the fundamentals related to sleep and the previous work on thermal comfort in sleeping environments, so that the effects of the thermal environment in a sleeping place on the quality of sleep may be clearly illustrated. A review on the previous studies on thermoregulation and its modeling is also reported. The issues related to applying numerical approaches to studying the thermal environment around a human body are also reviewed. Finally, a review on the types, the advantages and the ranges of operating parameters of TAC systems and their related studies for daytime applications is presented. A number of important issues where further in-depth research work in maintaining appropriate sleeping thermal environments in bedrooms at a low energy consumption is required have been identified. These are the expected targets of investigation in the project reported in this thesis.

The research proposal covering the aims and objectives, the project title and the methodologies adopted in this project is presented in Chapter 3.

Chapter 4 reports on two numerical studies on the micro-climate around, and the thermal neutrality of, a sleeping person placed in a space with a displacement ventilation system. A sleeping computational thermal manikin (SCTM) was developed and used to investigate the micro-climate around a naked SCTM, including air temperature and velocity distributions, and heat transfer characteristics.

Then, the results of the numerical study on the thermal neutrality for a sleeping person are presented, including the thermal neutrality for a naked sleeping person and the effects of the total insulation value of a bedding system on the thermal neutrality of a sleeping person. The results of the two numerical studies were validated by the experimental data from earlier related studies.

A study on developing a four-node thermoregulation model for predicting the thermal physiological responses of a sleeping person is presented in Chapter 5. The four-node thermoregulation model for a sleeping person was developed by modifying Gagge's two-node model. The four-node thermoregulation model was validated by comparing the predicted thermal physiological responses, including skin and core temperatures, using the model developed with the experimental data previously obtained by others. The comparison results demonstrated that the four-node thermoregulation model developed could be used to predict the thermoregulatory responses of a sleeping person with an acceptable accuracy. Therefore, the validated four-node thermoregulation model can be used as a useful tool to predict the influences of different indoor thermal parameters, such as air temperature and humidity, in a sleeping environment and different bedding systems on the thermoregulatory responses of a sleeping person.

Furthermore, a study on evaluating the operational and energy saving performance of a novel bed-based TAC system has been carried out. Both experimental and numerical approaches were employed in the study, and are separately reported in Chapter 6 and Chapter 7. In the experimental part reported in Chapter 6, the development of a novel bed-based TAC system placed in an experimental bedroom

and related experimental performance evaluations are presented. The experimental results demonstrated that the use of the novel bed-based TAC system can help achieve energy saving，compared to the use of a full air conditioning (FAC) system. The experimental results also suggested that the operational and energy saving performance of the novel bed-based TAC system would be affected by a number of factors, such as supply air flow rate and temperature, and supply vane angle. Given the limitations of the current experimental bedroom, where simulated space cooling load was only generated indoors, the energy saving potential when using the novel bed-based TAC system in an actual bedroom where there can be space cooling load from outdoors was studied through a theoretical analysis. The results of the theoretical analysis demonstrated that the energy saving potential when applying the novel bed-based TAC system to an actual bedroom can be significantly larger than that in the experimental bedroom. On the other hand, in the numerical part reported in Chapter 7, a numerical model for the novel bed-based TAC system placed in the experimental bedroom was established, and validated using the experimental data presented in Chapter 6. The validated numerical model was further used to analyze the operational performances of the novel bed-based TAC system developed at the non-experimental operating conditions other than the experimental conditions. The numerical study results showed that by suitably controlling its supply air flow velocity and temperature, supply vane angels, the bed-based TAC system can be operated to maintain an acceptable level of thermal comfort without cold draft in an occupied zone at a low energy consumption.

The conclusions of the thesis and the proposed future work are presented in the final Chapter.

Chapter 2

Literature Review

2.1 Introduction

A human being spends approximately one-third of his / her life in sleep. Sleep is not simply a state of rest, but has its own specific, positive functions [Hobson 1989]. Sleep can help people overcome tiredness and is very important to one's memory. For decades, numerous medical researchers have investigated various factors affecting the quality of sleep [Öhrström 1993, Morin et al. 1998, Shochat et al. 2001, Roehers and Roth 2005, Basner et al. 2011, Gooley et al. 2011]. It was commonly acknowledged that the quality of sleep was mainly determined by mental-physical factors of a sleeping person and environmental factors in a bedroom. Although the latter covered lighting, noise and thermal environment, the influence of thermal parameters in a sleeping environment on the quality of sleep was gradually understood [Haskell et al. 1981a, Muzet et al. 1984, Okamoto-Mizuno et al. 1999, Tsuzuki et al. 2008]. Previous experimental results have demonstrated that when the thermal environment in a bedroom deviated greatly from the so-called 'thermal comfort zone', sleep quality can be disturbed or even deteriorated as soon as the thermoregulatory responses were present. Consequently, different approaches, such as electric blanket [Fletcher et al. 1999, Okamoto-Mizuno et al. 1993, 2005] and water-perfused thermosuit [Raymann et al. 2008], were used to maintain a sleeping environment in the 'thermal comfort zone', so that sleep quality could be improved. Among them, using space air conditioning was a popular and important approach to maintain comfortable indoor thermal environments in bedrooms of residences,

guestrooms in hotels and wards in hospitals, at night time.

In the early 1900s, air conditioning technology was firstly developed by Willis H. Carrier, who has been recognized as the Father of air conditioning [Wang 1994]. Before 1922, air conditioning was primarily used for industrial processes, such as producing candy, gum, cheese, matches and textile. In 1922, the first comfort air conditioning system was installed in a theater in the United States [Lang 1979]. The earliest fully air conditioned high-rise office building was the Milam Building in San Antonio, Texas, built in 1928 [Pauken 1999]. Today, the use of air conditioning is to maintain comfortable indoor thermal environments not only in workplaces at daytime, but also in bedrooms of residences, guestrooms in hotels and wards in hospitals, at night time. This has been reflected in a survey on the situations of sleeping thermal environment and the use of air conditioning in bedrooms in residential buildings in Hong Kong. The results of the survey suggested that 68% of the respondents would leave their room air conditioners (RACs) on throughout the duration of their sleep and the rest would use their RACs only for certain hours during sleep [Lin and Deng 2006].

However, the current practices in air conditioning are mainly concerned with the situations in which people are awake in workplaces or other leisure places, such as shopping malls and restaurants. These may however not be directly applicable to air conditioning for sleeping environments. Therefore, it becomes necessary to study the thermal environment in an air conditioned sleeping space in order to provide people with a thermally comfortable sleeping environment at low energy consumption.

In this Chapter, the fundamentals related to sleep and the previous work on thermal comfort in sleeping environments are firstly reviewed, so that the effects of the thermal condition in a sleeping environment on the quality of sleep may be clearly illustrated. Secondly, a review on the previous studies on thermoregulation and its modeling is reported. This is followed by a review on applying numerical approaches to studying the thermal environment around a human body. Finally, a review on the types, the advantages and the ranges of operating parameters of task/ambient air conditioning (TAC) systems and their related studies for daytime applications is presented.

2.2 Sleep and thermal comfort in sleeping environments

2.2.1 Sleep

To understand the relationship between the sleep quality for a human being and his / her sleeping thermal environment, it is necessary to understand the definition of sleep and the methods to evaluate the sleeping quality currently used in medical or other related subject areas.

Sleep is indisputably a basic need, thought its duration varies, often considerably, from person to person. It is, in fact, possible to go without food longer than without sleep [Lavie 1996]. Not simply the absence of waking, sleep is a special activity of the brain, controlled by elaborate and precise mechanisms. Sleep is not simply a state of rest, but has its own specific, positive functions [Hobson 1989]. For example, sleep can help people overcome tiredness, and is very important to one's memory. In

recent years, sleep has been becoming increasingly an issue of concern. A survey conducted by the Hospital Authority in Hong Kong suggested that 15% of Hong Kong residents were significantly troubled by insomnia [Website_1 2011]. In addition, a survey carried out on March 21, 2011, the International Sleep Day, showed that 40% of Shanghai residents suffered from insomnia, or at least they had sleep disorder problems [Website_ 2 2011].

Modern sleep research is conducted principally in a sleep laboratory, where polysomnographic recordings (including electoencephalogram-EEG, electrooculogram-EOG, and electromyogram-EMG) depicting the course of sleep are made. Standardization of sleep stages and procedures for its scoring have generally been adopted [Rechtschaffen and Kales, 1968]. The appearance of sleep stages during a night is not a random process but an organized and definitive one. The sleep sequence can be best described with the aid of a hypnogram of sleep recording [Lavie 1996, Brebbia and Altshuler 1965]. Fig. 2.1 shows the hypnogram of a young adult.

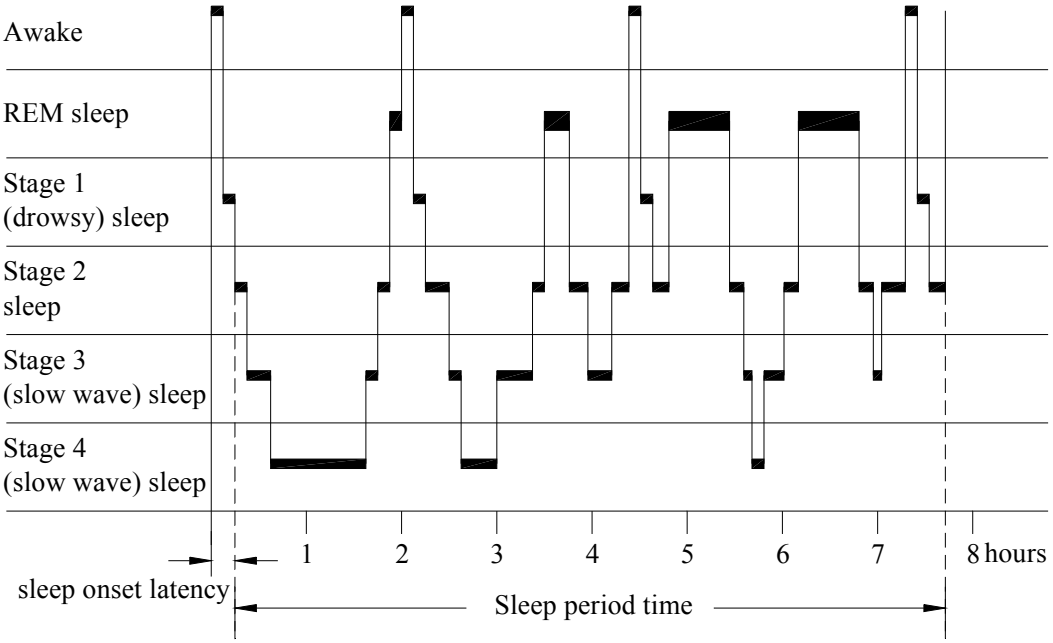

Fig. 2.1 The hypnogram of a young adult [Lavie 1996]

When human subjects pass from arousal to relaxed waking, to drowsiness, to light sleep, and finally to deep sleep, their brain waves change in a characteristic way. The characteristic patterns seen from light sleep to deep sleep have become known as the four stages of sleep.

Although the progression of EEG waves has been divided into discrete stages, it is actually gradual and continuous. Once Stage 4 is reached, the process reverses itself, and a sleeper goes back through Stage 3, 2 to 1. This clear cyclical process tends to repeat itself, from Stage 1 to Stage 1, at 90- to 100-minute intervals throughout a night [Hobson 1986]. At the end of each sleep cycle, there is a special period, called rapid eye movement (REM) stage, which can be regarded as the symbol of the start of next sleep cycle or the end of the last cycle. The number of sleep cycles per night depends on the duration of sleep; a younger person's sleep usually has four or five

cycles, while an older one has fewer.

2.2.2 Factors affecting the quality of sleep

Sleep deprivation would lead to daytime sleepiness and fatigue, and can hence affect coping skills, accomplishment of tasks, mood, relationships, and family and social life [Hui et al. 2002, Durmer and Dinges 2005, Roehers and Roth 2005]. Therefore, for decades, numerous medical researchers have investigated various factors affecting the quality of sleep. It was commonly acknowledged that the quality of sleep was mainly determined by the mental-physical factors of a sleeping person and the environmental factors in a sleeping environment.

More than 80% of people suffering from depression have disordered sleeping patterns and habits, often resulting in sleep deprivation [National Institute of Mental Health 2001]. It has been estimated that between 50% and 88% of patients with chronic pain had significant sleep complaints [Pilowsky et al. 1985, Morin et al. 1998, Smith et al. 2000]. A study found that more than two-thirds of institutionalized elderly people in the US had sleep disorders [Shochat et al. 2001]. People require less sleep as they get older, and an individual typically need approximately 30-60 minutes less per night in their late 70s than in their early 20s [Harbison 2002]. Moreover, sleep of elder people tends to be more fragmented, with a longer time taken to fall asleep.

Noise stimuli can be processed by the sensory functions of a sleeper, despite of a non-conscious perception of their presence [Muzet 2007, Basner et al. 2011]. It has

been reported that noises with intermittent peak levels of not less than 45dB (A) can increase the time duration for a sleeper to fall asleep by a few minutes to 20 minutes [Öhrström 1993]. The World Health Organization recommended a guideline level of 30dB for undisturbed sleep [World Health Organization 2007]. Light, as one of the most important environmental factors, can affect the quality of sleep. It does so both directly by making it difficult for people to fall asleep, and indirectly by influencing the timing of the internal clock of a human being and affecting his/her preferred time to sleep. Exposure to light in the late evening tends to delay the phase of the internal clock and to lead him/her to prefer to sleep late [Gooley et al. 2011]. Exposure to light in the middle of night can have more unpredictable effects, but can certainly be enough to cause a human being's internal clock to be reset, and may make it difficult to return to sleep. In addition to noise and light, the influence of thermal parameters in a sleeping environment on the quality of sleep has been also gradually understood [Haskell et al. 1981a, Muzet et al. 1984, Okamoto-Mizuno et al. 1999, Tsuzuki et al. 2008], which is presented in details in Section 2.2.3.

2.2.3 Thermal comfort in sleeping thermal environments

The last 30 years saw extensive research work on thermal comfort of people. These include establishing models [Fanger 1970, de Dear and Brager 1998], and indices [Gagge et al. 1986], carrying out experiments in climate chambers [Fanger 1970, Nakano et al. 2002], performing field surveys [Schiller 1990, Newsham 1997], establishing thermal comfort standards and evaluation methods [Olesen and Parsons 2002, de Dear and Brager 2002, Doherty and Arens 1988, Evin and Siekierski 2002，Höppe 2002, Zhang 2003], etc. However, almost all related studies were

concerned with the situations where people were awake. Nonetheless, there have been a few theoretical and experimental studies on the relationship between a sleeping thermal environment and the quality of sleep.

Strictly speaking, the term “thermal comfort” does not make too much sense for people during sleep. Basically, comfort was not a state of condition, but rather a state of mind. Therefore, to understand the relationship between the quality of a sleeping for a human being and his / her sleeping thermal environment, in medical or other related subject areas, a ‘thermal comfort zone’ was defined as: a range of ambient temperature around the thermal neutral temperature, within which the quantitative measures of sleep such as sleep stage latencies, time spent in each sleep stage, number and duration of awakening were only slightly modified [Muzet et al. 1984].

Numerous medical researchers have investigated the influence of thermal parameters in a sleeping environment on the quality of sleep. Different researchers carrying out experimental studies on the effects of high and low ambient temperatures on human sleep stages adopted different thermal neutral temperatures in sleep in the range of 20 to 32°C [Macpherson 1973, Karacan et al. 1978, Haskell et al. 1981b, Candas et al. 1982, Muzet et al. 1983, Sewitch et al. 1986, Palca 1986, Di Nisi et al. 1989, Dewasmes et al. 2003]. In the study [Haskell et al. 1981b] where subjects were naked, it was observed that the thermal neutral temperature was 29^{o}C. Miyazawa [1994] demonstrated that the range of thermal neutral temperature was about 22$\pm$ 3°C through a questionnaire survey and measuring the air temperature and humidity in a bedroom as well as the esophageal temperature of five junior college students for a period of 214 days. Table 2.1 lists the details of the different thermal neutral

temperature selected in various studies related to sleep. It can be seen that there is a fairly great range of thermal neutral temperature, indicating that a well-agreed single thermal neutral temperature has not been established. In most of the research studies related to sleep, only ambient air temperature was referred to, but the mean radiant temperature or operative temperature and air velocity were not taken into account. In cases where 20~25°C were selected, the test subjects were covered with bedding, while in others, the subjects may be naked. Although the thermal neutral temperatures determined by different researchers were different because of different experimental conditions (i.e., covered or naked), it can be clearly seen that the determined thermal neutral temperatures (20~25°C at covered condition; 28~32°C at naked condition) in sleeping thermal environments were different from the air temperature (24~26°C) normally maintained in workplaces in summer.

Table 2.1 Different thermal neutral temperatures adopted in studies related to sleep

Literature	Thermal neutral temperature (°C)	Condition of test subjects	Remark
Macpherson 1973	29~32	Naked	Air temperature
Karacan et al. 1978	22.2	Covered	Air temperature
Haskell et al. 1981b	29	Naked	Air temperature
Candas et al. 1982	32	Naked	Operative temperature
Muzet et al. 1983	19~22	Covered	Air temperature
Palca 1986	29	Naked	Air temperature
Sewitch et al. 1986	20~22	Covered	Air temperature
Di Nisi et al. 1989	30	Naked	Operative temperature
Dewasmes et al. 2003	25	Covered	Air temperature

Besides room ambient air temperature, other thermal environmental factors, such as air velocity and air humidity, also played an important role in the quality of sleep. In

a study carried out by Tsuzuki et al. [2008], 17 male subjects wearing short pajamas slept on a bed covered with a cotton blanket under three testing conditions: (1) air temperature 26°C, humidity 50% and air velocity 0.2 m/s (2) air temperature 32°C, humidity 80% and air velocity 1.7 m/s (3) air temperature 32°C, humidity 80% and air velocity 0.2 m/s. The experimental results suggested that having an appropriate air velocity inside a sleeping environment helped reduce the duration of wakefulness by decreasing the skin and rectal temperatures, and the body mass loss in a warm and humid condition. Okamoto-Mizuno et al. [1999] found that a high humidity exposure for a sleeping person at a high air temperature during nighttime increased the thermal load to suppress a decrease in rectal temperature, and thus increased wakefulness.

On the other hand, Lin and Deng [2008a] described the heat balance between a human body and its sleeping thermal environment as,

$$40 = \frac{34.6 - t_o}{R_t} + \frac{0.06 i_m L_R (p_{sk,s} - p_a)}{R_t} + 0.056(34 - t_a) + 0.692(5.87 - p_a) \quad (2.1)$$

Where, R_t, the total thermal resistance, is affected by as bedding, sleepwear, bed and mattress, the percentage coverage of body surface area by bedding and bed, air velocity, direction of airflow and posture, etc. [Lin and Deng 2008b].

By solving Equation (2.1), a comfort equation for sleeping environments, which combined both environmental and personal variables to produce a thermal neutral sensation, was derived:

$$40 = \frac{1}{R_t}\left[\left(34.6 - \frac{4.7\bar{t}_r + h_c t_a}{4.7 + h_c}\right) + 0.3762(5.52 - p_a)\right] + 0.056(34 - t_a) + 0.0692(5.87 - p_a) \quad (2.2)$$

There are five variables, R_t, $\bar{t}_r$, t_a, p_a, and h_c in Equation (2.2). The convective heat transfer coefficient, h_c, is the function of air velocity, v; therefore, four variables (i.e., $\bar{t}_r$, t_a, p_a, and v) are thermal environmental variables that determine a thermally neutral environment with a given bedding system.

By solving the Comfort Equation (2.2) at various combinations of variables, comfort charts (as shown in Fig. 2.2 and Fig. 2.3) were established, and can be used to determine a thermally neutral environment under a given bedding system.

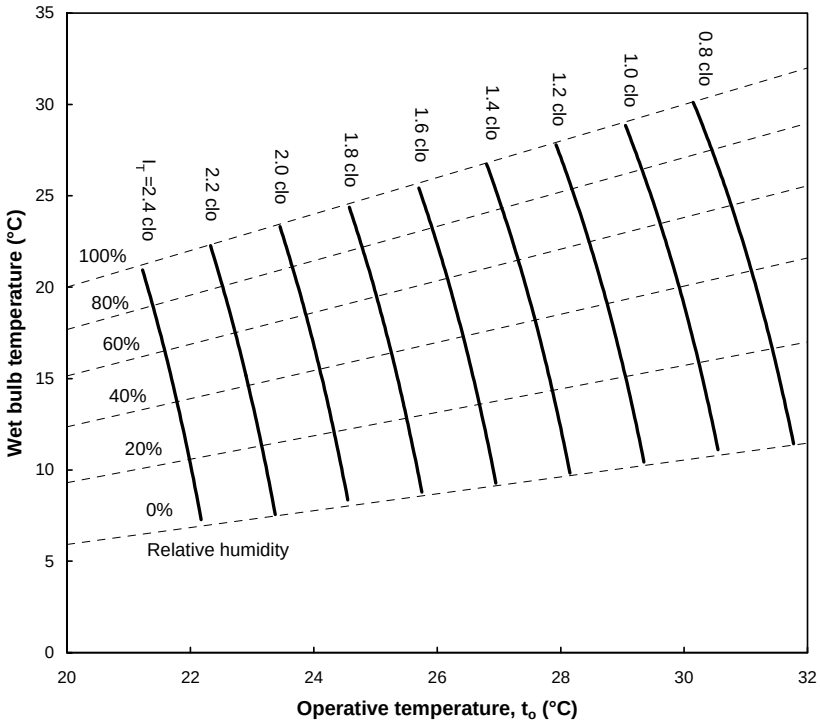

Fig. 2.2 Comfort lines (operative temperature vs. wet bulb temperature) with an indoor air velocity of not greater than 0.15 m/s [Lin and Deng 2008a]

Fig. 2.2 illustrates the comfort lines showing the combinations of operative temperature, wet bulb temperature and the total insulation value, under which thermal neutrality can be achieved. It can be seen that the influence of relative humidity on the thermal comfort of a sleeping person was relatively small. A change from absolutely dry air (RH = 0%) to saturated air (RH = 100%) can be compensated by only a 0.95 ~ 1.63°C (at the range of 2.4 ~ 0.8 clo total insulation values) decrease of operative temperature. The higher the total insulation value, the less the decrease in operative temperature. For example, when the total insulation value was 1.0 clo, a 1.5°C reduction in operative temperature would adequately compensate the change of relative humidity from 0% to 100%, compared to 1.1°C reduction in operative temperature at the total insulation of 2.0 clo.

On the other hand, the total insulation value provided by a bedding system significantly influenced the thermal neutral temperature for sleeping persons. This was clearly illustrated in Fig. 2.3, which shows the relationships between the thermal neutral temperature and the total thermal insulation of a bedding system under different indoor relative humidity levels. It can be seen from Fig. 2.3, that at 50% relative humidity, when the total insulation value increases from 1.0 clo to 2.0 clo, the thermal neutral temperature would decrease from 29.2°C to 23.4°C. It can also be seen from Fig. 2.3 that a linear relationship between the operative temperature and the total insulation value is demonstrated. Therefore, the relationship between the thermal neutral temperature and the total insulation value provided by a bedding system has been established. For example, the thermal neutral temperature was 29.3°C at 50% relative humidity for a naked sleeping person with the total insulation value of a bedding system being 0.98 clo. This agreed well with the range of 28 ~ 32°C for thermal neutrality temperature at naked conditions in various earlier studies related to sleep.

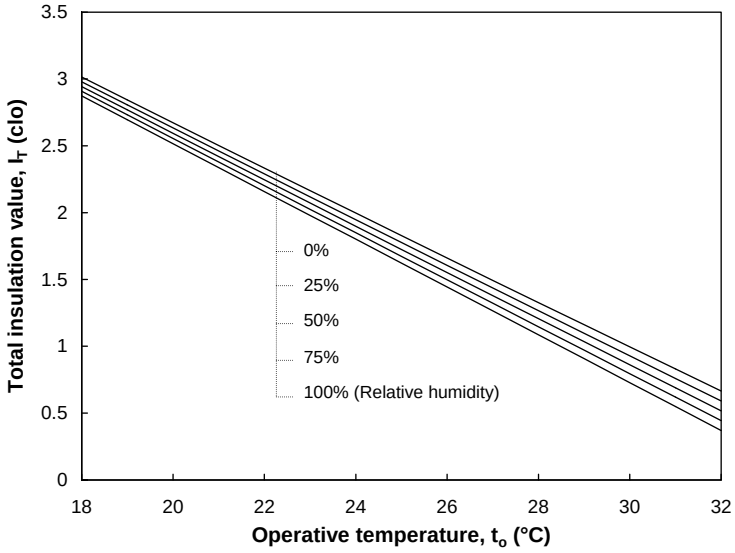

Fig. 2.3 Relationship between operative temperature and the total insulation value with an indoor air velocity of not greater than 0.15 m/s [Lin and Deng 2008a]

2.3 Thermoregulation and its modeling

2.3.1 Thermoregulation

A human being is a homoeothermic, warm-blooded animal whose heat production and heat loss are regulated to maintain an internal body or core temperature within a narrow range over a wide range of environmental conditions. A thermoregulatory system of a human being is physiologically responsible for maintaining the core temperature at a normal level by enhancing or inhibiting heat production and heat loss. Thermoreceptors, or temperature receptors, located in the skin, brain, spinal cord and possibly other sites inside the body of a human being respond to both local temperature and its changes [Guyton and Hall 2005]. Signals from the thermoreceptors are transmitted by the central nervous system to the hypothalamus where the signals are integrated. The overall thermal state of the body from these

signals will then be determined and the appropriate effector commands issued.

There are three types of thermoregulatory responses which could either inhibit or enhance body's heat production and heat loss: vasomotor, sudomotor and metabolic [Guyton and Hall 2005]. The three thermoregulatory functions control the body core temperature by either inhibiting or enhancing heat production and heat loss according to the commands issued by hypothalamus.

If the core temperature rises to above a normal level, the following thermoregulatory responses for decreasing it come into effect:

(1) Vasodilation (vasomotor): in most areas of a human body, the skin blood vessels are intensely dilated. Full vasodilation increases the rate of heat transfer to the skin surface by as much as eight-fold. When a vessel is dilated, much of the blood passes to the skin where it may be cooled before returning to the body core.

(2) Sweating (sudomotor): if vasodilatation is not sufficient to bring the core temperature back to its normal level, the anterior hypothalamus in the thermoregulatory system initiates a sweating process by sending a sweat-promoting signal to all of the sweat glands of the body through the sympathetic nerves. Sweating is a powerful and sensitive thermal regulatory mechanism. The evaporation of sweat on the skin surface allows a large amount of heat to be dissipated in a hot environment.

On the other hand, if the core temperature falls below its normal level, the following

thermoregulatory responses for increasing it come into effect:

(1) Vasoconstriction (vasomotor): it lessens the flow of warm blood from the internal structures to the skin, decreasing the heat transfer to the body surface from those organs producing the most heat. When vasoconstriction occurs, the skin temperature falls to near the temperature of the surroundings; this causes heat loss to be greatly diminished, allowing both the internal body to retain its heat and the core temperature to rise.

(2) Metabolic response (shivering): shivering begins to generate heat in muscle tissue. This muscular activity caused by shivering can increase the rate of heat generation in a human body by several-fold. Consequently, when the body is exposed to an extremely cold environment, shivering is a very powerful force to maintain normal body temperature.

In summary, the thermoregulatory system of a human body regulates heat production and heat loss through vasodilatation, vasoconstriction, shivering and sweating using temperature feedbacks from thermoreceptors.

2.3.2 Thermoregulation models developed for a waking person

A human being's thermoregulation is very complicated due to numerous variables involved in many control loops [Hensel 1973]. Using a thermoregulation model to predict human thermal physiological responses is a very useful tool in investigating the thermoregulation capability of a human body. Therefore, a large number of

thermoregulation models have been developed [Crosbie et al. 1961, Gagge et al. 1971, Stolwijk 1980, Wissler 1964, Smith 1991, Fu 1995, Fiala 1998, Huizenga et al. 2001 and Tanabe et al. 2002]. From early 40's to late 60's, human thermoregulation was studied primarily using analogue simulation [Crosbie et al. 1961, Smith 1962 and Atkins 1963]. In 1970s, there was a transition from the use of analogue simulation to digital simulation which was powerful in computational capability. Since then, a number of thermoregulation models have been developed, including the Gagge's two-node model [Gagge et al. 1971], the Stolwijk model [Stolwijk 1971] and the Wissler model [Wissler 1964]. With the further advancement of computer technology, Smith-Fu finite element thermoregulation model [Smith 1991, Fu 1995] and a 65-node thermoregulation model [Tanabe et al. 2002] were developed to predict three-dimensional body temperature distributions, local sweat rates, and latent and sensible heat losses from a human body surface. In addition, Fiala's dynamical model [Fiala 1998] was able to predict the transient thermal sensation based on available test data using human subjects. The results from the work by Huizenga et al. [2001] enabled the prediction of human physiological and psychological response to transient, non-uniform thermal environments. Sakoi's model [Sakoi et al. 2005, 2006] was proposed to predict local skin temperatures and heat losses under non-uniform thermal environments and various clothing conditions. It can numerically analyze the three-dimensional temperature distributions, three-dimensional distributions of body heat loss due to blood circulation, the promotion of heat conduction in skin tissue by conduction of blood flow, the respiratory heat loss, and the total heat loss at the skin surface using a finite element method.

Both the Gagge's two-node model and Stolwijk model have been the best known in

the field and they were very often used as a base on which other models were developed.

The Gagge's two-node model [Gagge et al. 1971, Gagge 1973] was a lumped parameter model dividing a human body into two concentric layers, an outer skin layer and a core layer representing internal organs, bone, muscle and subcutaneous tissue. Fig 2.4 shows the schematic of the Gagge's two-node model. It consisted of a controlled system and a controlling system.

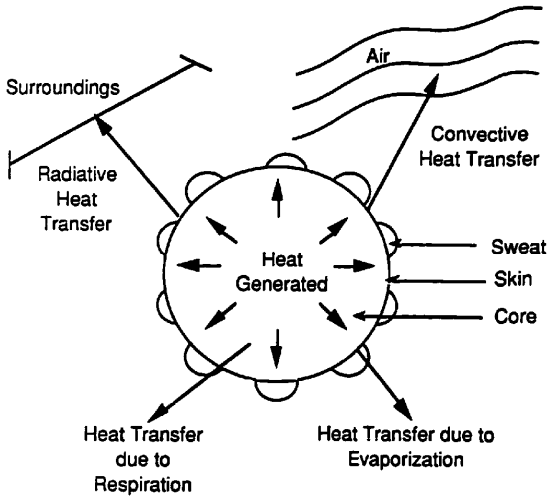

Fig.2.4 Schematics of the Gagge's two-node model [Gagge et al. 1971]

In the controlled system, the heat balance inside a human body and that between a human body and its surroundings were described. Firstly, assuming the temperature of each layer to be uniform, energy balances were written for the core and skin layers, respectively. The heat storage, conductive heat transfer between the two layers, and convective heat transfer due to blood flow were considered in the two layers. Secondly, sensible and latent heat losses caused by respiration and the effects of

metabolic heat generated during exercise and shivering were included in the core energy balance. Thirdly, heat exchange processes between the skin surface and its surroundings due to convection, radiation, and the evaporation of moisture were included in the skin energy balance.

The controlling system described the closed loop control processes and was further divided into two parts. In the first part where the thermal states of the controlled system were recognized, the error signals were the differences between the actual temperatures in two layers and their settings. A negative value of an error represented a cold signal, and a positive value a warm signal. In the second part, the controlling system equations were written as functions of these signals. For the blood flow rate equation, a cold signal from the skin governed a vasoconstriction process and a warm signal form the core a vasodilation process. In the case of a cold core signal and a warm skin signal, the blood flow rate was equal to its basal value. The rate of sweat production was controlled by both a warm body temperature signal, which was related to the mass weighted average of warm temperature signals from the core and skin, and a factor which incorporated the effects of local skin temperatures. Cold core and skin temperature signals made no contribution to the sweat rate equation. Furthermore, the shivering metabolic rate was expressed in relation to cold core and skin temperature signals.

This Gagge's two-node model was generally applicable to moderate levels of activity and uniform environmental conditions expressed by dry bulb temperature ranging between 5°C and 45°C with a minimum relative humidity of 10%.

On the other hand, the Stolwijk model [Stolwijk 1971, Stolwijk 1980] used five cylindrical elements to represent body trunk, arms, legs, hands and feet, and a spherical element for the head. Each element was divided into four concentric shells, representing core, muscle, fat and skin tissue layers. The core layers for head and trunk were assumed to be made of brain tissue and internal organs, respectively, while the core layers of all remaining elements were assumed to be made of bone. A network of blood vessels was used to transport blood from a central blood pool, or heart, to each tissue layer. The model consisted of a controlled system and a controlling system.

In the controlled system, energy balance equations were written for each tissue layer and the blood pool. Fig. 2.5 shows the schematics of the relevant heat exchange processes for one element. Firstly, heat storage, conductive heat transfer between adjacent tissue layers, convective heat transfer due to blood flow, and basal metabolic heat generation were included in the energy balances for all tissues. Secondly, latent heat losses due to respiration were equally divided between the head and trunk cores, which seemed inappropriate because latent heat loss occurred predominantly in the head. Finally, the energy balance equations for all skin layers included the heat losses due to convection, radiation and the evaporation of moisture on the body surface.

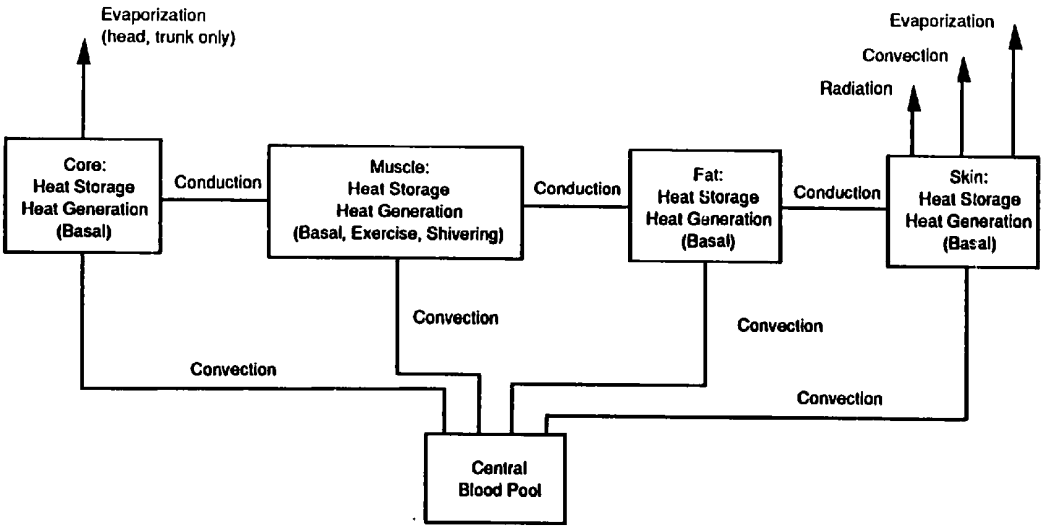

Fig. 2.5 Schematics of the Stolwijk model [Stolwijk 1971]

In the controlling system, controlling equations for the blood flow rate, the rate of heat production due to shivering, and the rate of heat loss due to the evaporation of moisture from the skin surface were presented. Similar to Gagge's two-node model, these controlling equations were assumed to be the functions of tissue temperature signals, defined in terms of both the deviation of tissue temperatures from their set point values and the rate of change in tissue temperatures. Warm head core and skin temperature signals governed both the effects of vasodilatation and the rate of evaporative heat loss at the skin surface. Cold signals from both of these regions governed the shivering metabolic heat generation rate while a cold skin temperature signal determined the vasoconstriction.

2.3.3 Thermoregulation for a sleeping person

Thermoregulation was present not only in wakefulness, but also during sleep. The interaction between thermoregulation and sleep led to different thermoregulatory

responses depending on the sleep stage and alterations in sleep of a sleeping person when in a cold or warm environment [Bach et al. 2002]. The experimental evidence showed that the interaction between thermoregulatory and sleep processes occurred at the level of a preoptic-hypothalamic thermostat [Parmeggiani 2003].

When exposed to a warm sleeping environment, vasodilation was present during NREM and REM stages [Haskell et al. 1981b, Candas et al. 1982]. Sweating was observed during NREM stages but depressed during REM stages [Ogawa et al. 1967, Takagi 1970, Shapiro et al. 1974, Henane et al. 1977, Sagot et al. 1987]. This sweating activity was consistent with both the down-regulation of set point for core temperature during NREM stages, with respect to wakefulness, and the fact that thermoregulation responses were still able to be proportional to thermal load. However, experimental results gave strong evidences that a greater sweating rate occurred during NREM stages than that during REM stages.

When exposed to a cold sleeping environment, shivering was occasionally present during NREMS stages but inhibited during REM stages [Kreider et al. 1958, Haskell et al. 1981b, Candas et al. 1982]. Haskell et al. [1981b] found that a low ambient temperature which was sufficient to induce vasoconstriction during NREM stages did not lead to vasoconstriction during REM stages. Vasoconstriction was present but inhibited in REM stages [Kreider et al. 1958, Haskell et al. 1981b].

2.4 Numerical approaches to studying thermal environment around a human body

2.4.1 Governing equations

With the rapid advancements in computer capacity and speed, computational fluid dynamics (CFD) has been widely used in many subject areas, including aerospace, food processing, buildings and environment. Among its many applications, the use of CFD techniques has become a powerful tool in building HVAC related studies for predicting indoor air flow patterns, indoor air temperatures and humidity, etc. [Nielsen 1974, Liddament 1991, Jones and Whittle 1992, Moser 1992, Chen 1996, Ladeinede and Nearon 1997, Emmerich 1997, Nielsen 1998, Spengler and Chen 2000, Chen and Zhai 2004, Stamou and Katsiris 2006, Zhai 2006 and Zhang et al. 2007].

Since indoor air is regarded as an uncompressible and viscous fluid, and its flow as of turbulent nature, the fundamental governing equations for indoor air flow could be written as:

1) Mass continuity equation:

$$\frac{\partial U_i}{\partial x_i} = 0 \tag{2.3}$$

2) Momentum equation:

$$\frac{\partial U_i}{\partial t} + U_j \frac{\partial U_i}{\partial x_j} = -\frac{1}{\rho}\frac{\partial P}{\partial x_i} + \nu \frac{\partial^2 U_i}{\partial x_j x_j} + \frac{1}{\rho}\frac{\partial}{\partial x_j}\left(-\rho\overline{u'u'_j}\right) - g_i \beta \Delta T \tag{2.4}$$

3) Energy equation:

$$c_p \frac{\partial T}{\partial t} + c_p U_j \frac{\partial T}{\partial x_j} = \frac{\lambda}{\rho} \frac{\partial^2 T}{\partial x_j x_j} + \frac{1}{\rho} \frac{\partial}{\partial x_j} \left(-\rho c_p \overline{u'_j \theta'} \right) + \frac{Q}{\rho} \tag{2.5}$$

A number of turbulence modeling approaches have been developed to solve the above governing equations. Proper selection of a turbulence modeling approach was a key issue that would directly affect the calculation accuracy and computational efficiency using CFD technique.

2.4.2 Turbulence modeling approaches and applications

2.4.2.1 Approaches

Generally, there were three turbulence modeling approaches [Heiselberg et al. 1998, Zhai et al. 2007]: direct numerical simulation (DNS), large-eddy simulation (LES) and Reynolds-averaged Navier-Stokes (RANS) simulation by turbulence transport models, as shown in Fig. 2.6.

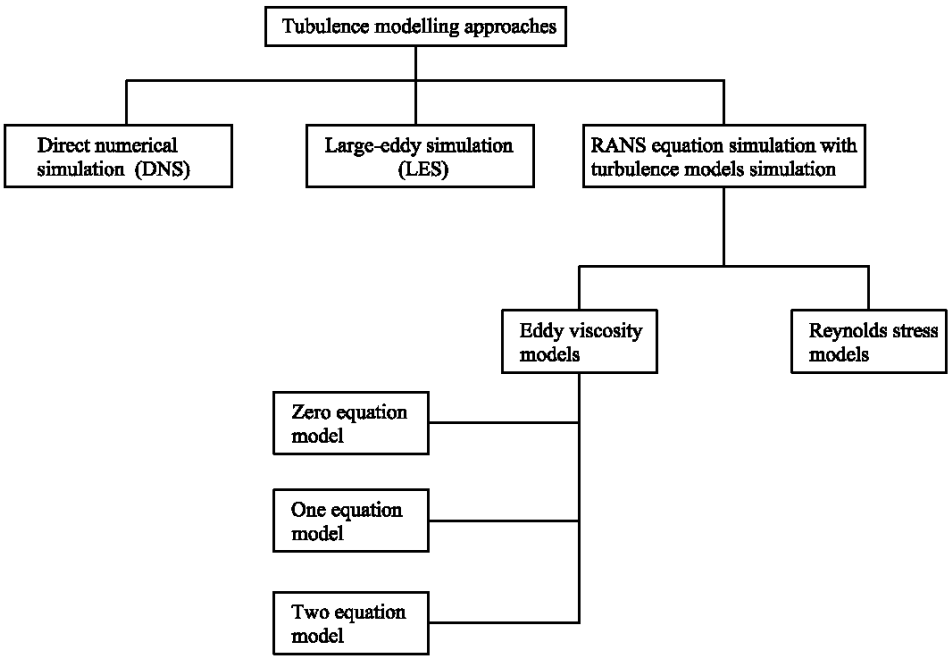

Fig. 2.6 The concept of different turbulence modeling approaches [Zhai et al. 2007]

DNS evaluates a turbulent flow by directly solving the highly reliable Navier-Stokes equation without approximations. Since DNS requires a very fine grid resolution to capture the smallest eddies in the turbulent flow and very small time steps, applying DNS to indoor air flow is not feasible and common.

LES is based on the hypothesis that turbulence could be separated into large eddies and small eddies such that the separation between the two does not have significant impact on the evolution of large eddies [Smagorinsky 1963, Deardorff 1970]. The large eddies can be directly simulated using the governing equations, shown in Section 2.4.1, while turbulent transport approximations are made for small eddies, eliminating the need for a very fine spatial grid and small time step. LES provides detailed information on instantaneous airflow and turbulence at the cost of

considerable computational efforts.

The RANS approach calculates statistically the averaged variables for both steady-state and transient flows and simulates the fluctuation effect of turbulence on the mean air velocities by using different turbulence models. Many turbulence models have been developed since the 1970s. Depending on how the Reynolds stress was determined and whether or not the Boussinesq concept was used, a turbulence transport model can be classified into an eddy viscosity model or a Reynolds stress model. The former can further be divided into a zero equation model [Chen and Xu 1998], or a one equation model [Baldwin and Barth 1990, Spalart and Allmaras 1992] or a two equation model [Launder and Spalding 1974, Yakhot and Orszag 1986, Shih et al. 1995]. At present, two equation models are the ones mainly applied to building HVAC studies.

2.4.2.2 Applications

Airflow inside buildings is characterized by a display of various flow elements. For example, air movement at a supply opening and an exhaust can be described as jet flow and potential flow, respectively, and the airflow in a room may be divided into natural convection, forced convection, or mixed convection according to its driving force. Certain turbulence models are only good at dealing with certain flow elements. It has been almost impossible so far to find out a single model that can be used to evaluate all room air flow patterns economically and accurately.

The performances of different turbulence models in modeling indoor air flow have

been continuously evaluated [Chen 1995, Lai and Yang 1997, Nielsen 1998, Murakami 1998, Walsh and Leong 2004, Zhang et al. 2007]. Up to the present moment, k–ε models are still most commonly used in practical engineering applications. Strictly speaking, a standard k-ε model was only applicable to fully turbulent flow. In the region near a solid surface, this model should be applied in conjunction with wall functions considering the dominant effects of viscosity, and the simulation accuracy would be greatly impacted by the location of the first grid close to the wall boundaries [Niu and Kooi 1992]. On the other hand, a low Reynolds number k-ε model differed from a standard k-ε model by using damping functions in a viscous sub-layer to replace wall functions. This brought in the benefit of more accurate modeling of transport phenomena in boundary layers and the penalty of finer grids near the wall at the same time [Launder and Sharma 1974]. A renormalized group k-ε model had the same form as a standard k-ε model except that its coefficients were derived from renormalization group theory [Yakhot and Orszag 1986], rather than experiments. However, all these three kinds of k–ε models mentioned above had their shortcomings. For example, the turbulence energy was over-predicted by a standard k-ε model [Wright and Eason 1999, Murakami 1998]. Very fine grids should be used near the wall and computational stability was probably a problem if a low Reynolds number k-ε model was employed. A RNG k-ε model still required to be used in conjunction with wall functions.

Table 2.2 shows the performance of different turbulence models used in four different enclosed environments. It can be seen that when selecting models, generally speaking, using complex turbulence models such as Reynolds-stress models would produce better accuracy, with the penalties in regard to computational

stability and duration. In most cases, using a standard k-ε model or a RNG k-ε model was able to predict room air flow pattern satisfactorily [Chen and Sebric 2002, Zhang et al. 2007]. Table 2.3 shows the performance of different k-ε models used for predicting indoor air flow.

Table 2.2 Performance of different turbulence models for predicting indoor air flow in four different enclosed environments[a] [Zhang et al. 2007]

Flow type	Compared Items	Turbulence Models							
		0-eq.[b]	RNG k-ε[c]	SST k-w[d]	LRN-LS[e]	V2f-dav[f]	RSM-IP[g]	DES[h]	LES[i]
Natural convection	Mean temperature	★★★	★★★★	★★★★	★★	★★★★	★★★★	★★	★★★★
	Mean velocity	★	★★★	★★★★	★★★	★★★★	★★★	★	★★★
	Turbulence	n/a	★★	★★	★★	★★★★	★★	★★	★★★★
Forced convection	Mean temperature	★★	★★★★	★★	★★★★	★★★★	★★★	★★	★★★★
	Turbulence	n/a	★★★	★★	★★★	★★★	★★★	★★	★★★
Mixed convection	Mean temperature	★★★★	★★★★	★★★★	★★★★	★★★★	★★★	★★★	★★★★
	Mean velocity	★★★★	★★★	★★★	★★★	★★★★	★★★★	★★★	★★★
	Turbulence	n/a	★★★★	★	★★★	★★★★	★★★★	★★★	★★★
Strong buoyancy convection	Mean temperature	★★★★	★★★★	★★★★	★★★★	★★★★	n/c	n/a	★★★
	Mean velocity	★★★	★★★★	★★★★	★★★★	★★★★	n/c	n/a	★★★★
	Turbulence	n/a	★★	★★★★	★★★	★★★	n/c	n/a	★★★
Computational time (unit)		1	2-4		4-8		10-20	10^2-20^3	

[a] ★★★★: Good, ★★★: Acceptable, ★★: Marginal, ★: Poor, n/a: not applicable, n/c: not converged; [b]the zero-equation model (0-eq.) from Chen and Xu [1998]; [c]the standard k-ε model from Yakhot and Orszag [1986]; [d]the SST k-w model (SST) from Menter [1994]; [e]a low-Reynolds-number k-ε model (LRN-LS) from Launder and Sharma [1974]; [f]a modified v2f model (v2f-dav) from Davidson et al. [2003]; [g]a Reynolds-stress model (RSM-IP) from Gibson and Launder [1978]; [h]a detached eddy simulation (DES) from Germano et al. [1991] and Lilly [1992]; [i]the large eddy simulation (LES) with a dynamic subgrid scale model from Shur et al. [1999].

Table 2.3 Performance of different *k-ε* models for predicting indoor air flow[a] [Chen 1995]

Flow type	Parameters	k-ε[b]	LB k-ε[c]	2L k-ε[d]	2S k-ε[e]	RNG k-ε[f]
Natural convection	Mean velocity	⋆⋆⋆	⋆⋆⋆⋆	⋆⋆⋆	⋆⋆⋆	⋆⋆⋆
	Turbulence	⋆⋆	⋆⋆	⋆	⋆	⋆⋆
	Temperature	⋆⋆⋆	⋆	⋆⋆⋆	⋆⋆⋆	⋆⋆⋆
	Heat transfer	⋆⋆	⋆⋆⋆	⋆⋆⋆⋆	⋆⋆	⋆⋆
Forced convection	Mean velocity	⋆⋆	⋆⋆	⋆⋆	n/a	⋆⋆
	Turbulence	⋆	⋆	⋆	⋆	⋆
Mix convection	Temperature	⋆⋆⋆⋆	⋆⋆⋆⋆	⋆⋆	⋆⋆⋆⋆	⋆⋆⋆⋆
Impinging jet	Mean velocity	⋆⋆	⋆⋆	⋆⋆	⋆⋆⋆⋆	⋆⋆⋆⋆
	Turbulence	⋆	⋆	⋆	⋆⋆	⋆⋆

[a] ⋆⋆⋆⋆: Excellent, ⋆⋆⋆: Good, ⋆⋆: Fair, ⋆⋆: Poor, n/a: not applicable; [b]the standard *k-ε* model from Lauder and Spalding [1974]; [c]a low-Reynolds-number *k-ε* model from Lam and Bremhorst [1981]; [d]a two-layer *k-ε* model from Rodi [1981]; [e]a two-scale *k-ε* model from Kim and Chen [1989]; [f]a *k-ε* model based on a renormalization group (RNG) method from Yakhot et al. [1992].

2.4.3 Related numerical studies on the thermal environment around a human body

In order to correctly evaluate thermal comfort of an individual and indoor air quality, the thermal environment around a human body needed to be known. To facilitate carrying out the related studies, thermal manikins have been used for many years [Holmér 2004]. They were first introduced half a century ago to measure the thermal resistance of clothing. In 1977, Mihira et al. [1977] developed a thermal manikin not only for measuring clothing insulation, but also for evaluating thermal environments. Afterwards, more complex thermal manikins were further developed to investigate the thermal reactions of a human body to indoor thermal environments [Fanger et al. 1980, 1986, Tanabe et al. 1989]. Although it was possible to obtain the parameters of a thermal environment (e.g., air velocity and turbulence intensity, air and wall temperatures, etc.) through an experimental study using a thermal manikin, it would be rather costly and time-consuming. Hence, a growing number of Computational Thermal Manikins (CTMs) have been proposed for the purpose of identifying and evaluating parameters that were either very expensive or very difficult to be experimentally obtained.

A CTM was firstly defined and proposed by Murakami et al. [1997]. In their study, five CTMs were placed in five different rooms, which were air conditioned with five different air distribution systems. The air flow fields around each CTM and the convective heat transfers between each CTM and its surroundings were numerically analyzed and compared. In a further study, the same CTM mentioned was employed to numerically examine the convective and radiative heat transfers, and the moisture transfer between a CTM and its surroundings in a room with a displacement

ventilation system [Murakami et al. 2000]. The study consisted of two parts. In the first part, a two-node thermoregulation model was employed to simulate the thermoregulatory process and to calculate the heat transfer inside the CTM. In the second part, the heat and mass transfer between the CTM and its surroundings was numerically studied. The outputs from the first part of the study such as the sensible heat loss from skin, sweat rate generated from skin, etc., were used as the boundary conditions for the second part while the outputs from the second part of the study, such as the mean skin temperature, mean indoor air temperature, water vapor partial pressure, etc., were used as the inputs to the first part. Hayashi et al [2002a, 2002b], BjØrn and Nielsen [1998], Xing et al. [2001] simulated the contaminant distribution around a CTM and its impact on the quality of inhaled air. With the advancement in technology, a CTM with real geometry of a seated female was obtained by scanning a thermal manikin using laser scanning technique [Gao and Niu 2004, Gao et al. 2006]. This CTM was employed in a numerical study to assess the effectiveness of a personalized ventilation system and the related thermal comfort issues.

A review on certain important issues related CFD study on the thermal environment around a human body was reported by Gao and Niu [2005a]. These included geometric complexity, turbulence models, grid generation, boundary conditions and related simulation results obtained. Firstly, CTMs may differ in size, posture and the level of geometric complexity. The level of geometric complexity of CTMs depended on the purpose of study. The geometries of CTM can be often obtained from computer aided design, but a CTM having a complicated geometry may be obtained using laser scanning technique [SØrensen and Voigt 2003, Gao and Niu 2004, Gao et al. 2006]. The use of CTMs with simple geometry required fewer

computational resources and less time for modelling and grid generation. However, using a detailed representation of a human body can help better to reflect the reality to produce more accurate simulation results. Toppe et al. [2002] investigated numerically the differences among using different shapes of CTMs with respect to both local and global air distributions as well as convective transfer. The study results showed that when a numerical research focused on global airflow pattern in a ventilated room, a CTM with simple geometry was enough; however, an accurate CTM geometry was necessary when the local flow pattern around a human body needed to be considered. Secondly, different types of flow elements, such as jet flow, buoyance driven flow, laminar flow and potential flow, may have to be dealt with when studying the air flow around a human body in a ventilated room. However, no turbulence model currently available can hand this perfectly. A low Reynolds number k-ε model performed better in predicting heat loss from human body [Murakami et al. 1997, SØrensen and Voigt 2003] while a standard k-ε model and a RNG k-ε model were sufficient if the emphasis was on airflow field [Gao and Niu 2004, Gao et al. 2006]. Thirdly, special attention should be paid to grid generation for a numerical study involving CTM and the correctness and accuracy of numerical study results depended very much on grid quality. Body-fitted coordinates and unstructured grids [Murakami et al. 1997, SØrensen and Voigt 2003, Gao and Niu 2004, Gao et al. 2006] were often used to represent the complex shape. Fourthly, two methods were usually used to describe the boundary condition of a human body: a fixed surface temperature or a fixed surface heat flux. Usually, the temperature of body surface was set between 31^{o}C [Murakami et al. 1997] and 33.7^{o}C [SØrensen and Voigt 2003]. The convective heat flux was set between 20W/m^2 [Hayashi et al. 2002a] and 25W/m^2 [Brohus and Nielsen 1996]. Lastly, radiative and convective

heat transfer from a human body has been be numerically investigated, and the study results have been used to assess the thermal comfort of a human being [Murakami et al. 2000, Silva and Coelho 2002, Yang et al. 2002, SØrensen and Voigt 2003, Gao and Niu 2004, Gao et al. 2006].

2.5 Task/ambient air conditioning (TAC) systems

Because of their excellent performance in local thermal environmental control and energy saving, TAC systems have attracted increasingly research attention. A TAC system permits the thermal conditions in a small, localized zone to be individually controlled by its occupants, while allowing thermal environmental conditions outside the zone to freely fluctuate [Bauman and Arens 1996]. Typically, the occupants could control over the speed and direction and in some cases the temperature of supply air to the zone. A TAC system is therefore designed to provide individual control and accommodate individual preferences over thermal environment, and to offer the potentials for improved productivity and energy saving for air conditioning.

2.5.1 Types

The original idea of TAC system was evolved from under-floor air distribution (UFAD) system [Matsunawa et al. 1995, Sodec and Craig 1990]. Over the years, different TAC systems have been developed, and may be divided into the following categories: floor-based, desktop-based, partition-based and ceiling-based.

A floor-based TAC system was the most utilized one. Floor-based TAC systems were

extensively developed and used in South Africa and Europe [Spoormaker 1990, Sodec and Craig 1991], as well as in the United States [Shute 1992, 1995] and Japan [Matsunawa et al 1995, Tanabe 1995]. For a floor-based TAC system, its supply outlets were designed to be incorporated into a raised access floor. Air was either drawn from a low-pressure underfloor plenum by local variable or constant-speed fans, or forced through a pressurized underfloor plenum by a central air handler, and delivered to a space through floor-level supply outlets. Fig. 2.7 shows a floor-based TAC system with Task Air Modules (TAM) [Bauman et al. 1995]. A floor-based TAM can provide required air-volume and allow occupants to control the direction of supply air.

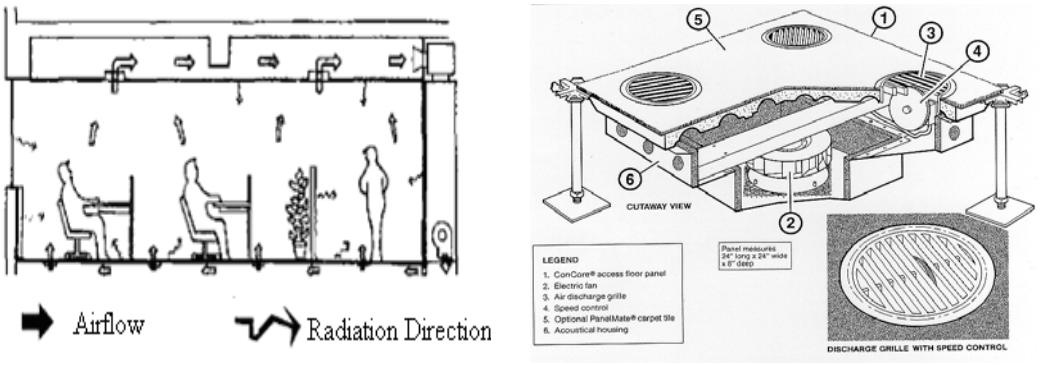

Fig. 2.7 A floor-based TAC system with Task Air Modules [Baumen et al. 1995]

For a desktop-based TAC system, its air supply outlet was installed in a desk. A variety of desktop supply outlets have been developed and used, such as desktop level grills at the back of a desk surface [Argon 1994], free-standing directable supply nozzles at the back of a work surface [Sodec 1984, Arens et al. 1991, Bauman et al. 1993] and a linear grill at a desk's front edge directly facing a seated occupant [Argon 1994, Wyon 1995]. A sketch of a typical desktop-based TAC system with a PEM (Personal Environmental Module) installation [Bauman et al. 1993] in a

workstation is shown in Fig. 2.8.

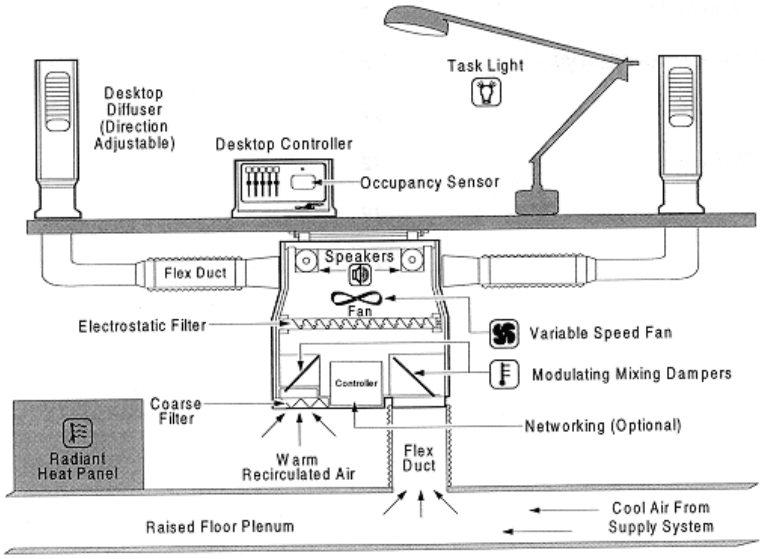

Fig. 2.8 A desktop-based TAC system [Bauman et al. 1993]

A partition-based TAC system [Argon 1994, Matsunawa et al. 1995, Pan et al. 2005] can be designed to be integrated into a partitioned workstation and was convenient to link it to a raised access floor. Supply air was delivered through a passageway that was integrated into the partition design to controllable supply grills that may be located just above desk level or just below the top of the panel (for personal comfort control), or to the outlets on top of the partitions (for ambient environmental control). Fig. 2.9 shows a terminal of a partition-based TAC system [Argon 1994]. A number of partition-based TAC systems installed in Japanese buildings were investigated by the Society of Heating, Air-conditioning and Sanitary Engineers of Japan [SHASE 1991] and Matsunawa et al. [1995].

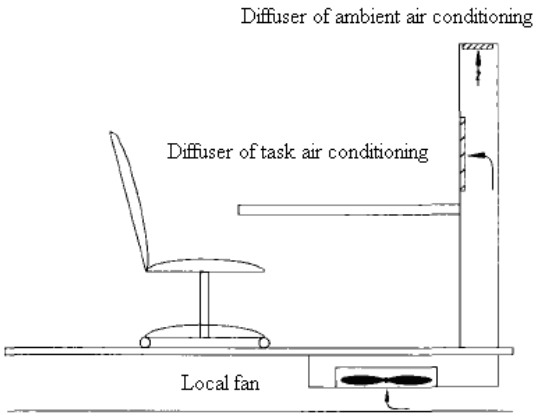

Fig. 2.9 A terminal of a partition-based TAC system [Argon 1994]

Ceiling-based TAC systems [Tamblyn 1995, Yang et al. 2008, 2009 and 2010] have been mostly seen in retrofit projects, where installing raised floor was difficult due to the limited floor-to-slab height. Similar to that in a conventional air conditioning system, the air supply outlets of ceiling-based TAC systems were above a work space. Fig. 2.10 shows a typical ceiling-based TAC system [Tamblyn 1995]. A remote controller was essential for this type of TAC system to be practically operable.

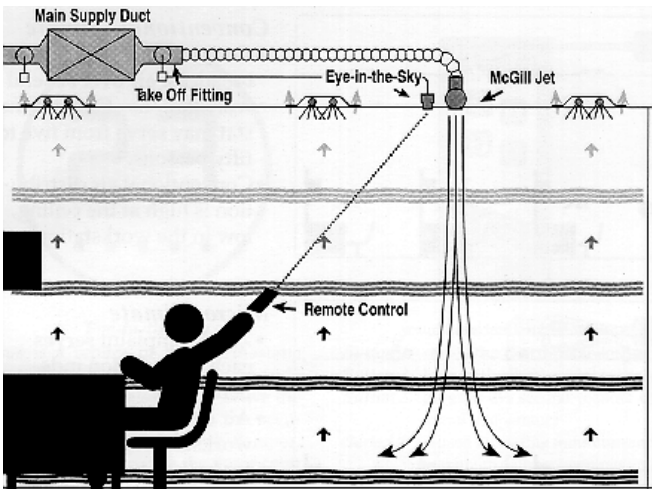

Fig. 2.10 A ceiling-based TAC system [Tamblyn 1995]

2.5.2 The advantages of using TAC systems

Studies have been carried out to investigate the operational performance of TAC systems used for daytime activities, through field measurement and experimentation. Results from these previous studies demonstrated that the use of TAC systems can help improve thermal comfort and indoor air quality, and reduce the energy consumption [Bauman et al. 1993, 1998, Shute et al. 1995, Faulkner et al. 1995, 1999, Tham et al. 2004, Pan et al. 2005, Amai et al. 2007].

By allowing personal control over local thermal environments, thermal comfort of occupants can be greatly improved using TAC systems. For example, the survey results by Bauman et al. [Bauman et al. 1993] showed that in office buildings, the use of desktop-based TAC systems led to a significant increase in overall occupants' satisfaction with indoor thermal, acoustical and air quality. Subjective surveys on different types of TAC systems were conducted by Amai et al. [2007] to evaluate their performances based on the level of thermal comfort and operational convenience that can be achieved by using each system.

The use of TAC systems can help improve indoor air quality, since fresh air can be directly delivered to occupants, and the contaminants from an occupied zone efficiently removed. Shute et al. [1995] studied indoor air quality in a room using a floor-based TAC system and concluded that the suspended substance concentration in the room was lower than that when using conventional air conditioning. Faulkner et al. [1999] carried out a laboratory-based study on a floor-based TAC system, and concluded that using two floor-supply units, the aging of air in the breathing zone

was about 20-40% slower than that using a mixed ventilation system. Spookmaker et al. [1990] studied indoor pollutants concentration in a building with a floor based TAC system, and the results indicated that each index of the pollutants was much lower than the standard value.

The use of TAC systems helped also achieve energy saving. This was because when a full air conditioning (FAC) system was used, a comfortable indoor environment for everywhere in a room would be maintained. However, when a TAC system was used, only a comfortable indoor environment within an occupied zone would be maintained, but air temperatures in unoccupied zone(s) were allowed to fluctuate even to outside comfort limits. Therefore, as compared to the use of an FAC system, the use of TAC systems can result in energy saving since air conditioning in an unoccupied zone was unnecessary. Pan et al. [2005] experimentally compared the performance of a personalized air-conditioning system, which was called an innovative partition-type fan-coil unit (PFCU), with that of a central air-conditioning system, in terms of the thermal comfort achieved and cooling energy consumed. The experimental results showed that the use of this personalized system can shorten the duration required in achieving the same level of thermal comfort, and save up to 45% of the energy consumed using a FAC system.

2.5.3 Ranges for operating parameter of TAC systems

The suitable ranges for operating parameters in various TAC systems have been investigated and are listed in Table 2.4. These included supply air temperature, velocity, supply direction, heat load level, etc. For a floor-based TAC system,

Bauman et al. [1995] recommended that local supply temperatures should be maintained at above 17°C to avoid uncomfortable cold draft for the occupants nearby. A floor supply module should be installed 1-1.5m away from a work station to avoid draft. For a desk-based TAC system, using larger nozzles to deliver a fixed amount of air at a lower velocity helped reduce the potential for draft discomfort while still maintaining an acceptable ventilation performance at a moderate to high air supply [Bauman et al. 1993, Faulkner et al. 1999]. Moreover, Gong et al. [2005, 2006] suggested that when a task/ambient supply outlet was 15 cm away from an occupant, a supply velocity of 0.3 to 0.45 m/s was suitable at a supply air temperature of 21°C, while the supply velocity of 0.3 to 0.9 m/s was better at a supply temperature of 23.5°C. Therefore, by suitably controlling its supply air velocity and temperature, supply direction, a TAC system can be operated to maintain acceptable thermal comfort and avoid draft in an occupied zone.

Table 2.4 Operating parameters of different types of TAC systems

Literatures	Types	Supply temperature (°C)	Supply flow rate (L/s)	Supply direction	Heat load level (W/m^2)
Bauman et al. 1991	Floor-based	18	16-33	Toward, inward and combined	35-55
Bauman et al. 1995	Floor-based	16 - 21.6	16-47	Toward and inward	25-50
Faulkner et al. 1995	Floor-based	15.9 - 22.9	27-82	Toward, inward	17.8-43.5
Mutsunawa et al. 1995	Floor-based	18 - 20	74-83	-	31-40
Bauman et al. 1993	Desktop-based	16.6 - 20.8	14-50	Toward and straight	24-51
Faulkner et al. 1993	Desktop-based	19	7-26.1	Vertical, horizontal, toward and parallel	-
Faulkner et al. 1999	Desktop-based	18.4 - 26.1	7-38	Vertical, horizontal, toward and parallel	-
Mutsunawa et al. 1995	Partition-based	18 - 20	74-83	-	31-40
Jeong et al. 2006	Partition-based	22 - 27	20	-	-

2.6 Conclusions

With the rapid economic growth and the continuous increase in people's living standard, air conditioning has been widely applied in various buildings, and the associated energy use has also significantly increased. Currently, air conditioning is mainly concerned with the situations in which people are awake in workplaces or other leisure places, such as shopping malls and restaurants. However, in tropical and

sub-tropical regions, air conditioning is required not only in daytime at a workplace, but also at nightime in a sleeping environment, such as bedrooms in residential buildings and guest rooms in hotels, as demonstrated in a survey on the use of air-conditioning in bedrooms in residential buildings in Hong Kong [Lin and Deng 2006]. Therefore, it has become highly necessary to study the thermal environment in an air conditioned sleeping space in order to provide people with a thermally comfortable sleeping environment at low energy consumption.

Previous medical research work on the factors affecting the quality of sleep has been undertaken, as reported in Section 2.2. It was commonly acknowledged that the quality of sleep was mainly determined by mental-physical factors of a sleeping person and the environmental factors in a sleeping environment. The most important environmental factors included indisputably the indoor thermal parameters such as air temperature, humidity. Therefore, a limited number of previous studies on surveying the sleeping thermal environments and bedroom air conditioning, studying the thermal comfort and developing an appropriate thermal comfort model for sleeping environments have been carried out.

Furthermore, numerical studies have been carried out to investigate the micro-climate around a human body using CTMs developed, as presented in Section 2.4. However, the reviewed studies were performed under the conditions that the CTMs were placed in a standing or seated position, which was for daytime activities but not applicable to a sleeping environment. This was because a sleeping person's posture was different from that when he or she stood or was seated. In addition, the metabolic rate of a sleeping person was also lower at 40 W/m^2 during sleep. This

implied that the mean skin temperature of a sleeping person in the state of thermal neutrality would be higher. More importantly, many related studies involving CTMs have overlooked the effects of thermal insulation of clothing. A recent study [Lin and Deng 2008a] suggested that in a sleeping environment, the total insulation value of a bedding system could play an important role in determining the thermal neutrality of a sleeping person, hence the total insulation value of the bedding system cannot be neglected. Consequently, a sleeping CTM (SCTM) should be developed and related numerical studies involving SCTM to examine the thermal environment around a sleeping person in a sleeping environment undertaken.

A human being's thermoregulation was very complicated due to numerous variables involved in many control loops. Using a thermoregulation model to predict human thermal physiological responses was a very useful tool in investigating the thermoregulation capability of a human body. The related review on existing thermoregulation models is presented in in Section 2.3.2. However, all reviewed thermoregulation models were for a waking person who was awake. For a sleeping person, his/her thermoregulatory process can be different from that of a waking person because of a number of reasons, as mentioned in Section 2.3.3. Firstly, a large part of the body surface of a sleeping person was in touch with mattress. Secondly, the total insulation value of a bedding system was different from that of clothing and would play an important role in a sleeper's thermal sensation. Thirdly, the set points for skin temperature and core temperature during sleep were different. Lastly, thermoregulatory responses of a sleeping person were sleep-stage dependent. Therefore, a thermoregulation model which is applicable to a sleeper should be developed.

Because of their excellent performance in local thermal environmental control and energy saving, TAC systems have attracted increasingly research attention. Different types of TAC systems have been reviewed in Section 2.5.1. Nevertheless, the current applications of TAC systems are mainly for daytime activities, such as in work stations, but not for bedrooms in residences or other sleeping environments. Unlike daytime activities such as shopping or walking, or even working in a work station, sleeping is confined to a relatively small space and a sleeping person is immobile. Therefore, TAC systems may be best applied to a sleeping environment. To this end, related studies on applying TAC to a sleeping environment should be carried out.

The extensive literature review presented in this Chapter has identified a number of important areas where further in-depth research work to maintain an appropriate sleeping thermal environment at a reduced energy consumption is urgently required. These are the expected targets of investigation to be reported in this Thesis.

Chapter 3

Proposition

3.1 Background

It is evident from Literature Review presented in Chapter 2 that the current numerical or experimental studies related to investigating micro-climate around a human body, thermoregulation models and the applications of TAC systems are basically concerned with situations in which people are awake in workplaces at daytime. Therefore, the outcomes of the related studies may not be directly applicable to the corresponding issues for sleeping environments. Consequently, relevant studies aiming at sleeping environments need to be carried out. This would help maintain an appropriate sleeping thermal environment at a low energy consumption.

Human thermal comfort has been one of focal points when developing air conditioning technology, for a workplace at daytime or a sleeping environment at nighttime. Currently, although there have been extensive research efforts in numerically studying human thermal comfort in workplaces at daytime, there has been a lack of numerical studies on human thermal comfort in sleeping environments at nighttime.

In addition, thermoregulation of a sleeping person to maintain a small oscillation of core temperature at nighttime is different from that of a waking person at daytime. This is because the total insulation value of a bedding system is different from that of

clothing and the thermoregulatory responses of a sleeping person are sleep-stage dependent. This suggests a need in developing a thermoregulation model for predicting the thermoregulatory responses of a sleeping person.

Furthermore, the current applications of TAC systems are mainly for daytime activities, but not for bedrooms in residences or other sleeping environments. Unlike daytime activities such as shopping or walking, or even working in a work station, sleeping is confined to a relatively small space and a sleeping person is immobile. However, the TAC systems developed for daytime applications might not be good enough for a sleeping environment. Consequently, there is a strong need to develop a TAC system that can be suitably applied to sleeping environments, using both experimental and numerical approaches.

3.2 Project title

This thesis focuses on three major pieces of work related to human thermal comfort in a sleeping environment: 1) studying numerically the micro-climate around and the thermal neutrality of a sleeping person; 2) developing a thermoregulation model to predict the thermoregulatory responses of a sleeping person; 3) developing experimentally and numerically a TAC system applicable to sleeping environments. The proposed research project is therefore entitled “An experimental and numerical study on the thermal environment in an air-conditioned sleeping space”.

3.3 Aims and objectives

The objectives of the research work reported in this thesis are as follows:

1) To develop a sleeping computational thermal manikin (SCTM) to investigate the micro-climate around, and the thermal neutrality of a sleeping person;
2) To develop and validate a thermoregulation model of a sleeping person to predict the thermoregulatory responses to different thermal environments;
3) To develop a TAC system applicable to sleeping environments and to study its operational and energy saving performance, both experimentally and numerically.

3.4 Research methodologies

Numerical, analytical and experimental approaches will be employed. Firstly, numerical approaches are used to study the micro-climate around, and the thermal neutrality of a sleeping person, using a commercially available CFD software package. A SCTM placed in a space conditioned by a displacement ventilation system will be developed. The micro-climates around a naked SCTM, including air temperature and velocity distributions, and heat transfer characteristics, etc., would be compared with the previous experimental results by others to validate the numerical study results. The thermal neutrality for a sleeping person will also be numerically studied, using the SCTM developed, covering the thermal neutrality for a naked sleeping person and the effects of the total insulation value of a bedding system on the thermal neutrality of a sleeping person.

Secondly, analytical approaches will be applied to studying thermoregulatory responses of a sleeping person. A thermoregulation model for a sleeping person will be developed by introducing appropriate modifications to Gagge's two-node model, to be validated by pervious experimental study results from other researchers.

Thirdly, both the experimental and numerical approaches will be employed in developing a TAC system applicable to sleeping environments. All the experimental work will be carried out in an experimental DX A/C station available in the HVAC laboratory in the Department of Building Services Engineering, The Hong Kong Polytechnic University. On the other hand, a numerical model for the TAC system developed will also be established, to be validated using the experimental data obtained. The validated numerical model will be further used to analyze the performances of the TAC system developed at the operating conditions other than the experimental conditions.

Chapter 4

Numerical studies on the micro-climate around a sleeping person and the related thermal neutrality issues

4.1 Introduction

As reported in Chapter 2, in both tropic and sub-tropic regions, the use of air conditioning is common for maintaining a thermally comfortable indoor environment not only at daytime, but also in sleeping environments at nighttime. Currently most studies related to air-conditioning are mainly concerned with environments in which people are awake. In order to provide people with a thermally comfortable sleeping environment at low energy consumption, it would be essential to study the thermal environment of an air conditioned sleeping space.

Previous medical research studies related to sleep mostly focused on the influence of room air temperature on thermoregulation, metabolism and stages of sleep. They have shown that during various sleeping stages, excluding the Rapid Eye Moment (REM) stage, the physiological response of a sleeping person to room air temperature changes was similar to that of a person who was awake [Lavie 1996]. Although the quality of sleep may be affected by a number of factors such as age, drug ingestion and noise level, the impact of thermal parameters in a sleeping environment on sleep quality has been gradually acknowledged. This has led to a number of studies that examined the relationship between a sleeping thermal environment and sleep quality over the last few decades [Muzet et al. 1983, Miyazawa 1994, Haskell et al. 1981a, Kubo et al. 1999, Okamoto-Mizuno et al.

1999, Tsuzuki et al. 2008]. However, these studies solely focused on the influence of room air temperature on sleep quality without considering other factors such as air velocity, air turbulence intensity, radiant temperature of internal walls and the total insulation value of a bedding system. Therefore, in order to maintain a thermally neutral sleeping environment, further studies should be conducted to examine the effects of other factors than air temperature on the thermal neutral environment, both experimentally and computationally. On the other hand, thermal manikins have been used for many years [Holmér 2004]. Although it was possible to obtain the parameters of a thermal environment (e.g., air velocity and turbulence intensity, air and wall temperatures, etc.) through an experimental study using a thermal manikin, it would be rather costly and time-consuming. Hence, a growing number of Computational Thermal Manikins (CTMs) have been proposed for the purpose of identifying and evaluating parameters that were either very expensive or very difficult to be experimentally obtained [Murakami et al. 1997, 2000, Gao and Niu 2004, Gao et al. 2006], as detailed in Chapter 2.

However, from the literature review presented in Chapter 2, it should be noted that the CTMs developed were placed in a standing or seated position, which would not be applicable to a sleeping environment. This is because during sleep, a person's posture is often different from when he or she is standing or seated. The metabolic rate of a sleeping person is also lower at 40 W/m^2 during sleep [ASHRAE Handbook 2009], suggesting that the mean skin temperature of a sleeping person in the state of thermal neutrality would be higher. More importantly, in many previous CTM related studies [Murakami et al. 1997, 2000, Gao et al. 2006, Zhu et al. 2007, 2008], the effects of thermal insulation of clothing were overlooked. Since a recent research

showed that in a sleeping thermal environment, the total insulation value of a bedding system could play an important role in determining the thermal neutrality of a sleeping person [Lin and Deng 2008a], the total insulation value of bedding system cannot therefore be neglected.

This Chapter reports on two numerical studies on the micro-climate around, and the thermal neutrality of, a sleeping person placed in a space with a displacement ventilation system. First, the development of a SCTM placed in a space air conditioned by a displacement ventilation system will be described. This is followed by reporting the results of the first numerical study on the micro-climate around a naked SCTM, including air temperature and velocity distributions, and heat transfer characteristics. Then, the outcomes of the other numerical study on the thermal neutrality for a sleeping person are presented, including the thermal neutrality for a naked sleeping person and the effects of the total insulation value of a bedding system on the thermal neutrality of a sleeping person.

4.2 Numerical method

4.2.1 Development of a Sleeping Computational Thermal Manikin (SCTM)

For the numerical studies reported, it was necessary to develop a SCTM. The geometry of the SCTM developed was a real and accurate representation of a nude sleeping female person, obtained by using 3-D laser scanning technique (Fig. 4.1). Its total surface area was 1.535 m^2, which was slightly smaller than 1.594 m^2 as

suggested by Sørensen and Voigt [2003], and 1.688 m^2 as proposed by Murakami et al. [1997, 2000].

The SCTM was placed on a bed with mattress which was simplified to a cuboid, measuring at 1900 mm (W)×920 mm (D)×300 mm (H), respectively (also shown in Fig.4.1). The percentage coverage of the SCTM's surface area by bed with mattress was 21.7%, which was close to 23.3% as proposed by McCullough et al. [1987].

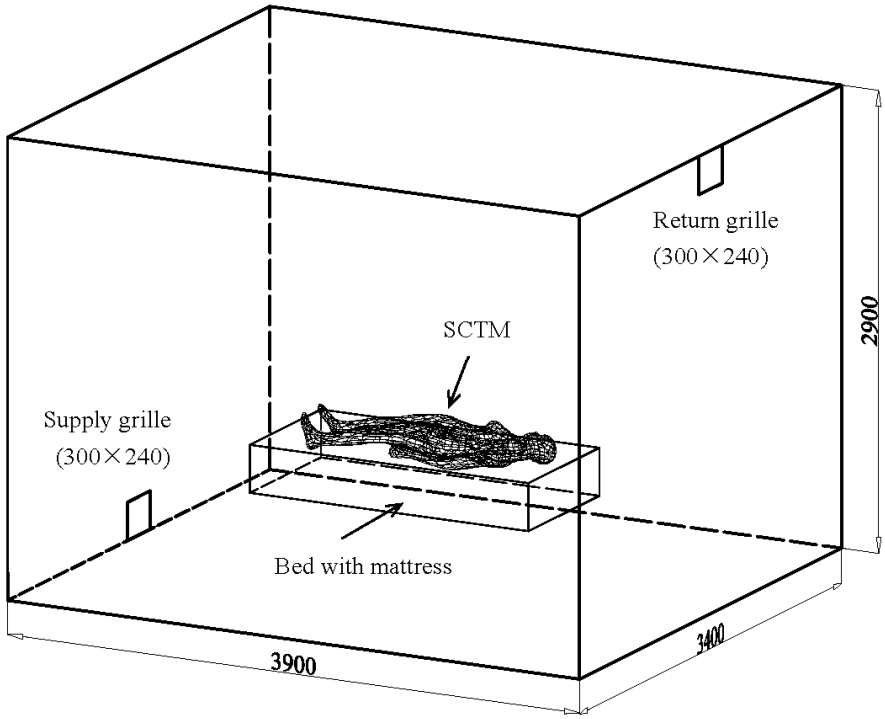

Fig. 4.1 The SCTM placed in a simulated space with a displacement ventilation system

4.2.2 Air-conditioned space with a displacement ventilation system

The above SCTM was placed in a simulated space installed with a displacement ventilation system (see Fig. 4.1), which was created by using a commercially available Computational Fluid Dynamics (CFD) software package. The origin of X-Y-Z axes for the simulated air conditioned space was at the centre point of the space. The detailed relative locations of the SCTM, the bed with mattress, supply and return grilles and the detailed dimensions of the simulated space are illustrated in Fig. 4.2 and Fig. 4.3. As seen from Fig. 4.1 to Fig. 4.3, conditioned air was supplied from the supply grille located at the centre-bottom on the left-hand side wall before travelling through the return grille located at the centre-top on the right-hand side wall. The above setting of the simulated space with a displacement ventilation system with both the SCTM and the bed with mattress placed inside made it possible to numerically study the micro-climate around the SCTM and to compare the numerical results with the experimental results previously obtained by others.

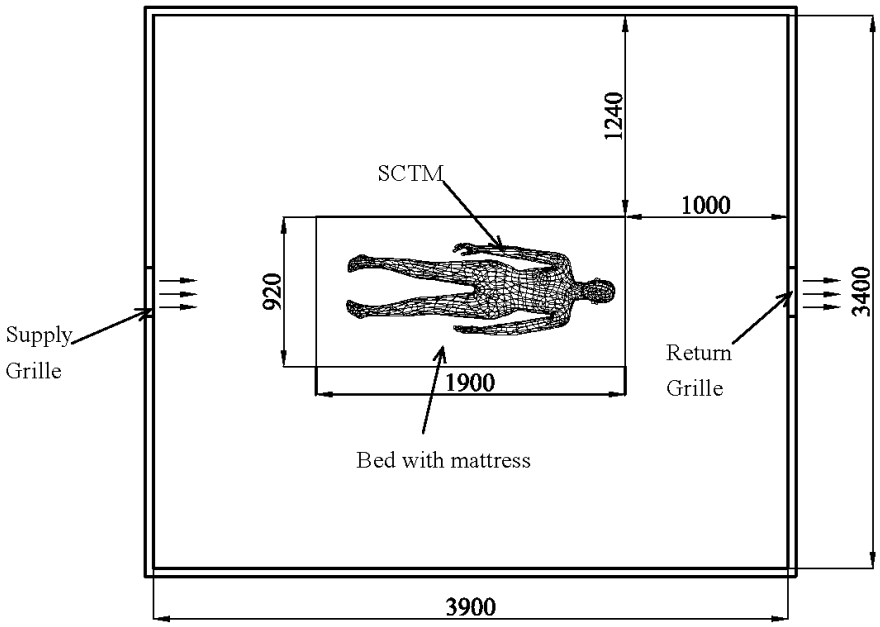

Fig. 4.2 Plan view of the simulated space with a displacement ventilation system

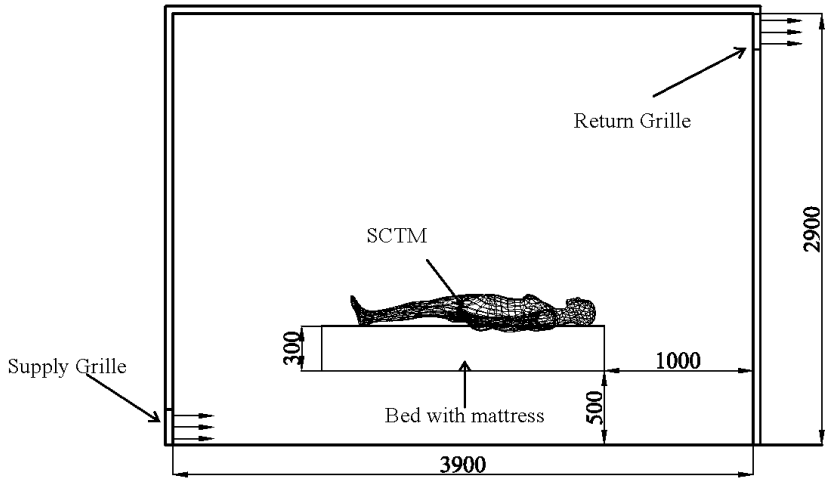

Fig. 4.3 Evaluation view of the simulated space with a displacement ventilation system

4.2.3 Grid generation for carrying out the numerical study

Given that the objective of the study was to examine the micro-climate around a sleeping person, the grid generated around the SCTM to be used in this numerical study was therefore carefully selected. The simulated space was divided into two parts (see Fig. 4.4): Part A enclosing the SCTM, and Part B for the remaining simulated space. For Part A, two boundary layers were first created around the SCTM to accurately simulate the viscous boundary before it was discretised with unstructured and fine grids to capture the boundary wall features. Part B was fragmented into structured and coarse grids so as to save computational time. Fig. 4.4 shows the generated grid at x = 0 plane (according to Fig. 4.1). The total number of cells generated was 1, 425, 264. The near-wall grids close to the SCTM were located in the region of y^+ <1. A finer grid system with four boundary layers and a total of 1, 819, 463 cells was also tested for grid independence. The two grid systems yielded similar simulation results.

On the other hand, a bed with mattress used in this numerical study was regarded as being adiabatic, so that no heat would be lost from a sleeping person through the bed with mattress [McCullough et al. 1987].

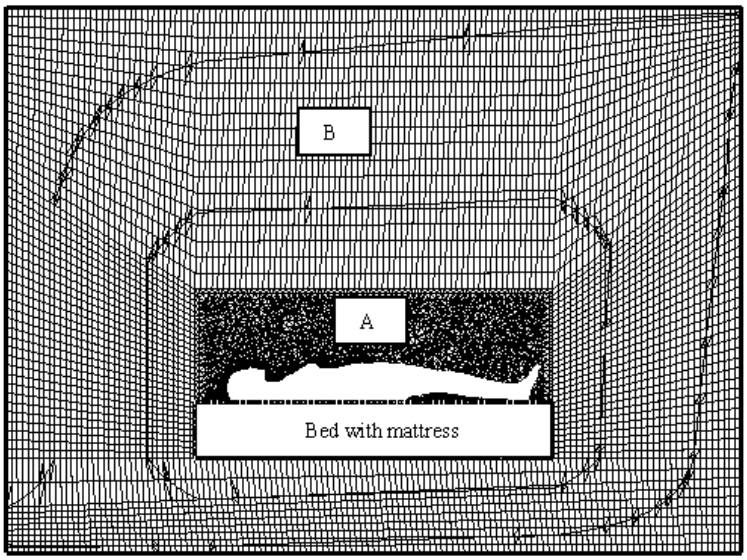

Fig. 4.4 The generated gird in the computational domain (at plane x=0)

4.2.4 Sub-models in the CFD software packages used

Various sub-models for evaluating the convective, radiative and conduction heat transfer were available in the CFD software package used. The Lauder-Sharma type Low-Reynolds-number k-ϵ sub-model [Lauder and Sharma 1974] was used for evaluating the turbulence flow within the simulated space. On the other hand, radiative heat transfer was calculated by using a surface-to-surface (S2S) radiation sub-model, which could account for the radiation exchange in an enclosure of gray-diffuse surfaces. Conduction heat transfer within a thin layer of solid material was evaluated by using a shell conduction sub-model.

4.2.5 Boundary conditions

Mean skin surface temperature, t_{sk}, was an important factor in influencing human's thermal sensation. The following linear regression equation, which was proposed as

a condition for optimal thermal comfort by Fanger [1970] was used to evaluate the value of t_{sk}:

$$t_{sk} = 35.7 - 0.0275(M - W) \tag{4.1}$$

In the state of thermal neutrality for a sleeping person whose activity level was lower than that of a seated person:

$$M = 40 \tag{4.2}$$

$$W = 0 \tag{4.3}$$

Its mean skin temperature would therefore be:

$$t_{sk} = 34.6 \tag{4.4}$$

Therefore, the skin temperature of the SCTM was set at a fixed value of 34.6°C, to represent a state of thermal neutrality of a sleeping person.

The turbulence intensity, I, and hydraulic diameter, D, for supply grilles were 5% and 0.27 m, respectively. Return grilles were pressure outlets.

When calculating radiative heat transfer, the emissivities for both the SCTM and the room walls, ε_{sk} and ε_{wall}, were set at 0.98 and 0.95, respectively [Murakami *et al*. 1997, 2000].

The total insulation value of a bedding system could play an important role in determining the thermal neutrality of a sleeping person [Lin and Deng 2008a] in

terms of the thermal resistance of a bedding, r_b, and the percentage coverage of body surface area by bedding and bed, A_C [McCullough et al. 1987, Lin and Deng 2008b, Pan et al. 2010].

A bedding material has a limited influence on the thermal resistance provided by the bedding. The thermal resistance of a bedding is mainly determined by its thickness, H_{fab}, rather than its weight per unit area [ISO 9920 2007]. Different beddings were simulated by adding a shell conduction sub-model, which could be used to evaluate the conduction heat transfer through a thin layer of solid material, such as a bedding, to the SCTM.

The thermal resistance of a bedding, r_b, can be evaluated by [Peirce and Rees 1946]:

$$r_b = 0.03984 \times H_{fab} \tag{4.5}$$

The thermal resistance of various beddings was simulated by setting the thickness of the shell in the shell conduction sub-model at a specific thermal conductivity. Table 4.1 shows the details of the three beddings [Lin and Deng 2008b].

Table 4.1 Measured thickness and evaluated thermal resistances of three beddings [Lin and Deng 2008b]

Bedding item	H_{fab} (mm)	r_b (m^2·K/W)
Blanket (B)	3.03	0.121
Summer Quilt 2 (Q2)	7.62	0.304
Summer Quilt 1 (Q1)	15.23	0.607

4.2.6 Simulated Study-cases in the numerical studies

Two related numerical studies were carried out and are reported in this Chapter. The first one was on the micro-climate around, and the other on the thermal neutrality of, a sleeping person in a space installed with a displacement ventilation system. The boundary conditions for SCTM, return grilles and walls, and the turbulence intensity and hydraulic diameter for supply grilles were the same for these two numerical studies, as given in Section 4.2.5. The results of the first numerical study are presented in Section 4.3 and those of the second one in Section 4.4, respectively.

In the first study, only one Study-case was investigated, while for the second study, twenty Study-cases were numerically examined, with their details explained in Table 4.2 and Table 4.3, respectively. In addition, the details of beddings used in the second study are given in Section 4.2.5.

Table 4.2 shows the details of 1-10 simulated Study-cases at a supply air velocity of 0.12 m/s, but at different supply air temperatures, bedding types and percentage coverages by bedding and bed. The purpose of Study-case 1 was to investigate the thermal neutrality of a naked sleeping person, and those of Study-cases 2 to 10 the effects of the total insulation value of a beddings system on the thermal neutrality of a sleeping person.

Table 4.2 Details of 1-10 simulated Study-cases at a supply air velocity of 0.12m/s

Study-case No.	Supply air temperature (°C)	SCTM covered by		Results shown in
		Bedding types	Coverage (%)	
1	20	None	21.7%	Fig. 4.9
	22	None	21.7%	
	24	None	21.7%	
	26	None	21.7%	
	28	None	21.7%	
2	14	B	100%	Fig. 4.11
	16	B	100%	
	18	B	100%	
	20	B	100%	
	22	B	100%	
3	4	Q2	100%	Fig. 4.11
	6	Q2	100%	
	8	Q2	100%	
	10	Q2	100%	
	12	Q2	100%	
4	6	Q1	100%	Fig. 4.11
	8	Q1	100%	
	10	Q1	100%	
	12	Q1	100%	
	14	Q1	100%	
5	14	B	79%	Fig. 4.11
	16	B	79%	
	18	B	79%	
	20	B	79%	
	22	B	79%	

Table 4.2 Details of 1-10 simulated Study-cases at a supply air velocity of 0.12m/s (Continued)

6	14	Q2	79%	Fig. 4.11
	16	Q2	79%	
	18	Q2	79%	
	20	Q2	79%	
	22	Q2	79%	
7	14	Q1	79%	Fig. 4.11
	16	Q1	79%	
	18	Q1	79%	
	20	Q1	79%	
	22	Q1	79%	
8	20	B	45%	Fig. 4.11
	22	B	45%	
	24	B	45%	
	26	B	45%	
	28	B	45%	
9	20	Q2	45%	Fig. 4.11
	22	Q2	45%	
	24	Q2	45%	
	26	Q2	45%	
	28	Q2	45%	
10	20	Q1	45%	Fig. 4.11
	22	Q1	45%	
	24	Q1	45%	
	26	Q1	45%	
	28	Q1	45%	

Table 4.3 shows the details of 11-20 simulated Study-cases at a supply air velocity of 0.24 m/s, but at different supply air temperature, bedding types and percentage coverage by bedding and bed. The purposes of Study-cases 11-20 were the same as those in Study-cases 1-10, but at a different supply air velocity.

Table 4.3 Details of 11-20 simulated Study-cases at a supply air velocity of 0.24m/s

Study-case No.	Supply air temperature (°C)	SCTM covered by		Results shown in
		Bedding types	Coverage (%)	
11	22	None	21.7%	Fig. 4.10
	24	None	21.7%	
	26	None	21.7%	
	28	None	21.7%	
	30	None	21.7%	
12	14	B	100%	Fig. 4.12
	16	B	100%	
	18	B	100%	
	20	B	100%	
	22	B	100%	
13	4	Q2	100%	Fig. 4.12
	6	Q2	100%	
	8	Q2	100%	
	10	Q2	100%	
	12	Q2	100%	
14	6	Q1	100%	Fig. 4.12
	8	Q1	100%	
	10	Q1	100%	
	12	Q1	100%	
	14	Q1	100%	
15	14	B	79%	Fig. 4.12
	16	B	79%	
	18	B	79%	
	20	B	79%	
	22	B	79%	
16	14	Q2	79%	Fig. 4.12
	16	Q2	79%	
	18	Q2	79%	
	20	Q2	79%	
	22	Q2	79%	
17	14	Q1	79%	Fig. 4.12
	16	Q1	79%	
	18	Q1	79%	
	20	Q1	79%	
	22	Q1	79%	

Table 4.3 Details of 11-20 simulated Study-cases at a supply air velocity of 0.24m/s (Continued)

18	20	B	45%	Fig. 4.12
	22	B	45%	
	24	B	45%	
	26	B	45%	
	28	B	45%	
19	20	Q2	45%	Fig. 4.12
	22	Q2	45%	
	24	Q2	45%	
	26	Q2	45%	
	28	Q2	45%	
20	20	Q1	45%	Fig. 4.12
	22	Q1	45%	
	24	Q1	45%	
	26	Q1	45%	
	28	Q1	45%	

4.3 Results of the first numerical study on the micro-climate around a naked SCTM placed in a space with a displacement ventilation system

In order to understand the micro-climate around a sleeping person, the first numerical study has been carried out, at a supply air temperature of 22°C and velocity of 0.12 m/s. Table 4.4 lists the detailed boundary conditions used in this study.

Table 4.4 Boundary conditions used in the first numerical study

Supply Grille	v=0.12 m/s; t_s=22 °C; I = 5 % ; D= 0.27m
Return Grille	Pressure outlet
SCTM	t_{sk}= 34.6°C, ε_{sk}=0.98
Room wall	Adiabatic wall , ε_{wall}=0.95

4.3.1 Simulated air flow field around the naked SCTM

Conditioned air was supplied at a supply velocity of 0.12 m/s from the supply grille located at the center-bottom on the left-hand side wall, and returned from the return grille located at the center-top on the right-hand side wall. The simulated velocity field and the velocity vector at the x=0 plane are shown in Fig. 4.5 and Fig. 4.6, respectively. It can be seen from Fig. 4.5 that the air flow field away from the SCTM was almost stagnant; however, a blanket of rising warm air stream was formed right above the SCTM due to buoyancy effect. On the other hand, it can be seen from Fig.4. 6 that the velocity vectors above the SCTM were similar to those above a hot plane cooled by cold air, and the air at the two ends of the SCTM flew towards the centre [Holman 2010]. The rising warm air stream above the SCTM reached a maximum velocity of 0.22 m/s, which agreed with the previous simulated result of 0.25 m/s [Gao et al. 2004].

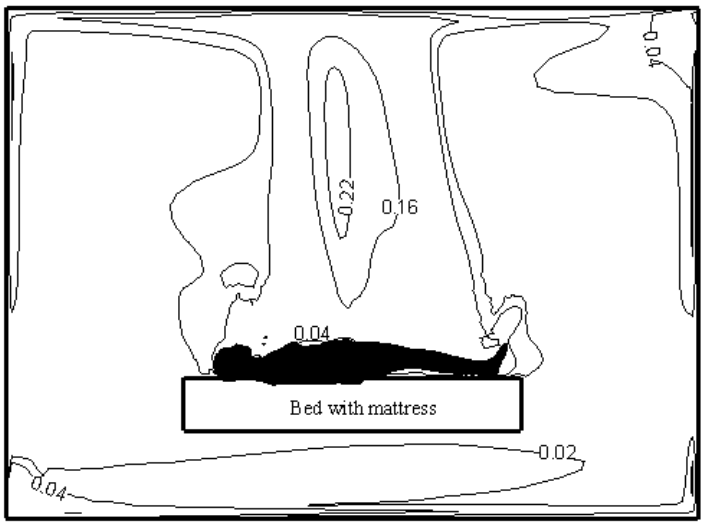

Fig. 4.5 Simulated air flow distribution around a naked SCTM, at x=0 plane

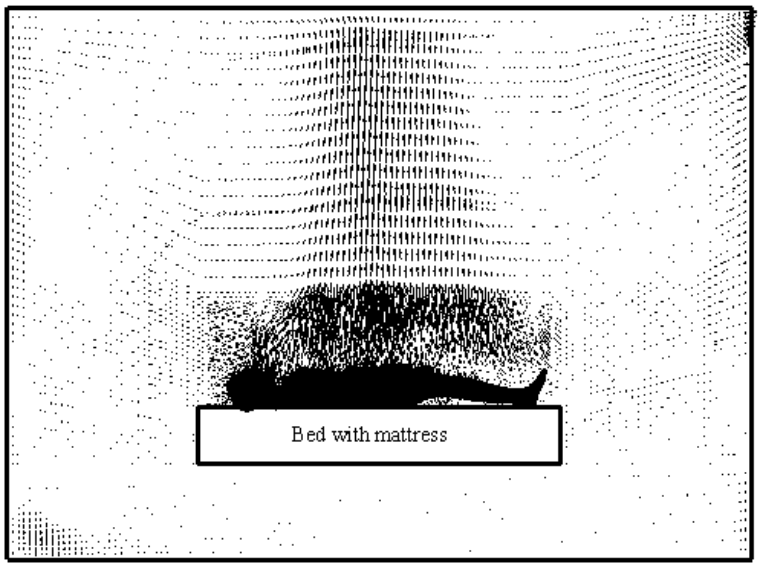

Fig. 4.6 Simulated velocity vectors around a naked SCTM, at x=0 plane

4.3.2 Simulated air temperature distribution around the naked SCTM

Fig. 4.7 and Fig. 4.8 show the simulated air temperature distributions around the naked SCTM at x=0 plane and y=0 plane, respectively. It can be seen that the displacement ventilation was in place, a vertical air temperature gradient was formed and the air temperature difference between the floor level and the SCTM level was

approximately 2°C. The air temperature above the SCTM was at about 28.1°C and the simulated mean indoor air temperature was at 28.4°C. Furthermore, because of the symmetry of the y-plane, the air temperature distribution at y=0 plane was almost symmetrical.

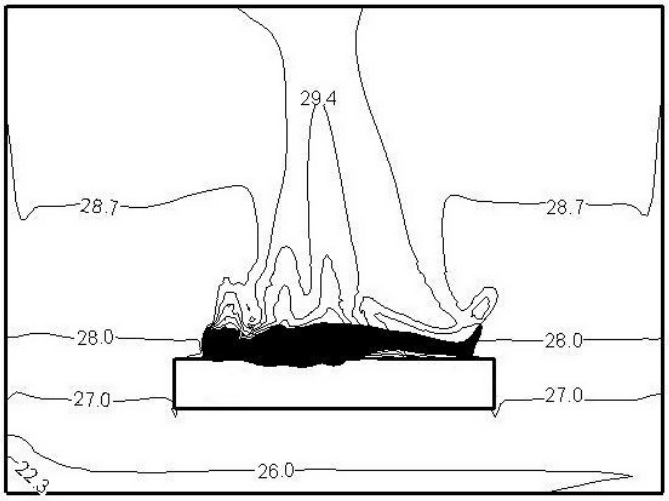

Fig. 4.7 Simulated air temperature distribution around the naked SCTM, at x=0 plane

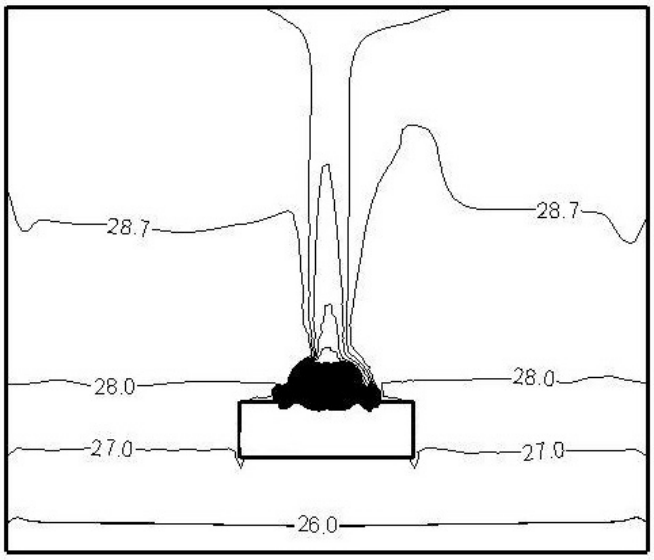

Fig. 4.8 Simulated air temperature distribution around the naked SCTM, at y=0 plane

4.3.3 Simulated mean internal surface temperatures

The simulated mean surface temperature of the floor was low at 27.5°C, whereas that of the ceiling was about 1°C higher at 28.4°C due to the use of displacement ventilation. Radiative heat transfer also took place among internal surfaces because the surfaces were at different temperatures. This led to the simulated mean temperatures on different internal surfaces becoming uniform.

The mean radiant temperature was evaluated by [ANSI/ASHRAE Standard 55-2004]:

$$t_r = \sum_{i=1}^{6} t_i F_{p \to i} \tag{4.6}$$

The angle factors from SCTM to internal surfaces, $F_{p \to i}$, were available as part of the outcome from the numerical study reported in this Section.

Therefore the mean radiant temperature was evaluated at:

$$t_r = 28.2 \tag{4.7}$$

4.3.4 Simulated heat transfer characteristics

The simulated heat transfer rates from the SCTM to indoor environment were 30.2W by convection, and 38.7W by radiation, or 44% by convection and 56% by radiation, respectively. This agreed reasonably well with the results in a previous numerical study [Gao et al. 2006], where the convective heat loss and the radiative heat loss

accounted for 40% and 60%, respectively, of the total heat loss from a CTM in a space with a displacement ventilation system. The present study further verified that radiative heat transfer could remarkably influence the thermal comfort of humans [ANSI/ASHRAE Standard 55-2004].

The convective heat transfer from an ordinary CTM to its surroundings can be affected by a number of factors, including body posture, the temperature difference between skin and its surrounding air, ΔT, air velocity near the CTM, etc. However, in this numerical study, the air flow around a SCTM induced by displacement ventilation was stagnant, as shown in Section 4.3.1, so that the convective heat transfer from a CTM was mainly determined by the natural convection induced by ΔT. Over the past few decades, a number of experimental and numerical studies were carried out to obtain and predict the mean convective heat transfer coefficient for a naked person in a stagnant air flow as summarized in Table 4.5. In this numerical study, the naked SCTM was placed in a space with a stagnant air flow and a ΔT of 6.5°C (34.6°C-28.1°C), and the mean convective heat transfer coefficient of the SCTM surface was evaluated at 3.03 W/(m^2·K), which agreed well with those from previous experimental and numerical results (Table 4.5). The findings were in particular in good agreement with the value of 3.3 W/(m^2·K) proposed by Winslow et al. [1939] for a reclining person in an air-conditioned room with a stagnant air flow.

Table 4.5 The mean convective heat transfer coefficients of a naked human body in stagnant air flow evaluated in previous related experimental and simulation studies

Item	Researchers	Posture	ΔT (°C)	h_c (W/(m^2·K))	Remarks
1	Gao et al. 2004	Sitting	9	4.95	S
2	Nishi and Gagge 1970	Sitting	2	3.1	E
3	Winslow et al. 1939	Sitting	9	4	E
4	de Dear et al. 1997	Sitting	12	3.3	E
5	Colin and Houdas 1967	Reclining	3.7	5.3	E
6	Winslow et al. 1939	Reclining	11±3	3.3	E
7	Murakami et al. 1997	Standing	5	3.9	S
8	de Dear et al. 1997	Standing	12	3.4	E
9	Nelson et al. 1947	Standing	14	4	E
10	Woodcock and Breckenridge 1965	Standing	4	4.3	E
11	Kurazumi et al. 2008	Standing	14	2.8	E

E: Experimental study; S: Simulation study

On the other hand, the mean radiative heat transfer coefficient of the SCTM was evaluated at 4.25W/(m^2·K). This was less than the value of 4.7W/(m^2·K), an estimated value for most typical indoor environment [ASHRAE Handbook 2009]. This may be caused by the differences in posture, temperature and emissivity of internal surface, etc.

In the first numerical study reported in this Section, the convective and radiative heat transfers from the naked SCTM, which dominantly determined human thermal comfort [Fanger 1970, ANSI/ASHRAE Standard 55-2004, ASHRAE Handbook 2009], can be predicted, and used in the second numerical study for studying both the thermal neutrality of a naked sleeping person and the impact of total insulation of a bedding system on thermal neutrality of a sleeping person, as reported in Section 4.4.

4.4 Results of the second numerical study on the thermal neutrality for a sleeping person

4.4.1 The definition of the thermal neutrality for a sleeping person

A primary condition for thermal comfort of a sleeping person is that thermal neutrality can be achieved during sleep. One requirement of maintaining a thermally neutral environment is by satisfying the following heat balance equation [Lin and Deng 2008a], as described in Equation (2.2) in Chapter 2.

In Equation (2.2), the value of $\frac{34.6 - t_o}{R_t}$ represented the rates of both convective and radiative heat transfers from the SCTM to its surroundings, which were obtained from the numerical study reported in Section 4.3. Because of the existence of the displacement ventilation, the air temperature distribution was not uniform and a vertical air temperature gradient was formed inside the simulated room, as described in Section 4.3.2. The mean air temperature, t_a, was represented by the mean air temperature in a designated space of 0.6 m high on top of the mattress bed, available from the numerical study. The water vapour partial pressure, P_a, was obtained after knowing t_a, under an assumed mean indoor air relative humidity of 50% , and the total insulation value of the bedding systems used for the SCTM, R_t, was obtained from a previous study by Lin and Deng [2008b].

The thermal load on the body, Q_{load}, was first defined as:

$$Q_{load} = 40 - (\frac{34.6 - t_o}{R_t} + \frac{0.3762(5.52 - P_a)}{R_t} + 0.056(34 - t_a) + 0.692(5.87 - P_a)) \quad (4.8)$$

When Q_{load} was equal to zero, Equation (4.8) would be satisfied and the thermal neutrality of a sleeping person could be achieved.

The operative temperature was calculated as an average of the mean indoor air temperature and mean radiant temperature when the difference between the two was small (< 4°C) [ANSI/ASHRAE Standard 55 2004]:

$$t_o = \frac{t_a + t_r}{2} \quad (4.9)$$

The simulated mean indoor air temperature, 28.1°C, was very close to the evaluated mean radiant temperature, 28.2°C, as reported in Sections 4.3.2 and 4.3.3. Hence, the operative temperature may be evaluated by:

$$t_o \approx t_a \quad (4.10)$$

Consequently, one may deduce that for a naked sleeping person, the thermal load on the body, Q_{load}, was mainly determined by the mean indoor air temperature, t_a.

When Q_{load} was equal to zero, the corresponding mean indoor air temperature was defined as the thermal neutral temperature.

4.4.2 The thermal neutrality for a naked sleeping person

In order to obtain the thermal neutral temperature for a naked sleeping person, in Study-case 1, at five different supply air temperatures (20°C to 28°C), but at a constant supply air velocity of 0.12 m/s, the thermal load on the body, Q_{load}, and the corresponding mean indoor air temperature, t_a, were each evaluated. A simulated relationship between the thermal load on the body, Q_{load}, and mean indoor air temperature, t_a, for a naked sleeping person was established, in a space with a displacement ventilation system and is shown in Fig. 4.9. It can be seen that t_a could significantly affect Q_{load}, with a positive correlation.

From Fig. 4.9, the thermal neutral temperature was estimated at 29.72°C. This agreed well with the thermal neutral temperature of 29.3°C obtained in an earlier study [Lin and Deng 2008a]. It should be noted that in a number of other studies [Haskell et al. 1981b, Macpherson 1973, Palca 1986, Dewasmes et al. 2000] as shown in Table 2.1 in Chapter 2, the thermal neutral temperatures were evaluated at between 28°C and 32°C and the thermal neutral temperature of 29.7°C obtained in this study was within this range.

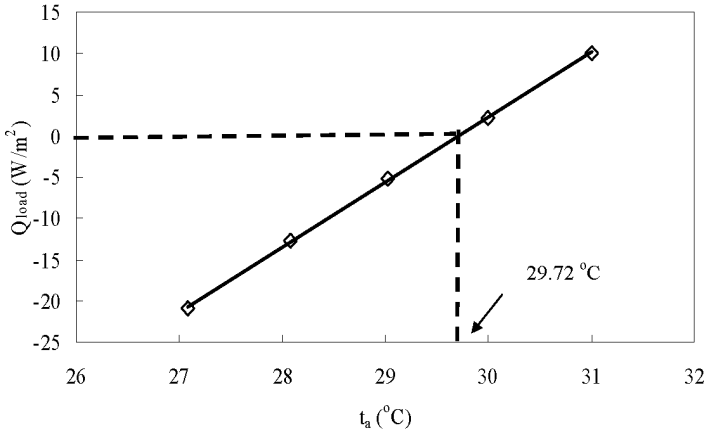

Fig. 4.9 The simulated relationship between thermal load on the body and mean indoor air temperature for a naked sleeping person at a supply air velocity of 0.12 m/s

Furthermore, in Study-case 11, at the five different supply air temperatures (22°C to 30°C), but at a different supply air velocity of 0.24 m/s, the thermal neutral temperature was estimated at 29.78°C, as shown in Fig. 4.10. This was very close to the thermal neutral temperature of 29.71°C obtained in Study-case 1, suggesting that the supply air velocity did not significantly affect the thermal neutral temperature when people were naked. This was possibly because when the supply air velocity was increased, the air velocity around the SCTM, which determined the convective heat transfer coefficient, did not increase significantly.

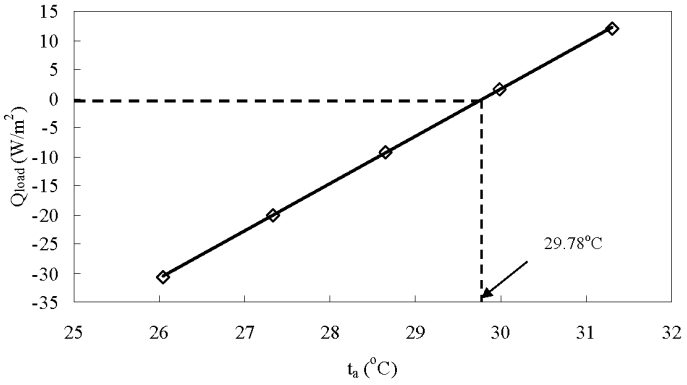

Fig. 4.10 The simulated relationship between thermal load on the body and mean indoor air temperature for a naked sleeping person at a supply air velocity of 0.24 m/s

4.4.3 Effects of total insulation value of a bedding system on the thermal neutrality of a sleeping person

In Study-cases 2 to 4, where the SCTM was covered with three different beddings at 100% A_C, at a supply air velocity of 0.12 m/s, the thermal neutral temperatures were numerically evaluated. The thermal neutral temperatures at the three different beddings, B, Q2, Q1 at 100% A_C, were 23.94°C, 15.5°C and 10°C, respectively, as shown in Fig. 4.11. The results agreed well with the values of 23°C, 15°C and 9.8°C reported in a previous study [Lin and Deng 2008a]. The findings show that the thermal resistance of a bedding could significantly affect the thermal neutral temperature of a sleeping person, i.e. the higher the thermal resistance of the bedding, the lower the thermal neutral temperature.

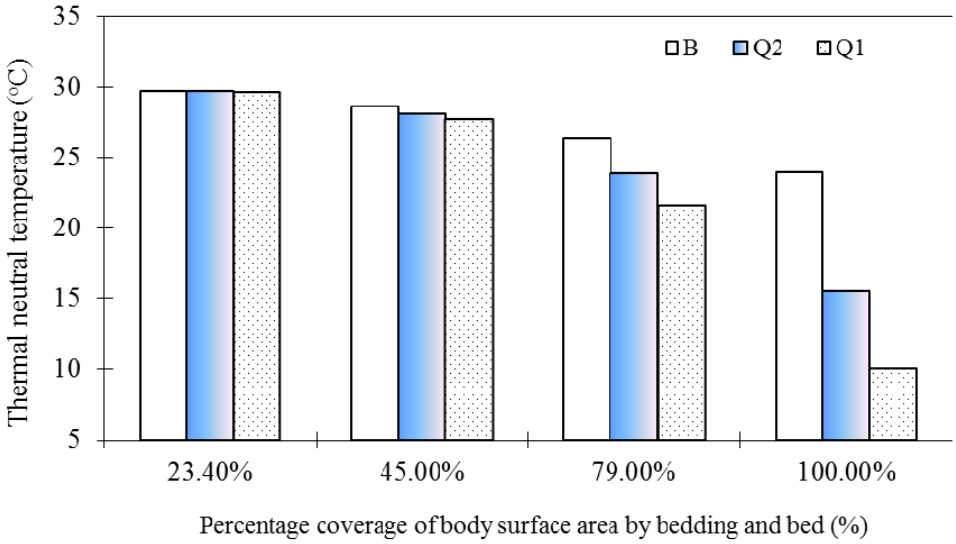

Fig. 4.11 The simulated relationship between the thermal neutral temperature and percentage coverage of body surface area by bedding and bed for the three different beddings at a supply air velocity of 0.12 m/s

In Study-cases 12 to 14, where the SCTM was covered with three different beddings at 100% A_C, but at a supply air velocity of 0.24 m/s, the thermal neutral temperatures were also numerically studied. The thermal neutral temperatures at the three different beddings, B, Q2, Q1 at 100% A_C, were 23.97°C, 15.8°C and 10.4°C, respectively, as shown in Fig. 4.12, which agreed with those at the supply air velocity of 0.12 m/s. It suggested that the supply air velocity did not significantly affect the thermal neutral temperature when people were covered with three different beddings at 100% A_C.

However, people seldom cover themselves completely with beddings and leave their heads exposed to air and the difference in A_C for the same bedding could result in different R_t. This would affect the thermal neutral temperature of a covered sleeping person. The thermal neutral temperatures in Study-cases 5 to 10, with different

values of A_C, at a supply air velocity of 0.12 m/s, were numerically studied. Fig. 4.11 shows the simulated relationship between the thermal neutral temperature and the percentage coverage of body surface area by bedding and bed, A_C, for the three different beddings at a supply air velocity of 0.12 m/s. Again it can be seen that A_C could remarkably affect the thermal neutral temperature, i.e. the higher the A_C, the lower the thermal neutral temperature. For a lightweight bedding, such as Blanket (B), the increase in A_C would lead to a smaller increase in thermal neutral temperature, when compared with that of a larger increase for heavyweight beddings, such as Quilt 1 (Q1) or Quilt 2 (Q2).

Furthermore, the thermal neutral temperatures in Study-cases 15 to 20, with different values of A_C, but at a supply air velocity of 0.24 m/s, were numerically studied. Fig. 4.12 shows the simulated relationship between the thermal neutral temperature and the percentage coverage of body surface area by bedding and bed, A_C, for the three different beddings at the supply air velocity of 0.24 m/s. The results further suggested that the supply air velocity did not also affect the thermal neutral temperature when people were covered with beddings.

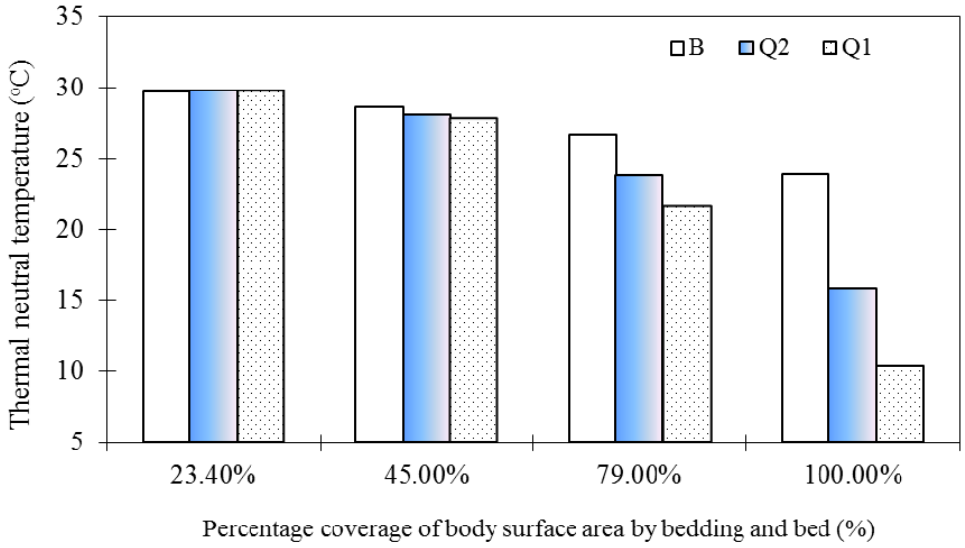

Fig. 4.12 The simulated relationship between the thermal neutral temperature and percentage coverage of body surface area by bedding and bed for the three different beddings at a supply air velocity of 0.24 m/s

4.5 Conclusions

Two numerical studies on the micro-climate around, and the thermal neutrality of a sleeping person a sleeping person placed in a space with a displacement ventilation system have been carried out and are reported in this Chapter. A sleeping computational thermal manikin (SCTM) was successfully developed and used in the two numerical studies. In the first numerical study, the micro-climate around the SCTM was, in terms of air temperature and velocity distributions and the heat transfer characteristics, numerically examined. The results of this numerical study were validated by comparing the simulated results with those obtained from previous related studies.

In the second numerical study, the thermal neutrality for a naked sleeping person was investigated and the effects of the total insulation value of a bedding system on the thermal neutrality of a sleeping person placed in a space with a displacement ventilation system were also examined. The results of the second numerical study obtained were in good agreement with those from earlier related studies.

Chapter 5

A four-node thermoregulation model for predicting the thermal physiological responses of a sleeping person

5.1 Introduction

Previous medical research results have demonstrated that when the thermal environment in a bedroom deviated greatly from the so-called ‘thermal comfort zone’, there were a remarkable increase in numbers and duration of wakefulness and a decrease in Rapid Eye Moment (REM) stage [Haskell et al. 1981a, Muzet 1984, Okamoto-Mizuno et al. 1999]. Although thermoregulatory responses were present across different sleep stages, they would be partly depressed in REM stage [Henane et al. 1977, Haskell et al. 1981b, Palca 1986, Sagot et al. 1987, Parmeggiani 2003]. Hence, an increase in wakefulness and a decrease in REM stage reflected a thermoregulatory need, and suggested that there was a competition between sleep maintenance and thermoregulation [Sakaguchi et al. 1979, Parmeggiani 2003]. Therefore, sleep quality became disturbed or even deteriorated as soon as the thermoregulatory responses were present. Consequently, it was necessary to investigate the thermoregulatory responses of a sleeping person in order to improve sleep quality.

A human being’s thermoregulation is very complicated due to numerous variables

involved in many control loops [Hensel 1973]. Using a thermoregulation model to predict human thermal physiological responses is a very useful tool in investigating the thermoregulation capability of a human body. Therefore, a large number of models for thermoregulation have been developed [Crosbie et al. 1961, Wissler 1964, Gagge et al. 1971, Stolwijk 1980, Smith 1991, Fu 1995, Fiala 1998, Huizenga et al. 2001, Tanabe et al. 2002].

However, as presented in Chapter 2, all thermoregulation models developed were for a person who was awake. For a sleeping person, his/her thermoregulatory process can be different from that of a waking person because of a number of reasons. Firstly, a large part of the body surface of a sleeping person was in touch with mattress [McCullough et al. 1987, Lin and Deng 2008b]. Secondly, the total insulation value of a bedding system was different from that of clothing and would play an important role in people's thermal sensation [Lin and Deng 2008a, Pan et al. 2010]. Thirdly, the set points for skin temperature and core temperature were different [Glotzbach and Heller 1976, Obal 1984, Lin and Deng 2008a]. Lastly, thermoregulatory responses of a sleeping person were sleep-stage dependent [Obal 1984, Parmeggiani 2003]. Therefore, thermoregulation models previously developed should be modified in order to predict thermal physiological responses of a sleeping person.

This Chapter reports on a study of developing a four-node thermoregulation model for predicting thermal physiological responses of a sleeping person, based on the

existing Gagge's two-node model. Firstly, the Gagge's two-node model is introduced in detail. This is followed by reporting the necessary modifications to Gagge's two-node model for developing the four-node thermoregulation model for a sleeping person. Thirdly, the four-node thermoregulation model is presented in detail. Lastly, the validation of the four-node thermoregulation model by comparing the predicted thermal physiological responses, including skin and core temperatures, using the model developed with the experimental data previously obtained by others is presented.

5.2 Development of a four-node thermoregulation model

5.2.1 Gagge's two-node model

The Gagge's two-node model has been widely used due to its simplicity, as compared to other complex models. Since the focus of the current study was to predict the thermal physiological responses of a sleeping person, not the complex heat transfers inside a human body, the Gagge's two-node model could be adequately used to simplify the model development without losing the sufficient representation of the actual heat and mass transfer between a sleeping person and his/her surrounding environment. Therefore, the four-node thermoregulation model reported in this Chapter was based on the Gagge's two-node model by incorporating necessary modifications appropriate for a sleeping person. While the Gagge's

two-node model is briefly introduced in Chapter 2, the mathematical equations to represent the Gagge's two-node model are reproduced in this Chapter.

The Gagge's two-node model [Gagge et al. 1971, Gagge 1973] was a lumped parameter model dividing a human body into two concentric layers (as shown in Fig. 5.1), an outer skin layer and a core layer representing internal organs, bone, muscle and subcutaneous tissue. It included two systems: one controlled system and the other controlling system.

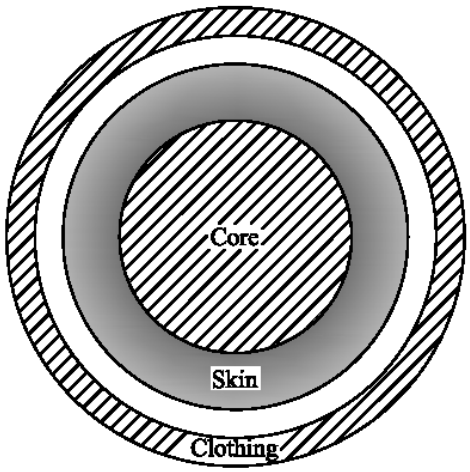

Fig. 5.1 Schematic diagram of the Gagge's two-node model [Gagge 1973]

5.2.1.1 Controlled system

The controlled system described the heat balances inside a human body and that between a human body and its surroundings. Heat was transferred between core layer and skin layer by virtue of conduction and mass transfer. A human body and its

surroundings exchanged heat by radiation, convection, evaporation and conduction. The mathematical equations for these heat transfer processes were as follows [Gagge et al. 1971, Gagge 1973].

The heat storage equations for core and skin layers, respectively, were:

$$S_{cr} = (M - W - Q_{res}) - Q_{cr-sk} = \frac{(1-\xi)mC_{p,b}}{A_D}\frac{dT_{cr}}{dt} \tag{5.1}$$

$$S_{sk} = Q_{cr-sk} - E_{sk} - (Q_c + Q_r) = \frac{\xi mC_{p,b}}{A_D}\frac{dT_{sk}}{dt} \tag{5.2}$$

In these two equations, the nude body surface area was evaluated by Dubois Formula [DuBois and DuBois 1916],

$$A_D = 0.202m^{0.425}l^{0.725} \tag{5.3}$$

The heat loss through respiration, Q_{res}, was evaluated by,

$$Q_{res} = 0.0014M(34 - t_a) + 0.0173M(5.87 - P_a) \tag{5.4}$$

The total sensible heat loss from skin, $Q_c + Q_r$,was evaluated by,

$$Q_c + Q_r = \frac{T_{sk} - T_{cl}}{R_{cl}} \tag{5.5}$$

and the evaporative heat loss from skin, E_{sk}, was calculated by,

$$E_{sk} = wE_{\max} \tag{5.6}$$

$$E_{\max} = \frac{P_{sk,a} - P_a}{R_{e,t}} \tag{5.7}$$

5.2.1.2 Controlling system

The controlling system in Gagge's two-node model described closed loop control processes (as shown in Fig. 5.2), and was further divided into two parts.

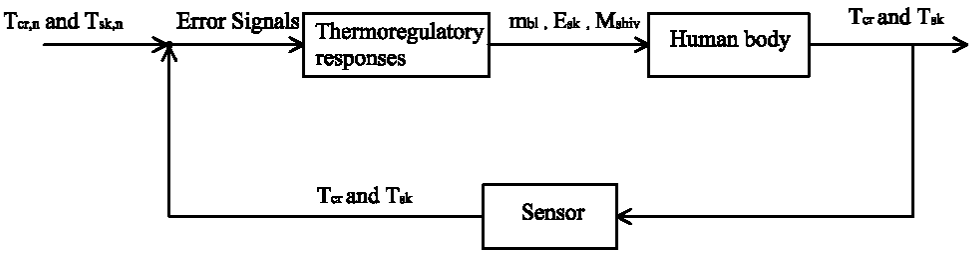

Fig. 5.2 Control processes in Gagge's two-node model

In the first part where the thermal states of the controlled system were recognized, the error signals were the temperature differences between the actual temperatures in two layers, T_{cr} or T_{sk}, and their set points, $T_{cr,n}$ or $T_{sk,n}$. Therefore, the warm and

cold signals from the core and skin layers were evaluated by the following equations [Gagge et al. 1971, Gagge 1973]:

$$WSIG_{cr} = \max((T_{cr} - T_{cr,n}),0) \tag{5.8}$$

$$CSIG_{cr} = \max((T_{cr,n} - T_{cr}),0) \tag{5.9}$$

$$WSIG_{sk} = \max((T_{sk} - T_{sk,n}),0) \tag{5.10}$$

$$CSIG_{sk} = \max((T_{sk,n} - T_{sk}),0) \tag{5.11}$$

The warm and cold signals from body temperature integrating the core and skin temperatures were evaluated by:

$$WSIG_{b} = \max((T_{b} - T_{b,n}),0) \tag{5.12}$$

$$CSIG_{b} = \max((T_{b,n} - T_{b}),0) \tag{5.13}$$

where,

$$T_{b} = \xi T_{sk} + (1-\xi)T_{cr} \tag{5.14}$$

$$T_{b,n} = \xi_{n} T_{sk,n} + (1-\xi_{n})T_{cr,n} \tag{5.15}$$

In the second part, based on the warm or cold signals, the thermoregulatory responses of the controlling system, such as vasomotion, sweating and shivering, were determined, respectively. The control equations for these thermoregulatory

responses were expressed as follows.

Vasomotion consisted of vasoconstriction and vasodilatation to regulate the rate of blood flow, m_{bl}, and also the fraction of body mass of the skin layer, ζ, which were, respectively, determined by,

$$m_{bl} = \frac{(6.3 + 200WSIG_{cr})}{(1 + 0.5CSIG_{sk})3600} \tag{5.16}$$

$$\xi = 0.042 + \frac{0.745}{3600m_{bl} + 0.585} \tag{5.17}$$

Therefore, the heat transfer between the core and skin layers was determined by:

$$Q_{cr-sk} = (K + C_{p,bl}m_{bl})(T_{cr} - T_{sk}) \tag{5.18}$$

Sweating resulted in an increase in evaporative heat loss from skin through modifying the regulatory sweating rate,

$$m_{rsw} = 4.72 \times 10^{-5} WSIG_b \exp(WSIG_{sk}/10.7) \tag{5.19}$$

and,

$$w = w_{rsw} + 0.06(1 - w_{rsw}) \tag{5.20}$$

$$w_{rsw} = 0.06 + 0.94\frac{E_{rsw}}{E_{\max}} \tag{5.21}$$

where,

$$E_{rsw} = m_{rsw} h_{fg} \tag{5.22}$$

Shivering which generated additional metabolic heat under a cold environment was evaluated by:

$$M_{shiv} = 19.4 CSIG_{sk} CSIG_{cr} \tag{5.23}$$

5.2.2 Modifications to the Gagge's two-node model

Considering the differences between the thermoregulatory responses of a sleeping person and that of a waking person, the following necessary modifications to the Gagge's two-node model were made.

5.2.2.1 Modifications to the skin layer

For sleeping environments, a bedding system included beddings and a mattress, and a large part of the body surface of a sleeping person was in direct contact with the mattress. Moreover, according to a previous study [Lin and Deng 2006], most people would not like to be covered by beddings completely. Therefore, for sleeping applications, a human body may be divided into four parts: core, naked skin, covered skin and skin in touch with mattress (as shown in Fig. 5.3). As compared to Gagge's two-node model, the outer skin layer in Gagge's two-node model was further divided into three different parts, to truly reflect the relationship between a sleeping person

and his/her environment during sleep. Each part was represented by a node, with the subscripts ’1’, ‘2’ and ‘3’ to denote the node for naked skin, the node for covered skin and the node for the skin in touch with mattress, respectively. In addition, Fig. 5.3b shows the heat transfer both between the core part and the three different skin parts and between the three different skin parts and the surrounding environments, as shown in Fig. 5.3a. Therefore, the resultant modifications due to dividing the outer skin layer to three different parts were as follows:

1) For the controlled system, the heat transfer processes related to the out skin layer would be modified, accordingly. Firstly, Equations (5.1) and (5.2) shown in Section 5.2.1.1 were modified to Equations (5.24) and (5.25), respectively, to be shown in Section 5.2.3.1. Secondly, since a bedding system rather than clothing was present in a sleeping environment, the intrinsic clothing resistance, R_{cl}, in Equation (5.5), cannot be determined because the clothing area factor, f_{cl}, was meaningless when a person was lying on a bed [Lin and Deng 2008a]. Equation (5.5) shown in Section 5.2.1.1 should be re-written to become three equations, with R_1, R_2 and R_3, to represent the thermal resistances associated with the three parts, respectively [Pan et al. 2010]. Consequently, Equations (5.5) to (5.7) shown in Section 5.2.1.1 were modified to Equations (5.28), (5.32) and (5.33), respectively, to be shown in Section 5.2.3.1.

2) For the controlling system, the control processes related to the out skin layer

would be modified, accordingly. Firstly, corresponding changes in the warm or cold signal from the original skin layer had to be made. Therefore, Equations (5.10) and (5.11) shown in Section 5.2.1.2 were modified to Equations (5.35) and (5.36), respectively, to be shown in Section 5.2.3.2. Secondly, corresponding changes in three thermoregulatory responses, including vasomotion, sweating and shivering, related to the original skin layer had also to be made. Therefore, Equations (5.19) and (5.23) shown in Section 5.2.1.2 were modified to Equations (5.45) and (5.46), (5.51) and (5.52), respectively, to be shown in Section 5.2.3.2.

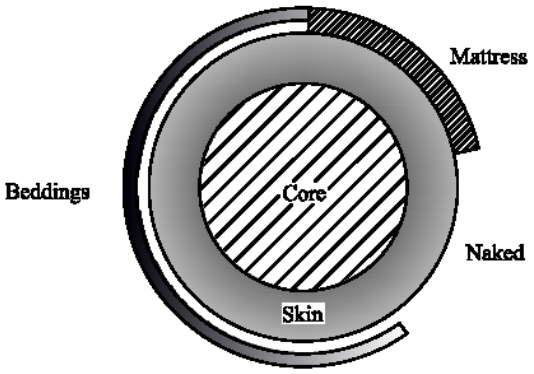

(a) The four-node thermoregulation model

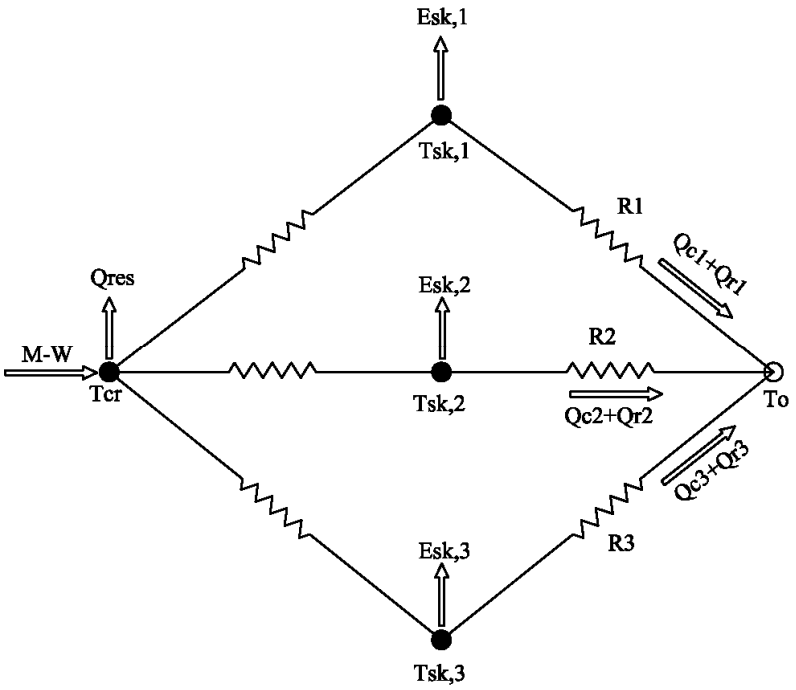

(b) Thermal resistance network

Fig. 5.3 Schematic diagrams of the four-node thermoregulation model for sleeping applications

5.2.2.2 Modifications to the set points for skin and core temperatures

The set point temperatures for the three skin parts, $T_{sk,n,i}$ (i=1-3), were all at 34.6^{o}C [Haskell et al. 1981b, Okamoto-Mizuno et al. 1999, Lin and Deng 2008a]. However, for the core temperature, previous experimental results suggested that its set point temperature, $T_{cr,n}$, was varied with the time but can be adjusted to a lower level during sleep than at daytime [Hammel et al. 1963, Glozbach et al. 1976, Obal 1984]. This is expressed in Equation (5.41) in Section 5.2.3.2.

5.2.2.3 Modifications to three different thermoregulatory responses

In the Gagge's two-node model, the control equation for each thermoregulatory response remained unchanged for an awaking person. However, sleep was divided into two distinct stages: Non Rapid Eye Movement (NREM) stage and Rapid Eye Movement (REM) stage [Hobson 1989]. NREM stage and REM stage appeared alternatively throughout a night. Previous experimental results showed that the thermoregulatory response of a sleeping person was different between NREM stage and REM stage [Glozbach et al. 1976, Henane et al. 1977, Haskell et al. 1981b, Obal 1984, Palca et al. 1986, Sagot et al. 1987, Parmeggiani 2003]. The major difference resulted from the change in the control gain, which controlled the magnitude of the outputs of thermoregulatory responses to error signals, and the basic form of control equations in Gagge's two-node model were retained. Therefore, each of three

different thermoregulatory responses in Gagge's two-node model would be modified and divided into two equations in terms of two sleep stages, respectively. Consequently, Equations (5.16), (5.19) and (5.23) shown in Section 5.2.1.2 were modified to Equations (5.40) and (5.41), (5.44) and (5.45), (5.50) and (5.51), respectively, to be shown in Section 5.2.3.2.

5.2.3 The four-node thermoregulation model for a sleeping person

According to the modifications described in Section 5.2.2, a four-node thermoregulation model for a sleeping person was developed. Similarly, it consisted of two systems: a controlled system and a controlling system. Model equations for these two systems are individually presented in this section.

5.2.3.1 The controlled system

Fig. 5.3 shows the schematic diagrams of the four-node thermoregulation model developed and its thermal resistance network.

The heat storage equations for both the core and the other three skin parts of a sleeping person, respectively, were:

$$S_{cr} = (M - W - Q_{res}) - \sum_{i=1}^{3} \alpha_i Q_{cr-sk,i} = \frac{(1-\xi) m C_{p,b}}{A_D} \frac{dT_{cr}}{dt} \qquad i = 1\text{-}3 \quad (5.24)$$

$$S_{sk,i} = Q_{cr-sk,i} - E_{sk,i} - (Q_{c,i} + Q_{r,i}) = \frac{\xi \mu_i m C_{p,b}}{A_D} \frac{dT_{sk,i}}{dt} \qquad i = 1\text{-}3 \quad (5.25)$$

where,

$$\alpha_i = \frac{A_i}{A_D} \qquad i = 1\text{-}3 \quad (5.26)$$

$$\mu_i = \frac{m_i}{m_{sk}} \qquad i = 1\text{-}3 \quad (5.27)$$

According to an earlier model for predicting the total insulation value of a bedding system [Pan et al. 2010], the total sensible heat losses from naked skin, covered skin and the skin in touch with mattress were respectively evaluated by:

$$Q_{c,i} + Q_{r,i} = \frac{T_{sk,i} - T_o}{R_i} \qquad i = 1\text{-}3 \quad (5.28)$$

where,

$$R_1 = \frac{1}{h_c + h_r} \quad (5.29)$$

$$R_2 = \frac{\frac{3}{5}}{\left(\left(0.03984 \times H_{fab}\right) + \frac{1}{h_c + h_r}\right)} + \frac{2}{5} \times h_c \times \left[\frac{\left(\frac{2}{\left(0.03984 \times H_{fab}\right) + \frac{1}{h_c + h_r}} + \frac{\sqrt{3}}{r_m} \right)}{\frac{2}{\left(0.03984 \times H_{fab}\right) + \frac{1}{h_c + h_r}} + \frac{\sqrt{3}}{r_m} + h_c} \right] \tag{5.30}$$

$$R_3 = r_m \tag{5.31}$$

Similarly, the evaporative heat losses from the three skin parts were respectively evaluated by:

$$E_{sk,i} = w_i E_{\max,i} \qquad i = 1\text{-}3 \tag{5.32}$$

$$E_{\max,i} = \frac{P_{sk,a,i} - P_a}{R_{e,i}} \qquad i = 1\text{-}3 \tag{5.33}$$

where,

$$i_m L_R = \frac{R_i}{R_{e,i}} \qquad i = 1\text{-}3 \tag{5.34}$$

Lastly, to predict the heat loss through respiration, in the four-node thermoregulation model, Equation (5.4) in Gagge's two-node model was retained.

5.2.3.2 The controlling system

The warm and cold signals from the three skin parts of a sleeping person were defined as:

$$WSIG_{sk,i} = \max(0, (T_{sk,i} - T_{sk,n,i})) \qquad i = 1\text{-}3 \tag{5.35}$$

$$CSIG_{sk,i} = \max(0, (T_{sk,n,i} - T_{sk,i})) \qquad i = 1\text{-}3 \tag{5.36}$$

The warm and cold signals from the averaged skin temperature were evaluated by:

$$WSIG_{sk,av} = \max(0, (T_{sk,av} - T_{sk,n})) \tag{5.37}$$

$$CSIG_{sk,av} = \max(0, (T_{sk,n} - T_{sk,av})) \tag{5.38}$$

where,

$$T_{sk,av} = \sum_{i=1}^{3} \alpha_i T_{sk,i} \tag{5.39}$$

The warm and cold signals from the core part of a sleeping person were evaluated by Equations (5.8) and (5.9) of Gagge's two-node model.

The warm and cold signals integrating the core and skin temperatures were assessed by Equations (5.12) and (5.13) of Gagge's two-node model. However, in these two equations, T_b was defined by:

$$T_b = \xi T_{sk,av} + (1 - \xi) T_{cr} \tag{5.40}$$

The set point of the core temperature, $T_{cr,n}$, was evaluated by [Kreider et al. 1958],

$$T_{cr,n} = 0.022234 \times (\frac{t}{3600})^2 - 0.27677 \times \frac{t}{3600} + 37.02 \quad (5.41)$$

Different thermoregulatory responses, including vasomotion, sweating and shivering, were respectively described for the two sleep stages, i.e., NREM stage and REM stage.

Vasomotion persisted during NREM stages [Haskell et al. 1981b, Candas et al. 1982]. However, there was a decrease in its control gain during NERM stages with respect to wakefulness. During NREM stages, the rate of blood flow from the core part to the skin part was evaluated by:

$$m_{bl,NREM} = \frac{6.3 + 200 \times 0.5 \times WSIG_{cr}}{3600(1 + 0.5 \times 0.5 \times CSIG_{sk,av})} \quad (5.42)$$

Vasodilatation persisted and vasoconstriction inhibited in REM stages [Haskell et al. 1981b, Candas et al. 1982], where the rate of blood flow from the core part to skin part was evaluated by:

$$m_{bl,REM} = \frac{6.3 + 200 \times 0.2 \times WSIG_{cr}}{3600} \quad (5.43)$$

The fraction of body mass of the total for the three skin parts, ζ, was determined by

Equation (5.17) of Gagge's two-node body.

Therefore, the heat transfers between the core layer and the three skin parts were determined by:

$$Q_{cr-sk,i} = (K + C_{p,bl} m_{bl})(T_{cr} - T_{sk,i}) \qquad i = 1\text{-}3 \tag{5.44}$$

When exposed to heat, sweating persisted in NREM stages [Henane et al. 1977, Sagot et al. 1987]. However, there was a decrease in its control gain during NREM stages with respect to wakefulness. Therefore, during NREM stages, the regulatory sweating rates for the three skin parts were predicted by:

$$m_{rsw,NREM,i} = 0.7 \times 4.72 \times 10^{-5} WSIG_b \exp(WSIG_{sk,i}/10.7) \qquad i = 1\text{-}3 \tag{5.45}$$

During REM stages, sweating was still present, but was of a lower control gain than that during NREM stages [Ogawa et al. 1967, Takagi 1970, Shapiro et al. 1974, Henane et al. 1977, Sagot et al. 1987]. The regulatory sweating rates for the three skin parts were predicted by:

$$m_{rsw,REM,i} = 0.2 \times 4.72 \times 10^{-5} WSIG_b \exp(WSIG_{sk,i}/10.7) \qquad i = 1\text{-}3 \tag{5.46}$$

Moreover, when water vapor partial pressure of air, P_a , was low, all the secreted sweat would be evaporated. When P_a was high, the percentage of wetted skin surface was increased and eventually 0-10% of the sweat, to be evaporated, would drip. Therefore the sweating evaporative efficiency decreased [Candas et al. 1979a, 1979b], and the decrease was related to skin wittedness and may be evaluated by [Candas et al. 1979b]:

$$\eta = \begin{cases} 1, & w \le 0.4 \\ -0.8w^2 + 0.42w + 0.93, & w > 0.4 \end{cases} \tag{5.47}$$

Therefore,

$$E_{rsw,i} = \eta_i m_{rsw,i} h_{fg} \qquad i = 1\text{-}3 \tag{5.48}$$

$$w_i = w_{rsw,i} + 0.06(1 - w_{rsw,i}) \qquad i = 1\text{-}3 \tag{5.49}$$

$$w_{rsw,i} = 0.06 + 0.94 \frac{E_{rsw,i}}{E_{\max,i}} \qquad i = 1\text{-}3 \tag{5.50}$$

When exposed to cold, shivering was generally found to be significantly lower in NREM stages than in wakefulness, and inhibited in REM stages [Kreider et al. 1958, Haskell et al. 1981b, Candas et al. 1982]. Therefore, shivering in the three skin parts of a sleeping person in NREM stages and in REM stages were repectively predicted by:

$$M_{shiv,NREM,i} = 0.5 \times 19.4 CSIG_{sk,i} CSIG_{cr} \qquad i = 1\text{-}3 \tag{5.51}$$

$$M_{shiv,REM,i} = 0 \qquad i = 1\text{-}3 \tag{5.52}$$

Moreover, a great difference was noted between cold and heat thermal loads: a mild cold thermal load may be experienced as an uncomfortable sensation, while a heat thermal load enough to activate sweating may result in a pleasant or comfortable feeling [Benzinger 1969]. When exposed to cold, NREM and REM stages decreased significantly and wakefulness increased [Haskell et al. 1981b]. When the core temperature was lower than 35.8^{o}C, a sleeping person would be awakened to maintain human body heat balance [Haskell et al. 1981a]. Compared with cold thermal load, a sleeping person would not be significantly affected under the influence of moderate heat load [Haskell et al. 1981a]. However, at an extreme heat induration, for example, when indoor air temperature and humidity rose to unbearable high levels, both NREM and REM stages were reduced, and wakefulness increased [Haskell et al. 1981a, Okamoto-Mizuno et al. 1999].

It should be noted that the four-node thermoregulation model developed can be used to predict the thermoregulatory behaviors of an adult only, since the thermoregulatory responses of an infant was different from that of an adult [Bach et al. 2002] and the sleep distribution of an aged was also different from that of an adult [Dijk et al. 2000].

5.3 Model validation

To validate the four-node thermoregulation model developed, thermal physiological responses of a sleeping person predicted using the model developed were compared to the experimental results previously reported in the literatures by Haskell [1978] and Okamoto-Mizuno [1999]. In Haskell's experiments, subjects were required to remain in bed for 7-h and thermoregulatory and electrophysiological variables were measured during sleep. In Okamoto-Mizuno's experiments, subjects were required to remain in bed for 8h and thermoregulatory and electrophysiological variables were also measured during sleep.

To use the four-node thermoregulation model for a sleeping person to predict thermal physiological responses, the following parameters need to be firstly determined：

1) Subjects parameters: weight and height;
2) Environmental parameters: air temperature, air humidity, air velocity and wall temperature;
3) Bedding parameters: the thickness of bedding and the thermal resistance of mattress. The determination of the values of R_1, R_2 and R_3 followed the method in a previously related study [Pan et al. 2010];

4) The area fraction and mass fraction of each skin parts: α_i (i=1-3) and μ_i (i=1-3);

5) Sleep stage parameters: a NREM stage lasted for 80 to 90 minutes [Hobson 1989], followed by a REM stage. One NREM stage and one REM stage formed a cycle. The number of cycles per night depended on the duration of sleep; a younger person's sleep usually had four or five cycles, while an older one has fewer.

The above parameters were determined according to the reported experimental conditions, so that the same conditions in bot experiments and simulation were maintained.

A relative error was defined when evaluating the four-node thermoregulation model developed, as follows:

$$\delta = \frac{T_{pre} - T_{ex}}{T_{ex}} \tag{5.53}$$

Fig. 5.4 shows the flowchart for solving all model equations.

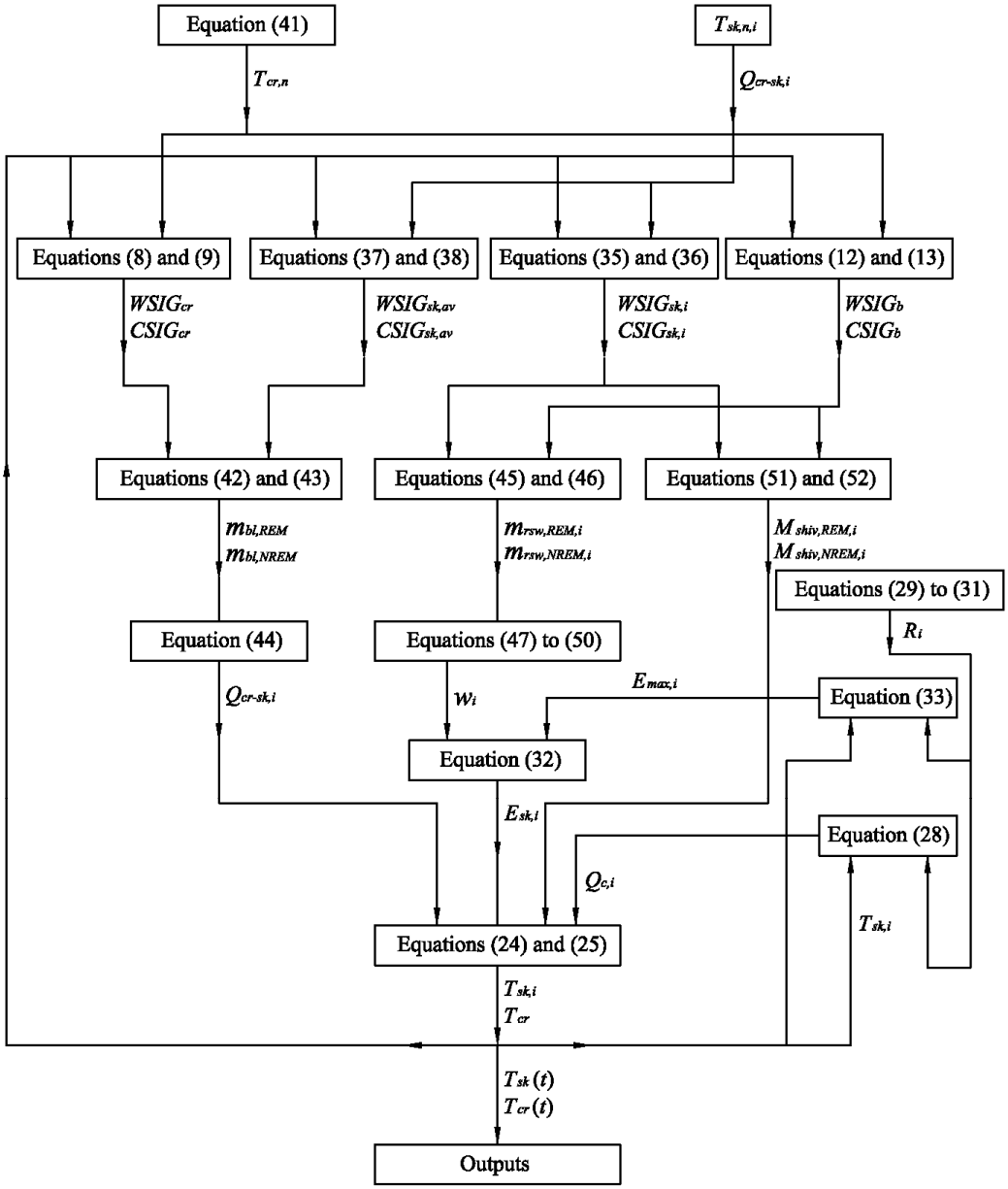

Fig. 5.4 The flowchart for solving all model equations

5.3.1 Validation using Haskell' s experiment results

According to the experimental conditions described by Haskell [1978], Table 5.1 lists the input parameters to the four-node thermoregulation model under three different experimental conditions. Since the purposes of carrying out the experiments

were to investigate the effects of indoor air temperature on metabolism and thermoregulation of a sleeping person, the values of three air temperatures used were considered representative.

Table 5.1 Input parameters to the four-node thermoregulation model under three different experimental conditions

Experimental conditions		1	2	3
Subjects parameters	Wight (kg)	70	70	70
	Height (m)	1.77	1.77	1.77
Environmental parameters	Air temperature (°C)	21	29	37
	Wall temperature (°C)	21	29	37
	Humidity (%)	50	20	20
	Air velocity (m/s)	<0.15	<0.15	<0.15
Bedding parameters	The thickness of bedding (mm)*	0	0	0
	The insulation resistance of mattress (m^2·K/W)**	0	0	0
Area fraction and mass fraction of each skin parts	α_1 (%)	1	1	1
	α_2 (%)	0	0	0
	α_3 (%)	0	0	0
	μ_1 (%)	1	1	1
	μ_2 (%)	0	0	0
	μ_3 (%)	0	0	0

*: Naked sleeping subject without using any beddings.

**: Subjects slept on a bed, constructed of woven strands of nylon webbing stretched taut across a metal frame, similar to a beach chair.

Fig. 5.5 shows the assumed sleep stage distribution in a 7-h period used by the model. A NERM stage lasted for 85 minute throughout a night [Hobson 1989, Haskell et al. 1981a, Okamoto-Mizuno et al. 1999], and there were four cycles through the 7-h sleep period.

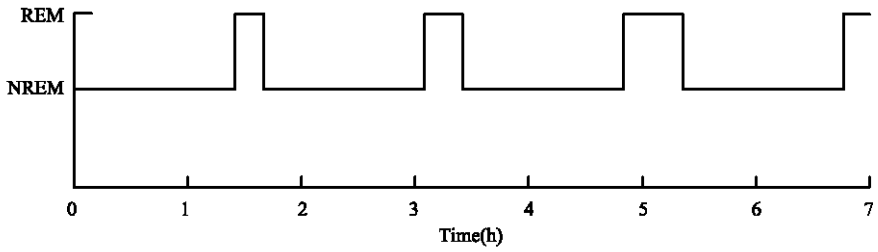

Fig. 5.5 The assumed sleep stage distribution in 7-h period

Using the parameters presented in Table 5.1 and Fig. 5.5, the skin temperature, which was the averaged value of the temperatures on three skin parts, and the core temperature were predicted using the four-node thermoregulation model developed. Fig. 5.6 shows comparisons between the experimental and predicted results of the skin temperature under three different experimental conditions. It can be seen that the predicted and experimental values agreed reasonably well, with a relative error of ±2%, except for the condition of 21°C.

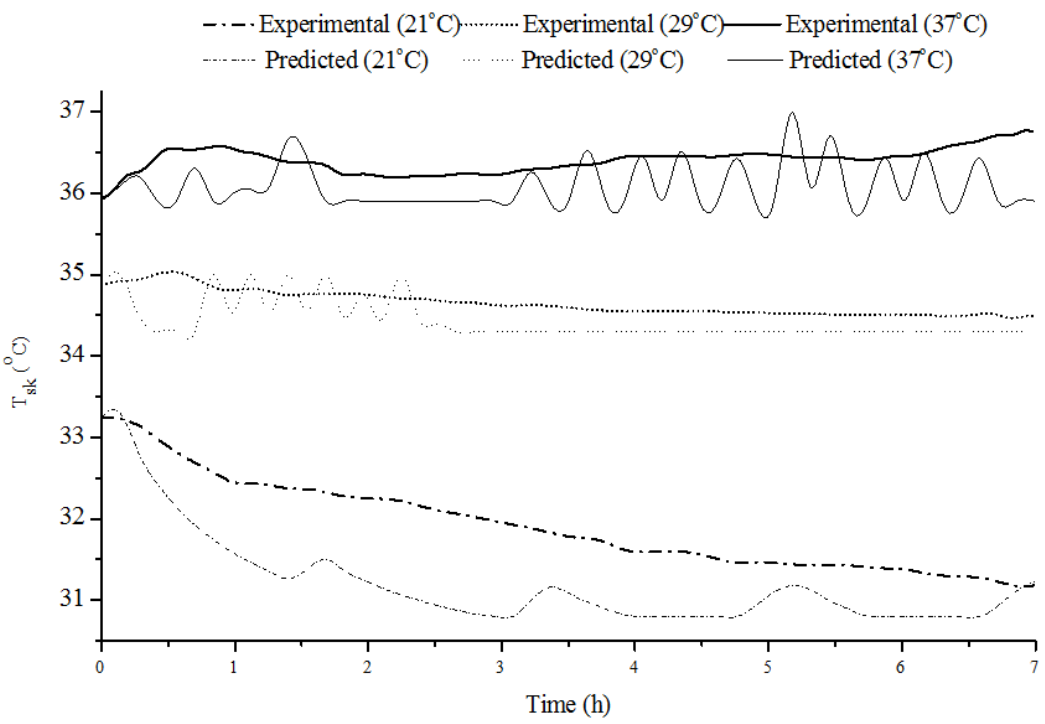

Fig. 5.6 Comparisons between the experimental and predicted results of skin temperatures under three different experimental conditions (21°C, 29°C and 37°C)

Fig. 5.7 shows comparisons between the experimental and predicted results of core temperature under three different experimental conditions. It can be seen that the predicted and experimental values agreed also reasonably well, with a relative error of ±1%.

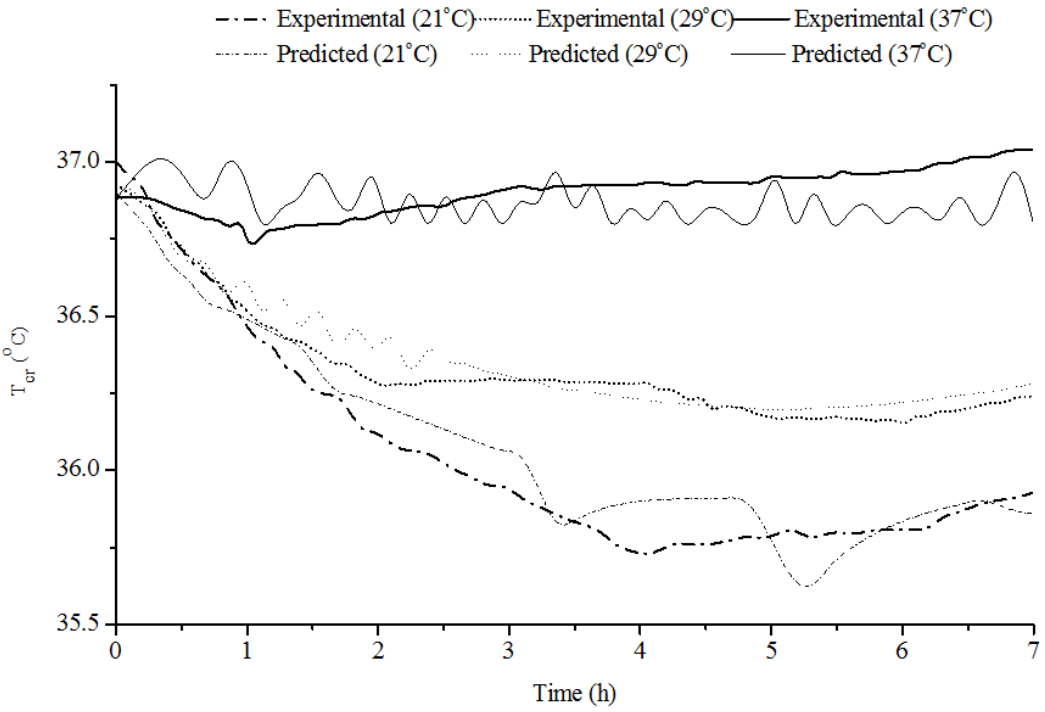

Fig. 5.7 Comparisons between the experimental and predicted results of core temperatures under three different experimental conditions (21°C, 29°C and 37°C)

Under the condition of an air temperature, 29°C, the predicted values agreed with the experimental values better than under the other two experimental conditions. This may be due to that thermoregulatory responses appeared in high and low air temperature, which deviated from 'thermal comfort zone', so that sleep stage distribution would be changed to some extent during experiments. However, it was assumed that sleep stage distribution remained unchanged for simulation. Moreover, under the condition of an air temperature, 21°C, the predicted values for skin temperatures was smaller than the experimental values. This may be due to that under cold condition, a sleeping person may be curl up to decrease the heat loss in experiments, which were not taken into account by the four-node thermoregulation

model developed.

Relatively high frequency fluctuations for the predicted values, and low frequency fluctuations for the experimental values are noted from Fig. 5.6 and Fig. 5.7. This may be because that there are a number of processes in a thermoregulatory system of a human being [Guyton and Hall 2005]. Thermoreceptors, or temperature receptors are the first one to respond to both local temperature and its changes, and then the signals from the thermoreceptors are transmitted by the central nervous system to the hypothalamus where the signals are integrated. The overall thermal state of a human body from these signals will then be lastly determined and the appropriate effector commands issued. All these processes need response time. However, the four-node thermoregulation model developed would respond immediately to the environments.

5.3.2 Validation using Okamoto-Mizuno' s experiment results

According to the experimental conditions described by Okamoto-Mizuno et al. [1999], Table 5.2 lists the input parameters to the four-node thermoregulation model under four different experimental conditions. Since the purpose of carrying out the experiments was to investigate the effects of air humidity on human sleep stages and body temperature, the values of air temperature and relative humidity used in the four experimental conditions were considered representative.

Table 5.2 Input parameters to the four-node thermoregulation model under four different experimental combinations

Experimental conditions		1	2	3	4
Subjects parameters	Wight (kg)	62	62	62	62
	Height (m)	1.725	1.725	1.725	1.725
Environmental parameters	Air temperature (°C)	29	29	35	35
	Wall temperature (°C)	29	29	35	35
	Humidity (%)	50	75	50	75
	Air velocity (m/s)	<0.15	<0.15	<0.15	<0.15
Bedding parameters	The thickness of bedding (mm)*	0	0	0	0
	The insulation resistance of mattress (m^2·K/W)	0.65	0.65	0.65	0.65
Area fraction and mass fraction of each skin parts	α_1 (%)	0.767	0.767	0.767	0.767
	α_2 (%)	0	0	0	0
	α_3 (%)	0.233	0.233	0.233	0.233
	μ_1 (%)	0.767	0.767	0.767	0.767
	μ_2 (%)	0	0	0	0
	μ_3(%)	0.233	0.233	0.233	0.233

*: Naked sleeping subject without using any beddings.

Fig. 5.8 shows the assumed sleep stage distribution in a 8-h period used by the model. A NERM stage lasted for 85 minute throughout a night [Hobson 1989, Haskell et al. 1981a, Okamoto-Mizuno et al. 1999] and there were five cycles throughout the 8-h sleep period.

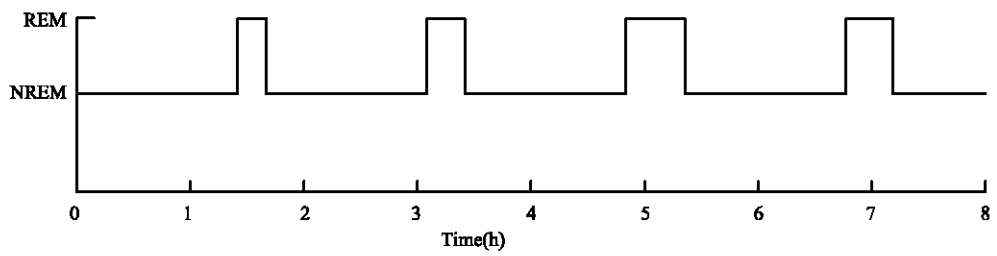

Fig. 5.8 The assumed sleep stage distribution in 8-h period

According to the parameters shown in Table 5.2 and Fig. 5.8, the skin temperature, which was the averaged value of the temperatures on the three skin parts, and core temperature were predicted using the four-node thermoregulation model developed. Fig. 5.9 shows comparisons between the experimental and predicted results of skin temperatures under four different experimental conditions. It can be seen that the predicted and experimental values agreed reasonably well, with also a relative error of ±1%.

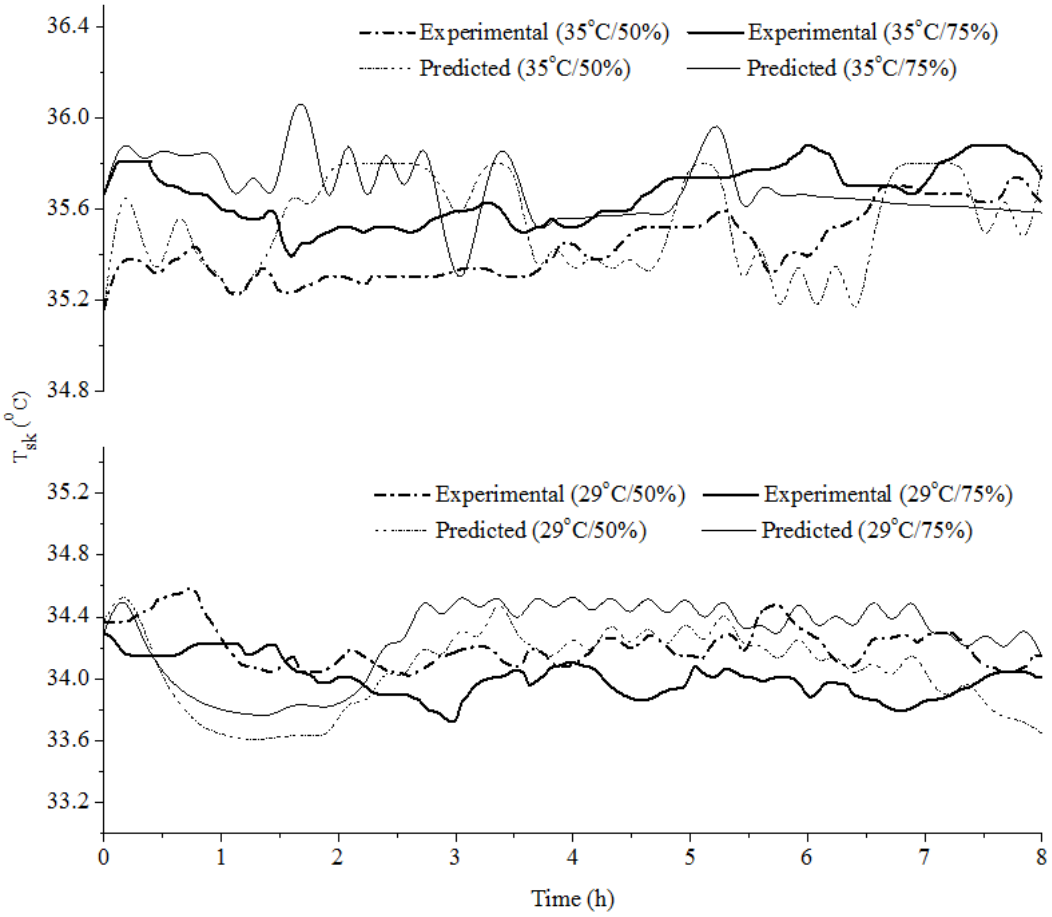

Fig. 5.9 Comparisons between the experimental and predicted results of skin temperatures under four different experimental conditions

Fig. 5.10 shows comparisons between the experimental and predicted results of core temperatures under four different experimental conditions. It can be seen that the predicted and experimental values agreed reasonably well, with a relative error of ±2%.

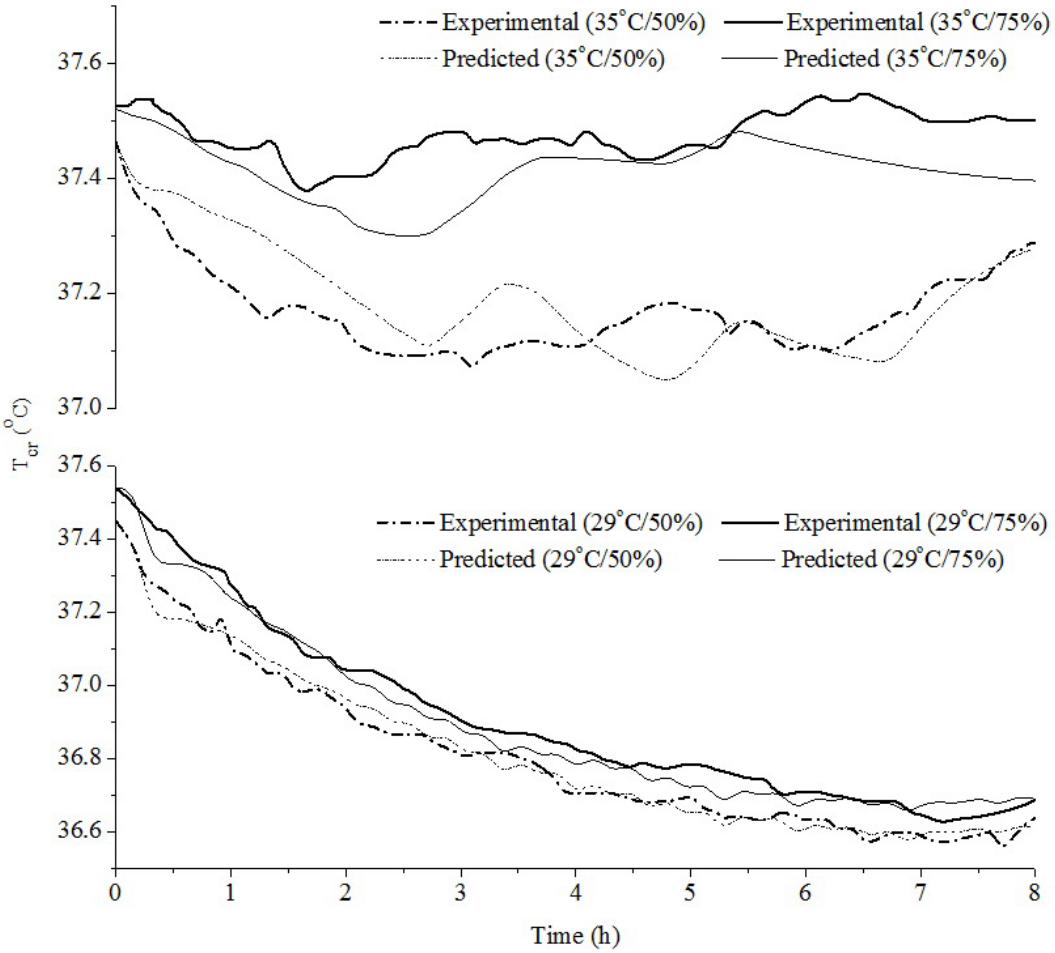

Fig. 5.10 Comparisons between the experimental and predicted results of core temperatures under four different experimental combinations

The above comparisons and discussion suggested that the four-node thermoregulation model could be used to predict the thermoregulatory responses of a sleeping person with an acceptable accuracy. However, the difference between the experimental and predicted values may be due to the following reasons:

1) Certain input parameters to the four-node thermoregulation model may be different from that used in the experiments, such as sleep stages distribution;

2) Some other factors, which possibly affect the core and skin temperatures during sleep, such as body movement, etc., were not taken into account by the four-node thermoregulation model developed.

5.4 Conclusions

A four-node thermoregulation model to predict the thermoregulatory responses of a sleeping person has been developed and is reported in this Chapter. The model was validated by comparing the predicted values with the experimental data available in open literature. The comparison results demonstrated that the four-node thermoregulation model developed could be used to predict the thermoregulatory responses of a sleeping person with an acceptable accuracy.

It is believed that the validated four-node thermoregulation model can be used to predict different indoor thermal parameters, such as air temperature and humidity, in a sleeping environment and different bedding systems on the thermoregulatory responses of a sleeping person. Therefore, the model is expected to be a powerful tool in the future studies on thermal comfort in sleeping environments and the related energy efficiency issues.

Chapter 6

Performance evaluation of a novel bed-based task/ambient conditioning (TAC) system

6.1 Introduction

Because of their excellent performance in local thermal environmental control and energy saving, TAC systems have attracted increasingly research attention. A TAC system allows the thermal conditions in small, localized zones in a building to be individually controlled by building occupants, while allowing thermal environmental conditions outside these zones to freely fluctuate [Bauman and Arens 1996]. Over the years, different TAC systems have been developed, and they may be divided into the following categories [Spoormaker 1990, Sodec and Craig 1991, Shute 1992, 1995, Matsunawa et al. 1995, Tamblyn 1995]: floor-based, desktop-based, partition-based and ceiling-based, as reported in Chapter 2.

Studies have been carried out to investigate the operational performance of daytime TAC systems, through field measurements and experimentations [Bauman et al. 1993, Faulkner et al. 1995, Shute 1995]. Results from these previous studies demonstrated that the use of TAC systems can help improve thermal comfort and indoor air quality, and reduce the energy consumption. Firstly, by allowing personal control over local thermal environments, the thermal comfort of occupants can be

greatly improved using TAC systems. Secondly, the use of TAC systems can help improve indoor air quality, since fresh air can be directly delivered to occupants, and the contaminants from an occupied zone efficiently removed. Lastly, the use of TAC systems helped achieve energy saving. This was because when a FAC system was used, a comfortable indoor environment for everywhere in a room would be maintained. However, when a TAC system was used only a comfortable indoor environment within an occupied zone would be maintained, but air temperatures in unoccupied zone(s) were allowed to fluctuate even to outside comfort limits. Therefore, as compared to the use of FAC systems, the use of TAC systems can result in energy saving since air conditioning in an unoccupied zone was unnecessary.

Nevertheless, the current applications of TAC systems are mainly for daytime activities, such as in work stations, but not for bedrooms in residences or other sleeping environments. Unlike daytime activities such as shopping or walking, or even working in a work station, sleeping is confined to a relatively small space and a sleeping person is immobile. Therefore, TAC systems may be best applied to a sleeping environment. Consequently, there is a strong need for studying the operational and energy performance of TAC systems when applied to sleeping environments.

This Chapter reports on an experimental study on evaluating the operational and

energy saving performance of a novel bed-based TAC system. Firstly, the novel bed-based TAC system is described in detail, and then a chamber used as an experimental bedroom introduced. This is followed by reporting experimental methods and conditions. Finally, experimental results of operational and energy saving performances, and their analysis and further discussions are presented.

6.2 Experimentation

6.2.1 The prototype novel bed-based TAC system

In Fig. 6.1, the prototype novel bed-based TAC system whose operational and energy saving performances were studied is sketched. Two supply air plenums, measuring at 1900 mm (L) × 300 mm (W) × 300 mm (H), were symmetrically placed on both sides of a mattress bed. The function of the supply air plenums was to ensure a uniform supply air distribution. Two supply grilles, whose outlet vanes were ± 90° adjustable, were each installed on one side of the supply air plenums. The size of each supply grille was at 900 mm × 100 mm, so that a low supply air velocity may be established, even with a larger supply air flow rate, to avoid draft.

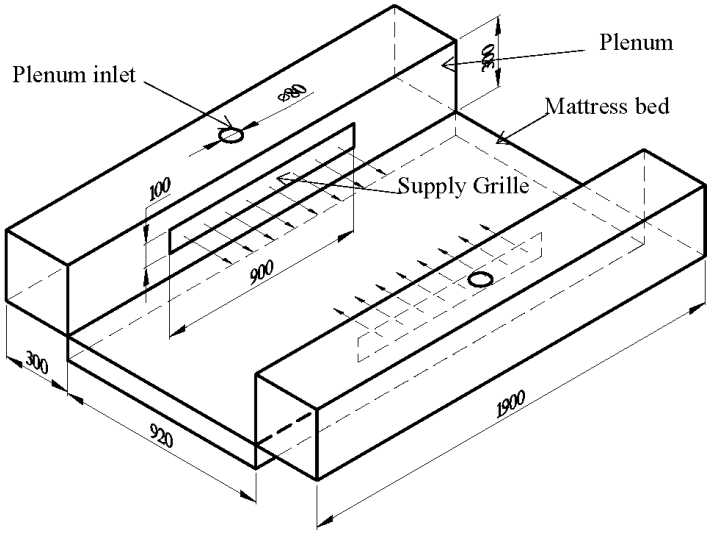

Fig. 6.1 The prototype novel bed-based TAC system

6.2.2 Experimental setup

The novel bed-based TAC system was placed in a chamber used as an experimental bedroom, as shown in Fig. 6.2. The chamber, measuring at 3600 (L) mm× 2500 (D) mm× 2550 (H) mm, was thermally insulated and placed inside a large air conditioned laboratory, so that the temperature difference across the envelope of the experimental bedroom was small. Therefore, the experimental bedroom could be treated as having no envelope cooling load, with all thermal load generated from indoor space during experiments. This was considered as a limitation of the experimental bedroom. The experimental bedroom was conditioned by a direct-expansion (DX) FAC system with both supply inlet and return outlet located on a side wall, also as shown in Fig. 6.2. Flexible air ducts were used to link the novel bed-based TAC system to both the supply inlet and return outlet, as shown in

Fig. 6.3(a) and Fig. 6.3(b), respectively. With such an arrangement, the novel bed-based TAC system may properly function as designed. On the other hand, when the flexible air ducts were not used, the chamber, or the experimental bedroom, itself may be fully air-conditioned by the DX FAC system.

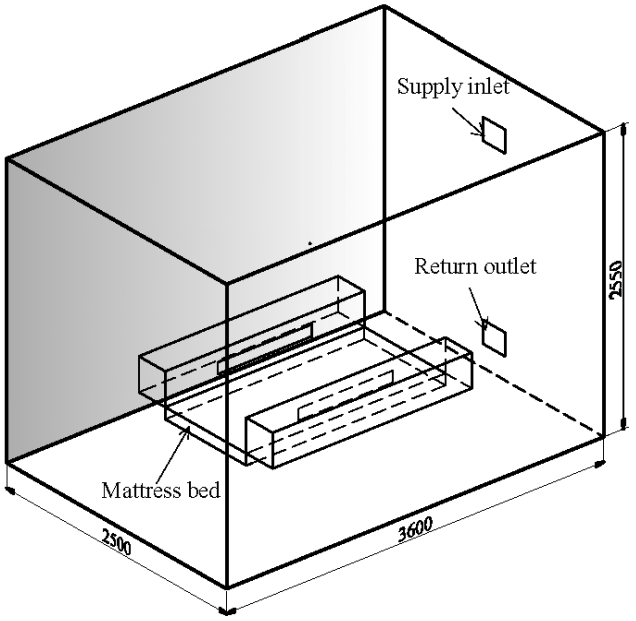

Fig. 6.2 The schematics of experimental setup

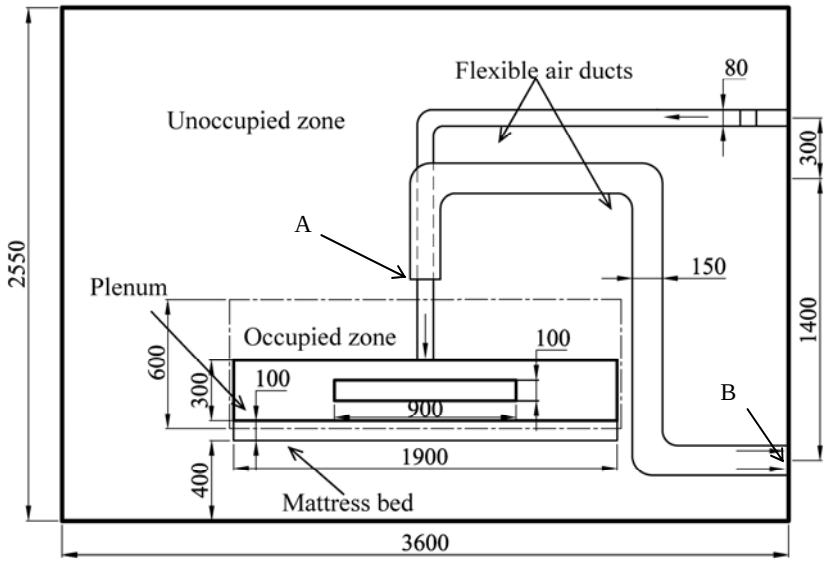

Fig. 6.3(a) Sectional view of the experimental setup

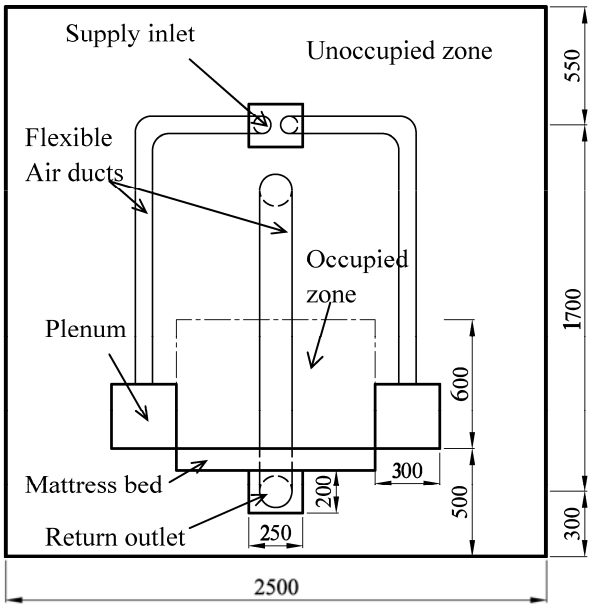

Fig. 6.3(b) Sectional view of the experimental setup

A conventional mattress of 100 mm thick was used in this study. Although a variety of different types of mattress were available, any conventional mattress would

provide considerably more local insulation than bedding. Therefore, it was assumed that in a steady-state there was no heat loss through the body surface in contact with the mattress. In addition, the firmness of a mattress might affect the amount of body surface area in contact with the mattress, but the resultant variation in insulation was minimal among conventional mattresses [McCullough et al. 1987].

According to results from a previous survey [Lin and Deng 2006], 90% of the respondents would cover themselves with quilts (50%) or blankets (40%) during sleep. Three bedding items, including two summer quilts and a blanket, termed Q1, Q2 and B, respectively were used in this experimental study. The physical properties of the three beddings were previously measured [Lin and Deng 2008b], and are shown in Table 4.1. in Chapter 4.

A thermal manikin, Alex, was placed in a supine position on the mattress bed to simulate a sleeping person. Its surface area was divided into 20 independent segments, each with its own temperature sensor, heating element and controller to approximately simulate the skin temperature distribution of a real human being. As described in Chapter 5, previous experimental results demonstrated that the skin temperature of a sleeping person remained stable at around 34.6°C throughout the sleep time under a thermally neutral sleeping environment except during approximately the first 30 minutes when skin temperature may experience some changes [Haskell et al. 1981b, Okamoto-Mizuno et al. 1999]. This was to say during

an entire normal sleep period of 8 hours, skin temperature remained stable for over 90% of the sleep duration. Therefore, the skin temperature settings for the thermal manikin were 34.6°C for all body segments, to simulate a sleeping person with an averaged skin temperature of 34.6°C in a thermally neutral state [Haskell et al. 1981b, Okamoto-Mizuno et al. 1999, Lin and Deng 2008a]. Since the thermal manikin was the only heat source that generated sensible thermal load in the experimental room in this Chapter, the analysis of energy saving would be based on the reduction in the sensible thermal load when using the novel bed-based TAC system.

6.2.3 Experimental methods and conditions

For the purpose of indoor air temperature measurement and results analysis, the chamber was divided into an occupied zone and an unoccupied zone, as shown in Figs. 6.3(a) and 6.3(b). The occupied zone was a designated space of 0.6m high on top of the mattress bed, and the rest of the chamber space was the unoccupied zone.

6.2.3.1 Measurement methods

Detailed air velocity and temperature measurements in the unoccupied zone were accomplished by using eight lightweight sensor rigs, whose locations each represented by a cross are shown in Fig. 6.4, allowing a vertical array of sensors to be positioned at four measuring heights: 0.1 m, 0.6 m, 1.1 m and 1.7 m. The first

three corresponded to the recommended measuring heights for seated subjects, as specified by AHSRAE Standard [ANSI/ASHRAE 2004]. The measured temperatures in these eight locations, totally 32 measuring points, were averaged to represent the average air temperature in the unoccupied zone. On the other hand, detailed air velocity and temperature measurements in the occupied zone were accomplished by using ropes, allowing a vertical array of sensors to be positioned at two measuring heights of 0.8 m and 1.0 m, respectively. The first corresponded to the breathing level of a sleeping person in this study. Six measuring locations within the occupied zone are also shown in Fig. 6.4 and the measured temperatures in these totally 12 measuring points were averaged to represent the average air temperature in the occupied zone. The purpose of air velocity measurement was to ensure that the air velocity in the occupied zone was maintained at not greater than 0.25 m/s [ANSI/ASHRAE 2004]. Temperatures were measured using K-type thermocouples and velocity using omnidirectional anemometers having a measuring range of 0-2.5m/s and an accuracy of ±1 % of full scale. All temperature and velocity data were sampled at an interval of one minute and recorded using a data logger. During each test, the power input to, and the mean skin temperature of each segment of, the thermal manikin were continuously monitored and recorded at an interval of one minute. The mean value of each parameter was calculated based on at least thirty number of its steady-state measured data.

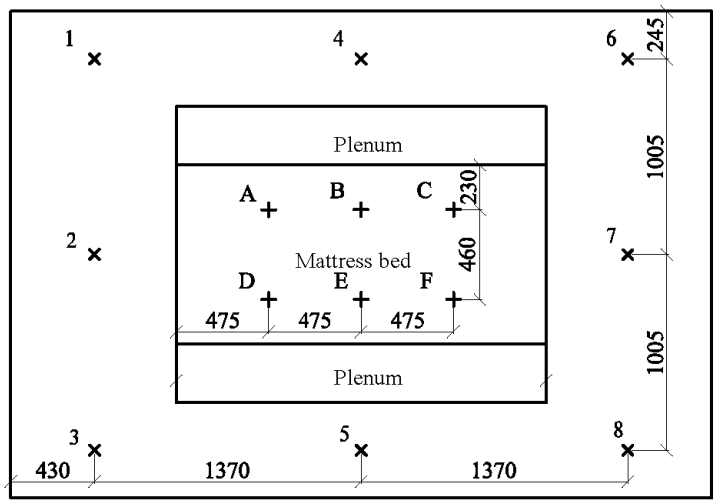

Fig. 6.4 Locations of air temperature and velocity measurement inside the experimental bedroom

6.2.3.2 Measurement conditions

The lowest and highest permissible supply air temperatures were restricted to achieve an acceptable level of thermal comfort. In Hong Kong, a survey done by Lin and Deng [2006] showed that 80% of the respondents would prefer a relatively low indoor air temperature setting at below 24°C. In another study [Gong et al. 2006], the supply air temperatures were between 20°C and 24°C, which were considered acceptable by tropically acclimatized human subjects. Therefore, a supply air temperature between 20°C and 24°C was adopted in this study. On the other hand, a TAC system had the responsibility for removing the cooling load so as to maintain the comfortable indoor thermal environment in an occupied zone, thus its supply air flow rate would be larger than that of a Personal Ventilation (PV) system which was

mainly to maintain the indoor air quality in an occupied zone. In this study, the supply air flow rate varied between 25 L/s and 75 L/s, lower than that used for workstations [Bauman et al. 1995]. This was because the metabolic rate of a sleeping person would be lower than that of a working person, and the cooling load at nighttime would be lower that in daytime [Lin and Deng 2004]. Furthermore, since the outlet vanes of the two supply grilles were ± 90° adjustable, experiments were carried out under three different supply vane angles of -45°, 0°and +45°, as shown in Fig. 6.5, respectively. Moreover, when the thermal manikin was covered by beddings, the percentage coverage of body surface area by beddings and bed was at 94.1% [Lin and Deng 2008b].

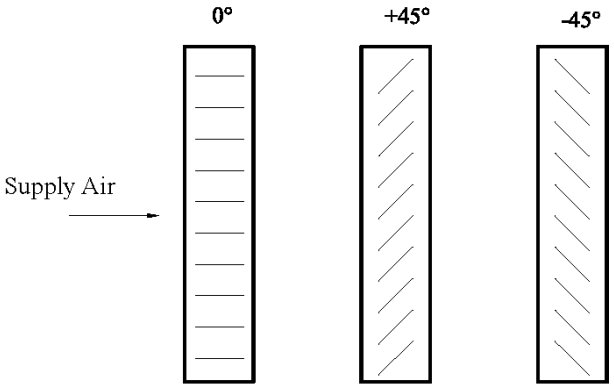

Fig. 6.5 Three different supply vane angles

Table 6.1 summarizes various groups of experimental conditions. Firstly, the purposes of carrying out Group 1 experiments were to compare the operational and energy saving performances between using the novel bed-based TAC system and a FAC system at different supply air temperatures, with all other parameters being the

same for both systems. Group 1 experimental results are shown in Figs. 6.6 and 6.7. Secondly, for Group 2 experiments whose results are shown in Fig. 6.8, their purposes were to exam the levels of thermal comfort achieved, at two different supply air flow rates of 50L/s for the novel bed-based TAC system and 100L/s for the FAC system, respectively. Totally there were nine experiments carried out, at three different supply air temperatures (i.e., 20°C, 22°C and 24°C) and three different beddings (i.e., B, Q2 and Q1). Thirdly, the purposes of doing Group 3 experiments were to investigate the effects of varying supply air flow rate on the operational and energy saving performance of the novel bed-based TAC system and their results are shown in Fig. 6.9. Finally, in Group 4 experiments whose results are illustrated in Fig. 6.10, the effects of varying supply vane angles on the operational and energy saving performance of the novel bed-based TAC system were studied.

Table 6.1 Groups of experimental conditions

Group	Series No.	Supply air temperature (°C)	Supply air flow rate (L/s)		Supply vane angle for TAC (°)	Thermal manikin covered by	Results shown in
			TAC	FAC			
1	1.1	20	50	50	0	None	Figs. 6.6 and 6.7
	1.2	22	50	50	0	None	
	1.3	24	50	50	0	None	
2	2.1	20	50	100	0	B	Fig.6.8
	2.2	20	50	100	0	Q2	
	2.3	20	50	100	0	Q1	
	2.4	22	50	100	0	B	
	2.5	22	50	100	0	Q2	
	2.6	22	50	100	0	Q1	
	2.7	24	50	100	0	B	
	2.8	24	50	100	0	Q2	
	2.9	24	50	100	0	Q1	
3	3.1	20	25	-	0	None	Fig.6.9
	3.2	20	50	-	0	None	
	3.3	20	75	-	0	None	
4	4.1	20	50	-	0	None	Fig.6.10
	4.2	20	50	-	45	None	
	4.3	20	50	-	-45	None	

6.3 Results analysis

6.3.1 Evaluation indexes

Firstly, the Predicted Mean Vote (PMV) equation applicable to a sleeping environment, which was obtained previously [Lin and Deng 2008a], was adopted to evaluate the level of indoor thermal comfort in the occupied zone:

$$PMV = 0.0998(40 - Q_t - Q_{res} - E_{sk}) \tag{6.1}$$

Where,

$$Q_{res} = 0.056(34 - t_{oz}) + 0.692(5.87 - p_{oz}) \tag{6.2}$$

$$E_{sk} = \frac{0.3762(5.52 - p_{oz})}{R_t} \tag{6.3}$$

In Equation (6.1), Q_t, the sensible heat losses from a sleeping person, was directly measured using the thermal manikin. Further, in Equations (6.2) and (6.3), all parameters were obtained experimentally except the value of R_t, which however was available by reference to previous experimental values [Lin and Deng 2008b]. According to ASHARE Standard [ANSI/ASHRAE 2004], when PMV was in the range between -0.5 to 0.5, indoor thermal environment would be accepted by most people.

Secondly, to evaluate the energy saving potential using the novel bed-based TAC system, an energy utilization coefficient (EUC), which was also adopted in previous studies [Gan 1995, Liu et al. 2008], was used:

$$EUC = \frac{t_{uz} - t_s}{t_{oz} - t_s} \tag{6.4}$$

Where, t_{uz}, t_{oz} and t_s are the average air temperature in an unoccupied zone, the average air temperature in an occupied zone and supply air temperature, respectively. The definition of EUC suggests that energy saving becomes possible if the EUC is over 1, and the energy saving potential is expected to increase as the EUC increases beyond 1. Therefore, for an FAC system, the resulted EUC should be close to 1. However, for a TAC system, the resulted EUC is expected to be greater 1.

6.3.2 The measured operational and energy saving performance of the novel bed-based TAC system

In this section, the comparisons of the measured operational and energy saving performance between using the novel bed-based TAC system and the FAC system at Groups 1- 4 experimental conditions are presented.

Fig. 6.6 shows the comparisons of EUCs between using the FAC and the novel bed-based TAC system at different supply air temperatures. It can be seen that the EUC values when using the TAC system were all greater than 1.0. This suggested that using the novel bed-based TAC system would have energy saving potential, since conditioned air was directly supplied to the occupied zone, without the need to cool down the air outside the occupied zone. As seen, when using the novel bed-based TAC system, EUC increased slightly with the decrease in supply air

temperature. This may be because when using the novel bed-based TAC system, supply air temperature mainly affected the average air temperature in the occupied zone. Therefore, a decrease in supply air temperature would result in a larger reduction in average air temperature in the occupied zone than that in the unoccupied zone, leading to a higher EUC. However, it was obvious that the energy saving potential was limited, since the EUCs in the current study when using the novel bed-based TAC system was around 1.8. This was because there was not much heat transferred from the outdoors, as described in Section 6.2.2 and the average air temperature in the unoccupied zone was lower. However, if the experimental bedroom was an actual bedroom with external walls or windows, the average air temperature in the unoccupied zone would be higher due to heat transferred from outdoors. Consequently, the EUC values when using the bed-based TAC system would be higher.

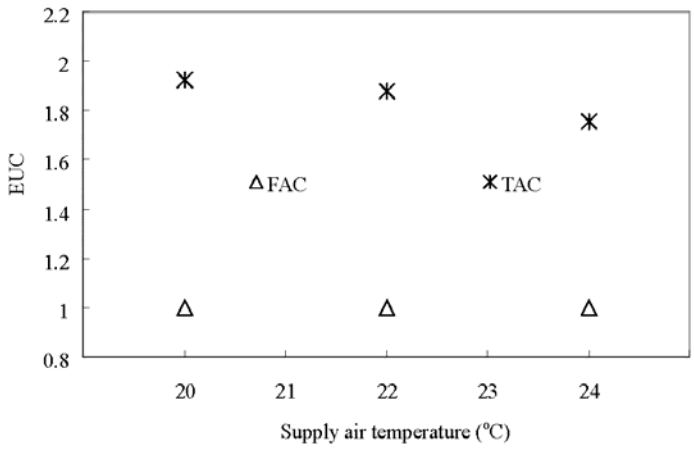

Fig. 6.6 The measured EUCs between using the FAC and the novel bed-based TAC system at different supply air temperatures

Fig. 6.7 shows the comparisons of PMVs between using the FAC and the novel bed-based TAC system at different supply air temperatures. It can be seen that to achieve the same level of thermal comfort in the occupied zone, a higher supply air temperature may be employed by using the novel bed-based TAC system, as compared to using the FAC system, which consequently led to energy saving potential. However, the PMVs for both systems were too low and hence not acceptable in this study, since the envelope cooling load was negligibly small, so that both systems only dealt with the cooling load from the thermal manikin.

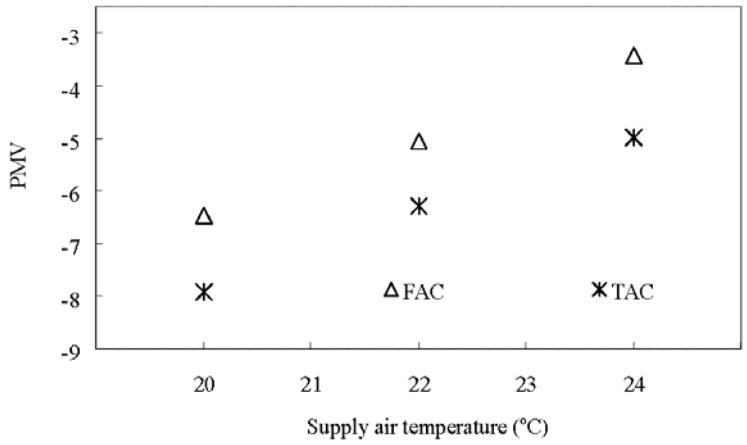

Fig. 6.7 PMVs in the occupied zone between using the FAC and novel bed-based TAC system at different supply air temperatures

Furthermore, from the Group 2 experimental results shown in Fig. 6.8, it can be seen that at the nine experimental points, PMV values when using the novel bed-based

TAC system at 50 L/s supply air flow rate were very close to those when using the FAC system however at 100 L/s supply air flow rate. This implied that the supply air flow rate could be reduced for energy saving when using the novel bed-based TAC system, while maintaining the same level of indoor thermal comfort in the occupied zone as if the FAC system was used. The PMVs for both systems when covered with Q2 were between -0.5 and +0.5 and hence acceptable, since the beddings decreased the sensible heat loss from the thermal manikin.

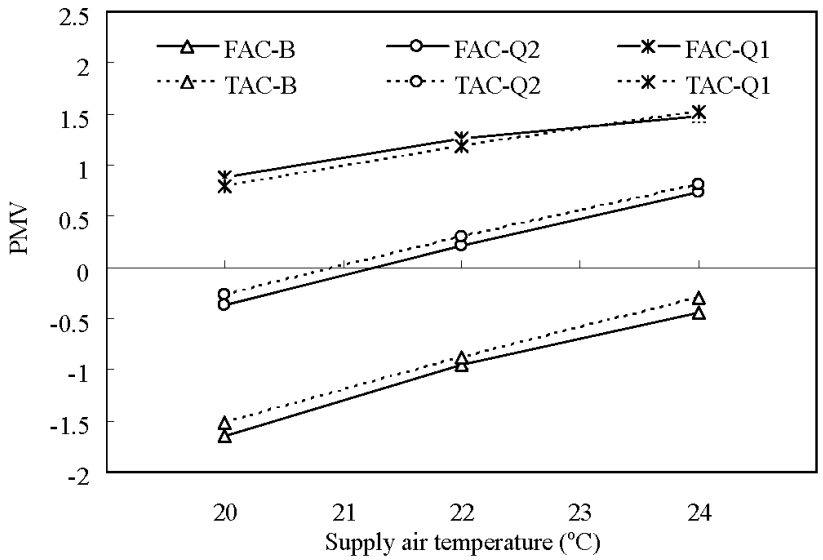

Fig. 6.8 PMVs in the occupied zone when using the FAC system at 100L/s and the novel bed-based TAC system at 50L/s, with three different beddings

Therefore, using the novel bed-based TAC system would help maintain a lower average air temperature in the occupied zone, but allow a higher average temperature in the unoccupied zone. Compared with the use of a FAC system, the use of the

novel bed-based TAC system would help save energy with either a higher supply air temperature or a smaller supply air flow rate, to maintain the same level of thermal comfort in an occupied zone.

6.3.3 Factors effecting the operational and energy saving performance of the novel bed-based TAC system

The results from Group 1 experiments, as shown in Figs. 6.6 and 6.7, demonstrated that the supply air temperature would affect the values of both EUC and PMV. Other factors, including supply air flow rate and supply vane angle, may also affect the operational and energy saving performance of the novel bed-based TAC system. These are reported in this Section.

6.3.3.1 Supply air flow rates

Fig. 6.9 shows the measured EUCs and PMVs under Group 3 experimental conditions. It can be seen that the EUC values increased, while the PMV values decreased, with the increase in supply air flow rate. Since the supply air mainly affected the thermal environment in the occupied zone. Therefore, a higher supply air flow rate would result in a larger reduction in average air temperature in the occupied zone than that in the unoccupied zone, leading to a higher EUC. Moreover, a reduction in average air temperature in the occupied zone led to an increase in

sensible heat loss from the thermal manikin; hence PMV values would be less according to Equation (6.1). Therefore, using a larger supply air flow rate would help improve energy saving, but at the expense of reducing thermal comfort level, for the novel bed-based TAC system.

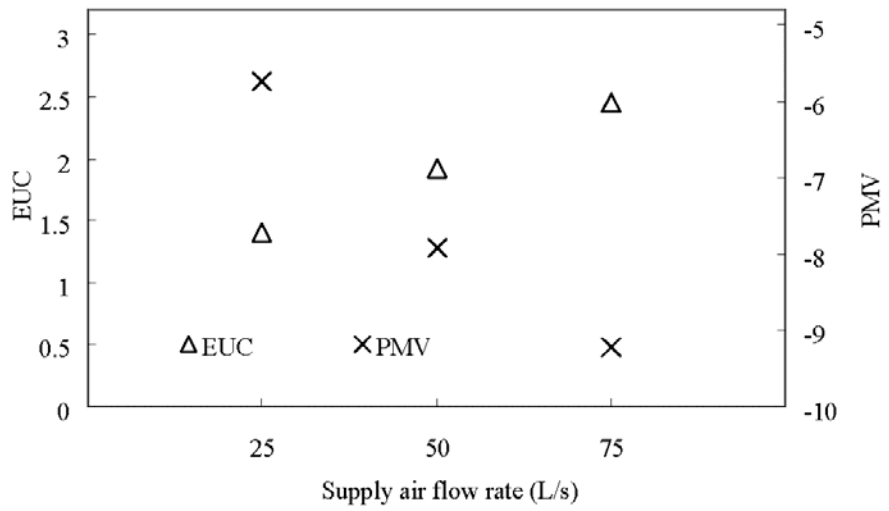

Fig. 6.9 Measured EUCs and PMVs when using the novel bed-based TAC system at different supply air flow rates

6.3.3.2 Supply vane angles

Fig. 6.10 shows the measured EUCs and PMVs under Group 4 experimental conditions at different supply vane angles when using the novel bed-based TAC system. It can be seen that the EUC values slightly decreased when supply vane angles changed from -45° to 0°, and then to +45°, while however the PMV values increased. At -45° supply vane angle, the conditioned air was supplied to the lower

part of the occupied zone, creating a lower average air temperature in the occupied zone, and resulting in a higher EUC value. At +45° supply vane angle, the conditioned air was supplied to the upper part of the occupied zone, so that some of it might well mix with the air in the unoccupied zone, creating a higher average temperature in the occupied zone and resulting in a lower EUC value. On the other hand, at -45° supply vane angle, the average air temperature in the occupied temperature would be lower than that at 0° or +45° angles, resulting in a higher sensible heat loss from the thermal manikin and hence a lower PMV.

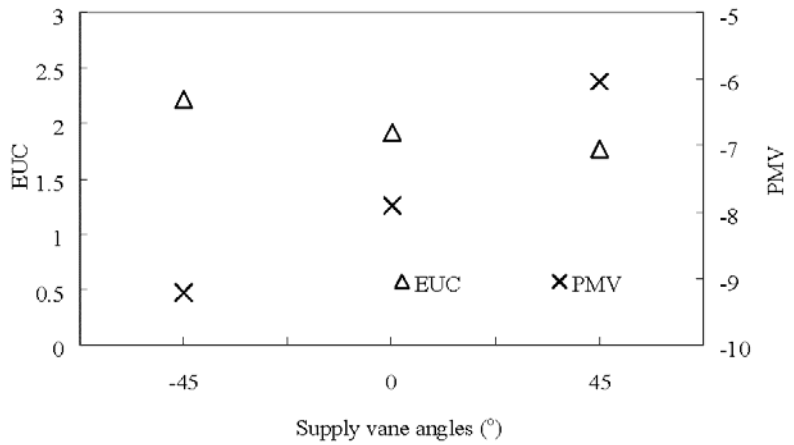

Fig. 6.10 Measured EUCs and PMVs when using the novel bed-based TAC system at different supply vane angles

6.4 Discussions

6.4.1 The energy saving potential of the novel bed-based TAC system in a simulated actual bedroom

The measured operational and energy saving performances of the novel bed-based TAC system installed inside the experimental bedroom are reported in Section 6.3. However, as mentioned in Section 6.2.2, the experimental bedroom did not have any thermal load from outdoors. In real applications, unlike the experimental bedroom, there should be external walls and windows in an actual bedroom and there would be thermal load transferred from outdoors, in addition to the loads generated indoors. Therefore, it was considered necessary to further study the energy saving potential of the novel bed-based TAC system installed inside a simulated actual bedroom through a theoretical analysis, which is reported in this Section.

The following assumptions were made in the analysis:

- The simulated actual bedroom was the same as the experimental bedroom, with the novel bed-based TAC system placed inside except that one of the walls, which is represented by the shaded surface in Fig. 6.2, was replaced by an external wall having a window on it, and being subjected to an indoor-outdoor air temperature difference;
- The combined thermal resistance and surface area of both the external wall and the window were R_{en} and A_{en}, respectively;
- The equivalent thermal resistance and surface area between an occupied zone and a unoccupied zone were R_a and A_a, respectively.

The envelope cooling load and the cooling load due to heat loss from occupants were removed by the TAC system, as shown in Fig. 6.11.

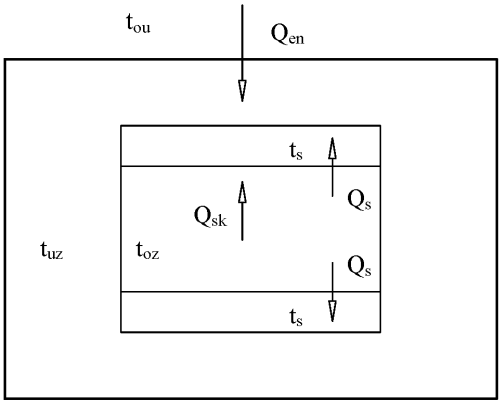

Fig. 6.11 Heat transfer processes in an actual bedroom

Based on the above assumptions and using the steady state heat transfer theory, the heat transfer processes shown in Fig. 6.11 could be represented by Fig. 6.12.

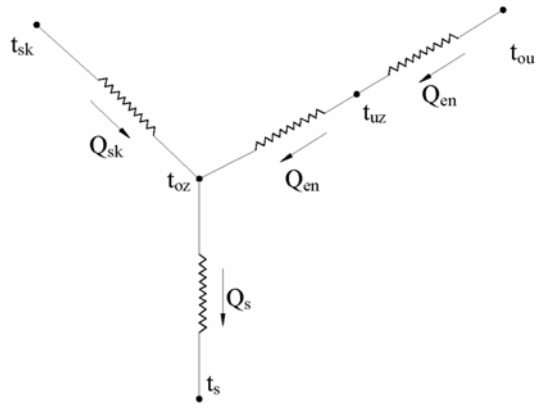

Fig. 6.12 Node network for the heat transfer processes shown in Fig. 6.11

Therefore, heat transfer was evaluated as follows:

$$Q_{en} = A_{en} \frac{t_{ou} - t_{uz}}{R_{en}} \tag{6.5}$$

$$Q_{en} = A_a \frac{t_{uz} - t_{oz}}{R_a} \tag{6.6}$$

The cooling capacity of the TAC bed-based system was calculated by:

$$Q_s = C_p V \rho (t_{re} - t_s) \tag{6.7}$$

According to the energy conservation, the following yielded:

$$Q_s = Q_{en} + Q_{sk} \tag{6.8}$$

Combining Equations (6.5) and (6.6), Q_{en} can be evaluated by:

$$Q_{en} = \frac{t_{ou} - t_{oz}}{\frac{R_{en}}{A_{en}} + \frac{R_a}{A_a}} \tag{6.9}$$

Putting Equations (6.9) into Equation (6.5) to obtain:

$$t_{uz} = t_{ou} - Q_{en} \frac{R_{en}}{A_{en}} \tag{6.10}$$

Compared with the novel bed-based TAC system in the experimental bedroom, the novel bed-based TAC system in the simulated actual bedroom would deal with additionally the thermal load transferred from the outdoors. Therefore, its supply air temperature should be reduced if its supply air flow rate remained unchanged, at the same thermal comfort level maintained.

In the following analysis, a superscript ,', is used to denote the parameters related to the experimental bedroom.

Combining Equations (6.7) and (6.8) Δt_s, can be evaluated by:

$$\Delta t_s = \frac{Q_{en}}{C_p V \rho} \tag{6.11}$$

Therefore, the supply air temperature from the novel bed-based TAC system in the simulated actual room was evaluated by:

$$t_s = t_s^{'} - \frac{Q_{en}}{C_p V \rho} \tag{6.12}$$

Putting Equations (6.10) and (6.12) into Equation (6.4), its EUC in the simulated actual room was then evaluated by:

$$EUC = \frac{t_{ou} - Q_{en}\frac{R_{en}}{A_{en}} - \left(t_s^{'} - \frac{Q_{en}}{C_p V \rho}\right)}{t_{oz} - \left(t_s^{'} - \frac{Q_{en}}{C_p V \rho}\right)} \tag{6.13}$$

Combining Equations (6.5) to (6.8), $\frac{R_a}{A_a}$ can be evaluated by:

$$\frac{R_a}{A_a} = \frac{t_{uz} - t_{oz}}{C_p V \rho(t_{re} - t_s) - Q_{sk}} \tag{6.14}$$

Since the ratio between the volume of an unoccupied zone and that an occupied zone was the same, and the air velocity in unoccupied zone was rather low, for both the experimental bedroom and simulated actual bedroom, the value of $\frac{R_a}{A_a}$ was considered to be the same as that of $\frac{R_a^{'}}{A_a^{'}}$. Therefore, using the experimental data obtained for the experimental bedroom, $\frac{R_a}{A_a}$ was estimated at 0.077 K/W.

On the other hand, $\frac{R_{en}}{A_{en}}$ was evaluated based on area and thermal resistance of the external wall and window. According to the design standard [Chinese Standard JGJ 75 2003] applicable to Hong Kong, the following were adopted:

- The window/wall ratio for the external wall was 0.3;
- The thermal resistances of external wall and window were 1.4 m^2·K/W and 0.4 m^2·K/W, respectively;
- The total surface area of the external wall including the window was 9.18 m^2 (3 m × 2.55 m).

Therefore, the value of $\frac{R_{en}}{A_{en}}$ was estimated at 0.1 W/K.

Finally, for t_{ou}, a value of 32.2°C was adopted, using the mean dry-bulb temperature in the summer design day in Hong Kong [ASHARE handbook fundamental 2009].

Consequently, the EUC for the simulated actual bedroom may be evaluated, according to the above analysis and using the experimental results under Group 1 experimental conditions. Fig. 6.13 shows the comparisons between the evaluated EUC for the simulated actual bedroom and the measured EUC for the experimental bedroom. It can be seen that the evaluated EUCs were significantly larger that the measured EUCs. Moreover, the evaluated EUCs when using the novel bed-based TAC system were just under three times as much as the EUC when using the FAC system. This suggested that the energy saving potential of the novel bed-based TAC system in a simulated actual bedroom would be larger than that in the experimental bedroom.

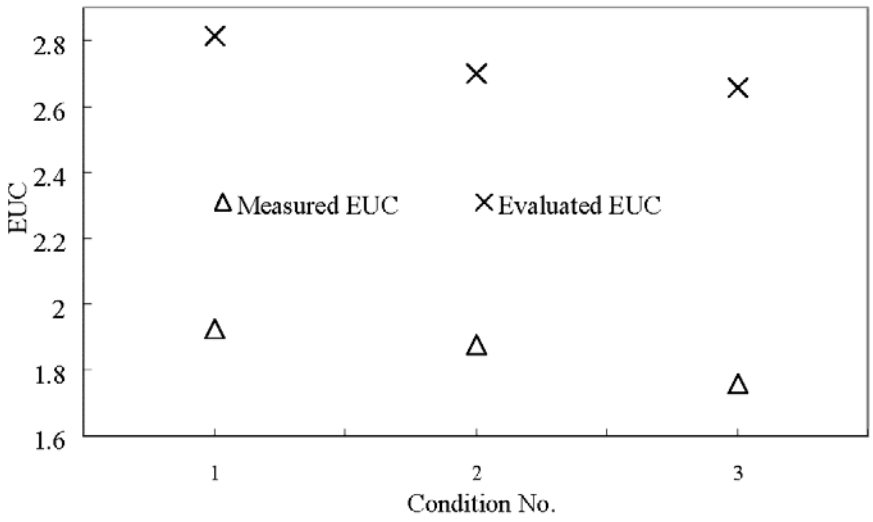

Fig. 6.13 The comparisons between the evaluated EUC and the measured EUC

6.4.2 Latent energy saving potential

As mentioned earlier in Section 6.2.2 in the current study, the analysis of energy saving focused on the sensible thermal load when using the novel bed-based TAC system. For a real air conditioning system, it could deal with not only sensible load but also latent load. If the latent load would also be considered, the total energy saving would have been even greater, as energy saving from dealing with the latent load can be similar to dealing with the sensible load.

6.4.3 The percentage of energy saving when using the novel bed-based TAC system

To further discuss the energy saving when using the novel bed-based TAC system quantitatively, an index, percentage reduction in cooling load, η_c, was defined, based on that the same indoor thermal comfort level was achieved when using either the novel bed-based TAC system and an FAC system. In the definition, the subscripts '1' and '2' represented "the FAC system" and "the novel bed-based TAC system", respectively.

Percentage reduction in total cooling load was defined by:

$$\eta_c = \frac{Q_{co,1} - Q_{co,2}}{Q_{co,1}} \tag{6.15}$$

It can be assumed that supply fresh air rate was at 10% of the total supply air flow rate [Gan 1995], so that the total cooling load may be evaluated by:

$$Q_{co} = 10\%\rho VC_p\left(t_{ou} - t_s\right) + 90\%\rho VC_p\left(t_{re} - t_s\right) \tag{6.16}$$

Putting Equation (6.15) into Equation (6.16) to obtain:

$$\eta_c = 1 - \frac{10\%V_2\left(t_{ou} - t_{s2}\right) + 90\%V_2\left(t_{re2} - t_{s2}\right)}{10\%V_1\left(t_{ou} - t_{s1}\right) + 90\%V_1\left(t_{re1} - t_{s1}\right)} \tag{6.17}$$

From the definition of η_c, a high value of η_c meant a larger reduction in total

cooling load, leading to a significant energy saving.

Table 6.2 shows the predicted values of η_c under four different cases. In Case 1 and Case 2, the supply air flow rates for both systems were the same. In Case 3 and Case 4, the supply air temperatures for both systems were the same. In Case 1, although the supply air flow rates were the same for both systems, the supply air temperature when using the novel bed-based TAC system can be 2°C higher than that when using the FAC system to achieve the same indoor thermal comfort level. The value of η_c was 6.15%. In case 3, although the supply air temperatures were the same for both systems, the supply air flow rate when using the novel bed-based TAC system can be 50 L/s less than that when using the FAC system to achieve the same indoor thermal comfort level. The value of η_c were 13.2 %. Therefore, the use of the novel bed-based TAC system would help save more energy through reductions in both the total cooling load and fan power consumptions, as compared to using the FAC system.

Table 6.2 The predicted values of η_c under four different cases

Case	FAC			TAC			η_c (%)
	t_{s1} (°C)	t_{re1}(°C)	V_1 (L/s)	t_{s2} (°C)	t_{re2} (°C)	V_2 (L/s)	
1	22	23.34	50	24	25.41	50	6.15
2	22	23.17	75	24	25.17	75	9.65
3	20	21.06	100	20	22.84	50	13.2
4	22	22.9	100	22	24.5	50	10.7

6.5 Conclusions

Unlike daytime activities such as shopping or walking, or evening working in a work station, sleeping is confined to a relatively small space and sleeping persons are immobile. Therefore, TAC systems may be best applied to a sleeping environment.

This Chapter reports on an experimental study where a novel bed-based TAC system has been developed and its operational and energy saving performance were investigated experimentally. The experimental results and their analysis demonstrated that the use of the novel bed-based TAC system can help achieve energy saving，compared to the use of a FAC system. The results analysis further suggested that the operational and energy saving performance of the novel bed-based TAC system would be affected by a number of factors, such as supply air flow rates and temperatures, and supply vane angles, etc. Given the limitations of the current experimental bedroom, the energy saving potential using the novel bed-based TAC system in an actual bedroom was studied through a theoretical analysis. The results of theoretical analysis demonstrated that the energy saving potential when using the novel bed-based TAC system in an actual bedroom can be significantly larger than that in the experimental bedroom.

Chapter 7

Numerical study on the operating performances of the novel bed-based task/ambient conditioning (TAC) system

7.1 Introduction

The use of TAC systems can help improve thermal comfort and indoor air quality, and reduce the energy consumption. Therefore, a study on developing a novel bed-based TAC system applicable to sleeping environments has been carried out and the experimental part of the study is reported in Chapter 6. The experimental results demonstrated that the use of the novel bed-based TAC system can help achieve energy saving compared to the use of a full air-conditioning (FAC) system, and its operational and energy saving performance would be affected by a number of factors, such as supply air flow rate and temperature, and supply vane angles, etc.

The suitable ranges of operating parameters for various TAC systems were experimentally studied previously and are listed in Table 2.4. These included supply air temperature, velocity, supply direction and heat load level, etc. Moreover, the results of the previous studies showed that by suitably controlling its supply air velocity and temperature, supply air direction, etc., a TAC system can be operated to maintain an acceptable level of thermal comfort and avoid draft in an occupied zone, with a low energy consumption.

Although experimental studies can provide essential performance data of TAC systems, they can be rather costly and time-consuming. Hence, computational tools have been used to numerically study the operating performances of various TAC or personized ventilation (PV) systems [Matsunawa et al. 1995, Gao and Niu 2005b, Jeong et al. 2006, Yang and Skhar 2007, Liu et al. 2008] This reflected that the numerical approach in studying the operating performance of TAC systems was effectively adopted.

Therefore, numerical approach was also employed in the study of developing the novel bed-based TAC system, in order to save study cost and time duration. This Chapter reports on the numerical part of the study. Firstly, the development of a numerical model for the novel bed-based TAC system placed in the experimental bedroom is presented. Secondly, the numerical model is validated using the experimental results at the experimental operating conditions presented in Chapter 6. Finally, the simulated operating performances of the novel bed-based TAC systems at non-experimental operating conditions using the validated numerical model are reported.

7.2 Numerical model development

7.2.1 Numerical model for the novel bed-based TAC system placed in the experimental bedroom

In Chapter 4, the development of a SCTM whose geometry was a real and accurate representation of a nude sleeping female person, obtained by using 3-D laser scanning technique, as shown in Fig. 4.1, is reported. This SCTM was used in the numerical part of the study. A numerical model for the experimental bedroom where the novel bed-based TAC system was installed, as detailed in Chapter 6, was created by using a commercially available Computational Fluid Dynamics (CFD) software package. The origin of X-Y-Z axes for the simulated experimental bedroom was at its geometric centre. The exact locations of the SCTM, the bed with mattress, the supply grille and the detailed dimensions of the simulated experimental bedroom except the return grille were the same as those in the experimental set-up shown in Fig. 6.3. However, the location of the return grille in the numerical model was changed from its original position, Point A on Fig. 6.3, to Point B, also on Fig. 6.3., since this change could help simplify simulations but did not significantly affect the air velocity and temperature in the simulated experimental bedroom, especially in an occupied zone.

Same as in the experimental study reported in Chapter 6, the simulated experimental bedroom was also divided into an occupied zone and an unoccupied zone, respectively. The grids generated in the two zones were different. For the occupied

zone, a two layer volume boundary (as shown in Fig. 7.1) was created around the SCTM in order to accurately simulate the viscous boundary and discretized with unstructured and fine grids, which enabled capturing the boundary wall features. For the unoccupied zone, it was fragmented into structured and coarse girds so as to save computational time. Fig. 7.1 shows the grid generated at x = 0 plane. The total number of cells generated was 1, 401, 885. The near-wall grids close to the SCTM were located in the region of y^+ <1. In order to test the grid independence, a finer grid system with four boundary layers around the SCTM and a total of 1, 708, 457 cells was also created. The two grid systems yielded similar simulation results. Therefore, the grid system with a two layer volume boundary and a total of 1, 401, 885 cells was adopted to save computational time.

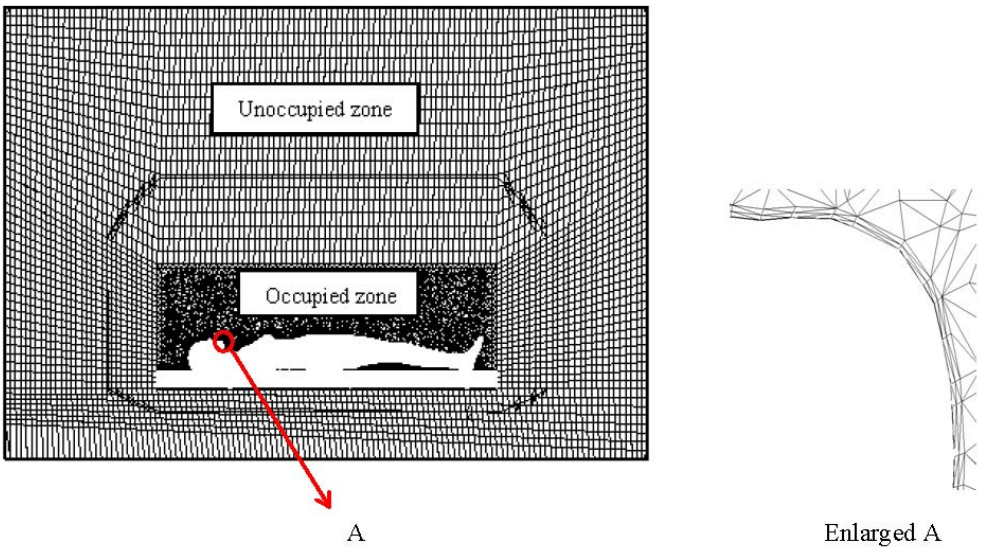

Fig. 7.1 The gird generated inside the simulated experimental bedroom and the local grid showing the two layer volume boundary (at plane x=0)

The sub-models for evaluating the convective, radiative and conduction heat transfer used in this numerical model were the same as those reported in Chapter 4.

The general boundary conditions for the numerical model are shown in Table 7.1. However, the simulated supply air temperatures and flow rates for the supply grilles will be detailed in Section 7.2.2, where different simulation cases are introduced.

Table 7.1 General boundary conditions used in the numerical model

Supply Grille	I = 2 % ; D= 0.18 m
Return Grille	Pressure outlet
SCTM	t_{sk}= 34.6°C, ε_{sk}=0.98
Room wall	Adiabatic wall , ε_{wall}=0.95

7.2.2 Simulation cases

Table 7.2 summarizes the four groups of simulation cases. The purpose of carrying out Group 1 simulation cases was to validate the numerical model for the novel bed-based TAC system placed in the experimental bedroom at the experimental operating conditions, using the experimental results reported in Chapter 6, and that carrying out Groups 2 to 4 simulation cases were to numerically study on the operating performances of the novel bed-based TAC system at non-experimental operating conditions using the validated numerical model. Firstly, in Group 2 simulation cases, the effects of varying supply air flow rate on the performance of

the novel bed-based TAC system were investigated and the results are shown in Fig. 7.14. Secondly, in Group 3 simulation cases whose results are shown in Fig. 7.18, the effects of varying supply air temperature on the performance of the novel bed-based TAC system were examined. Thirdly, in Group 4 simulation cases, the effects of varying supply vane angles on the performance of the novel bed-based TAC system were studied and their results are shown in Fig. 7.21.

Table 7.2 Groups of simulation cases

Group	Case No.	Supply air temperature (°C)	Supply air flow rate (L/s)	Supply vane angle (°)	SCTM covered by	Results shown in
1	1. 1	20	50	0	Nil	Figs.7.2 to 7.13
	1. 2	22	50	0	Nil	
	1. 3	24	50	0	Nil	
	1. 4	20	25	0	Nil	
	1. 5	20	75	0	Nil	
	1. 6	20	50	45	Nil	
	1. 7	20	50	-45	Nil	
	1. 8	20	50	0	B*	
	1. 9	20	50	0	Q2*	
	1. 10	20	50	0	Q1*	
2	2.1	28	25	0	Nil	Fig. 14
	2.2	28	50	0	Nil	
	2.3	28	75	0	Nil	
	2.4	28	100	0	Nil	
	2.5	28	125	0	Nil	
3	3.1	24	75	0	Nil	Fig. 18
	3.2	26	75	0	Nil	
	3.3	28	75	0	Nil	
	3.4	30	75	0	Nil	
	3.5	32	75	0	Nil	
4	4.1	28	75	60	Nil	Fig. 21
	4.2	28	75	45	Nil	
	4.3	28	75	30	Nil	
	4.4	28	75	15	Nil	
	4.5	28	75	0	Nil	
	4.6	28	75	-15	Nil	
	4.7	28	75	-30	Nil	
	4.8	28	75	-45	Nil	
	4.9	28	75	-60	Nil	

*: Details of these beddings are given in Table 4.1.

7.3 Numerical model validation using the experimental results

In the experimental part of the study reported in Chapter 6, both Predicted Mean Vote (PMV) and energy utilization coefficient (EUC) were adopted to evaluate the level of indoor thermal comfort in the occupied zone and the energy saving potential, respectively. The two indexes, defined by Equations (6.1) and (6.5), respectively, were also used in numerical part of the study reported in this Chapter. Using the numerical model described in Section 7.2, the following important parameters used to determine values of PMV and EUC: the sensible heat losses from a sleeping person, Q_{sk}, the average air temperature in the unoccupied zone, t_{uz}, and the average air temperature in the occupied zone, t_{oz}, can be obtained numerically under the given operating and boundary condition. Therefore, the numerical model was firstly validated by comparing the experimental and simulated values of Q_{sk}, t_{oz} and t_{uz}, respectively.

7.3.1 Sensible heat loss

Figs. 7.2 to 7.5 show the comparisons between the simulated and experimental values of Q_{sk} under different experimental operating conditions. It can be seen that the simulated values agreed reasonably well with the experimental values, with a relative error of ±5% for most cases, except for one case.

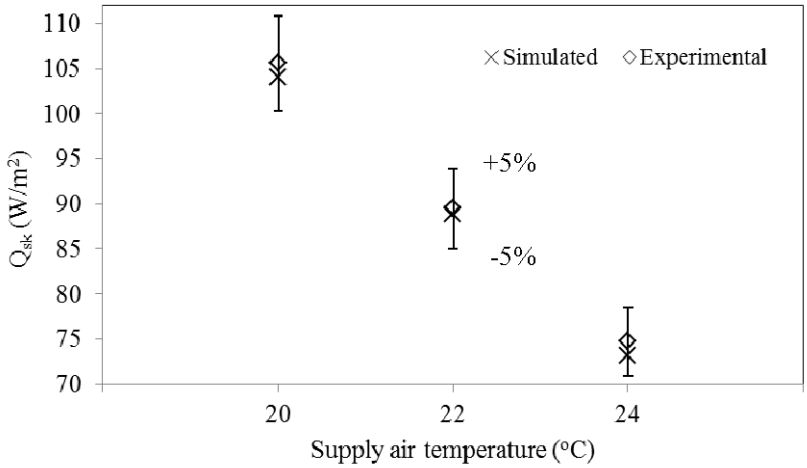

Fig. 7.2 Comparisons between simulated and experimental values of Q_{sk} at different supply air temperatures

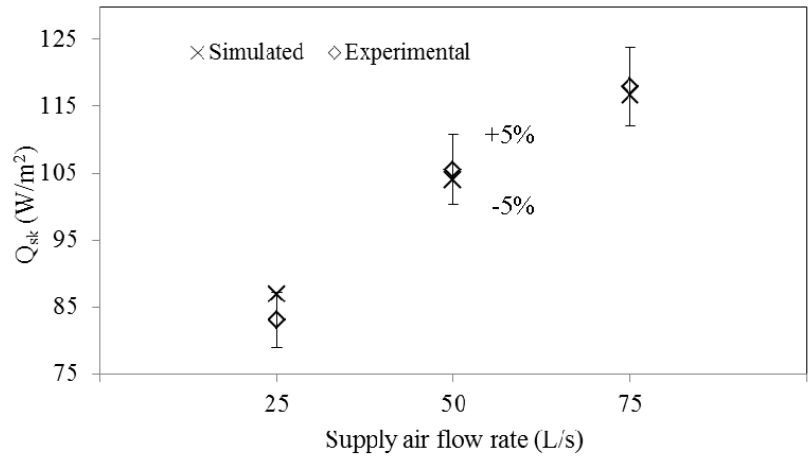

Fig. 7.3 Comparisons between simulated and experimental values of Q_{sk} at different supply air flow rates

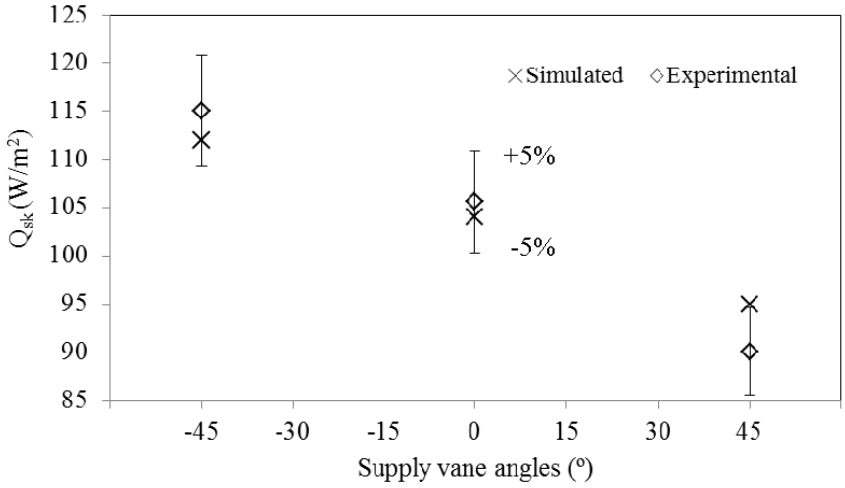

Fig. 7.4 Comparisons between simulated and experimental values of Q_{sk} at different supply vane angles

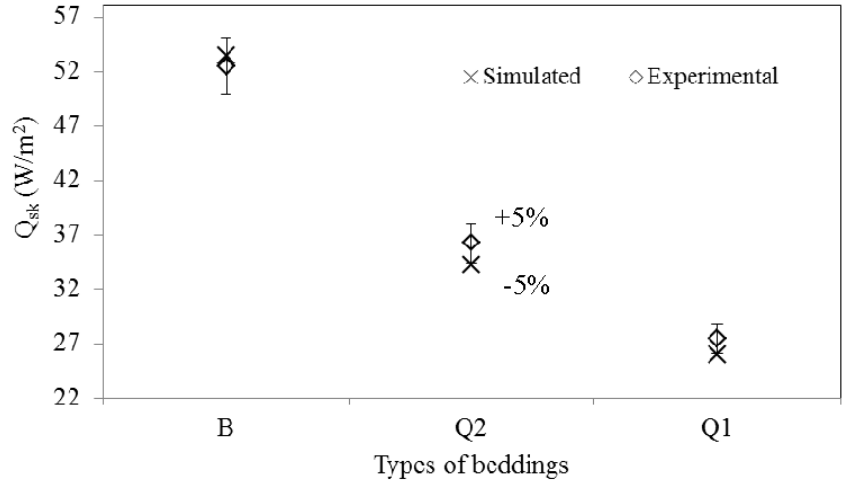

Fig. 7.5 Comparisons between simulated and experimental values of Q_{sk} with different types of beddings

7.3.2 Average air temperature in the occupied and the unoccupied zones

Figs. 7.6 to 7.9 show the comparisons between the simulated and experimental

average air temperatures in the occupied zone, t_{oz}, under different experimental operating conditions, respectively. It can be seen that the simulated values agreed reasonably well with the experimental values, with a relative error of ±2% for most cases.

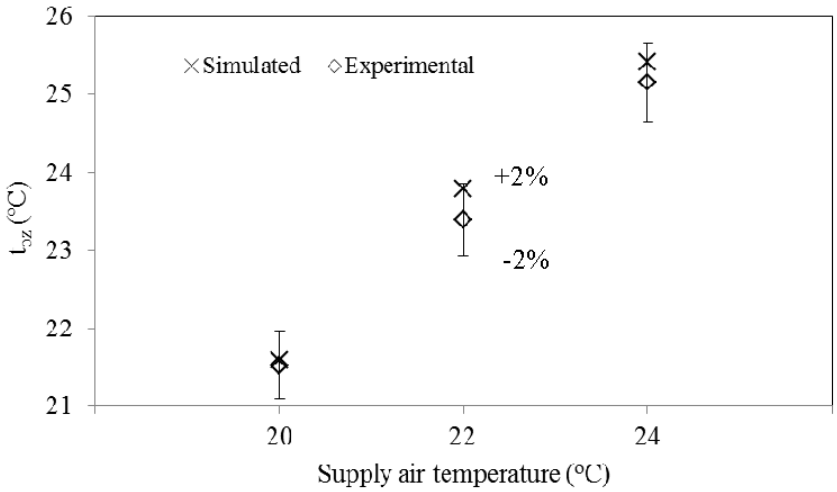

Fig. 7.6 Comparisons between simulated and experimental values of t_{oz} at different supply air temperatures

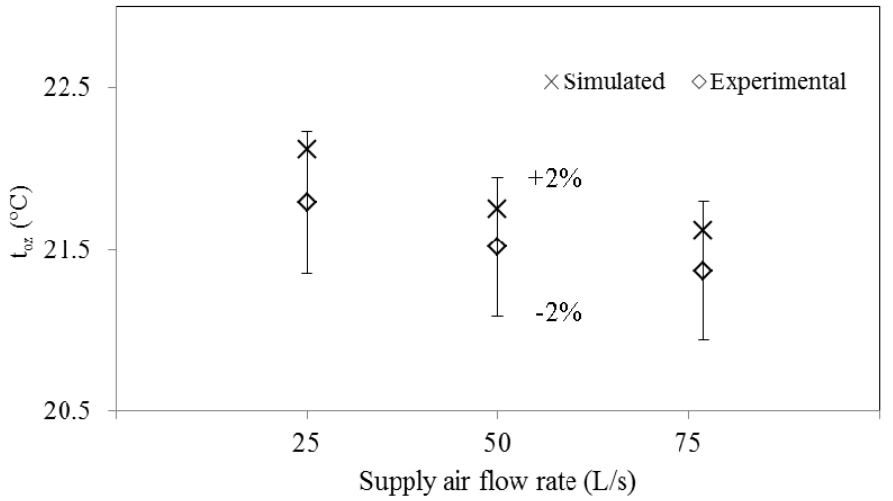

Fig. 7.7 Comparisons between simulated and experimental values of t_{oz} at different supply air flow rates

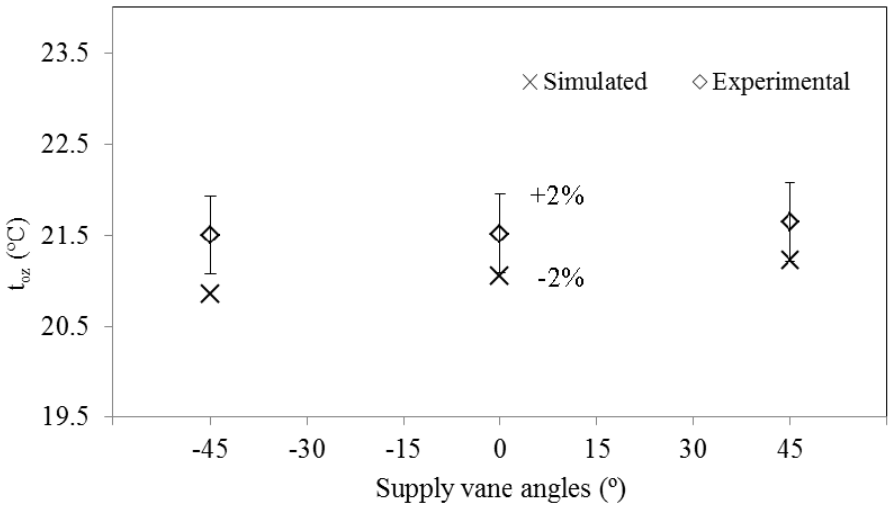

Fig. 7.8 Comparisons between simulated and experimental values of t_{oz} at different supply vane angles

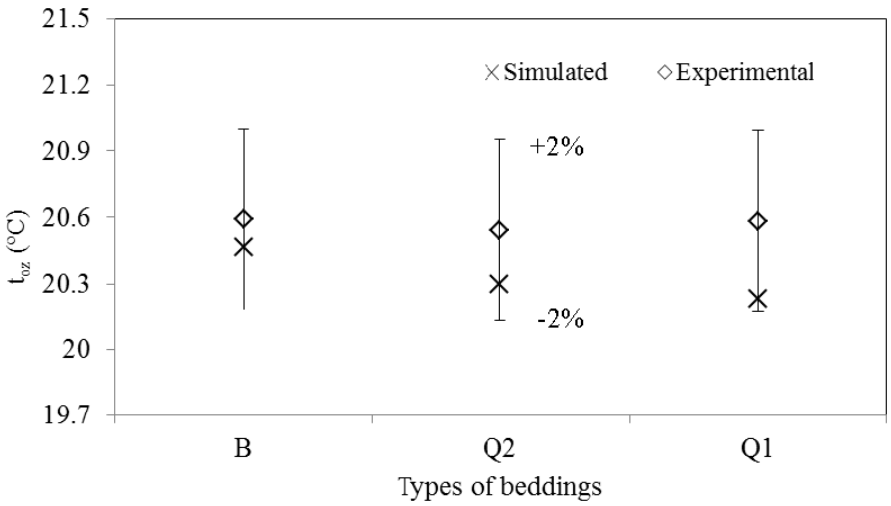

Fig. 7.9 Comparisons between simulated and experimental values of t_{oz} with different types of beddings

Figs. 7.10 to 7.13 show the comparisons between the simulated and experimental average air temperature in the unoccupied zone, t_{uz}, under different experimental operating conditions, respectively. It can be seen that the simulated values agreed reasonably well with experimental values, with a relative error of ±3% for most cases.

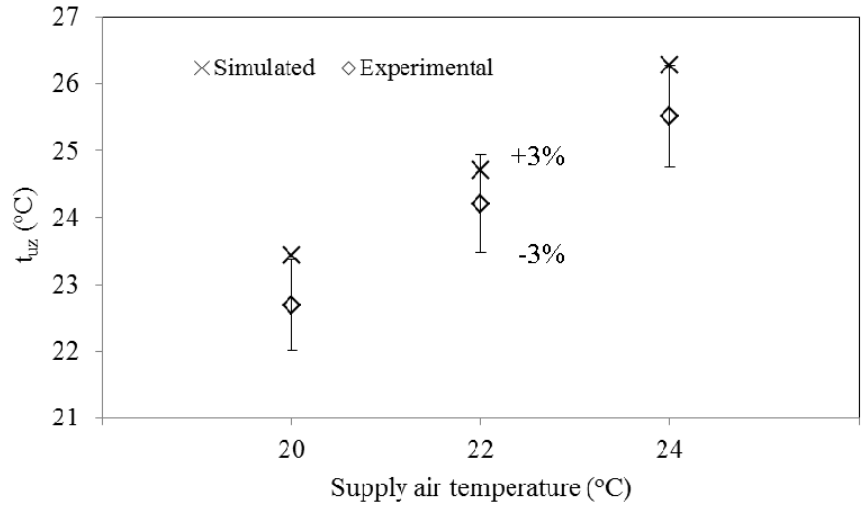

Fig. 7.10 Comparisons between simulated and experimental values of t_{uz} at different supply air temperatures

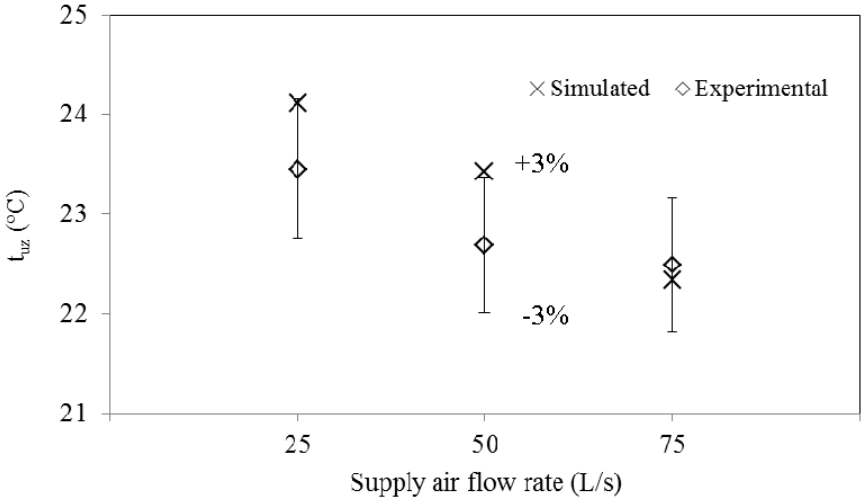

Fig. 7.11 Comparisons between simulated and experimental values of t_{uz} at different supply air flow rates

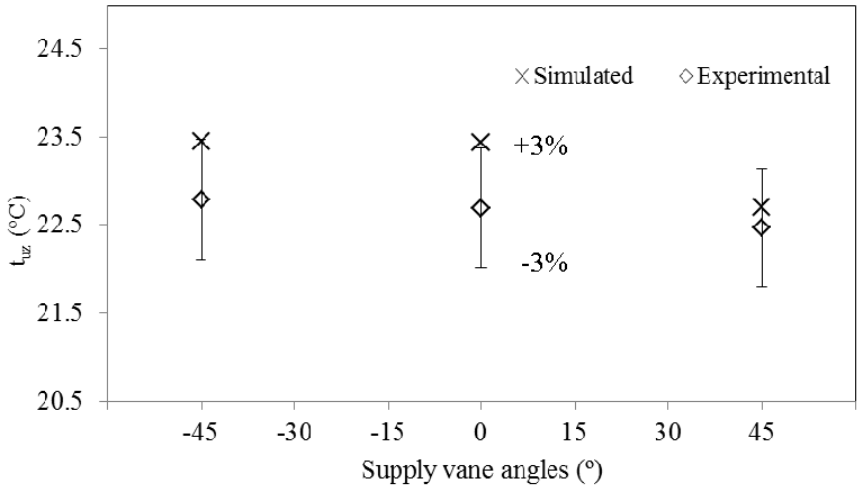

Fig. 7.12 Comparisons between simulated and experimental values of t_{uz} at different supply vane angles

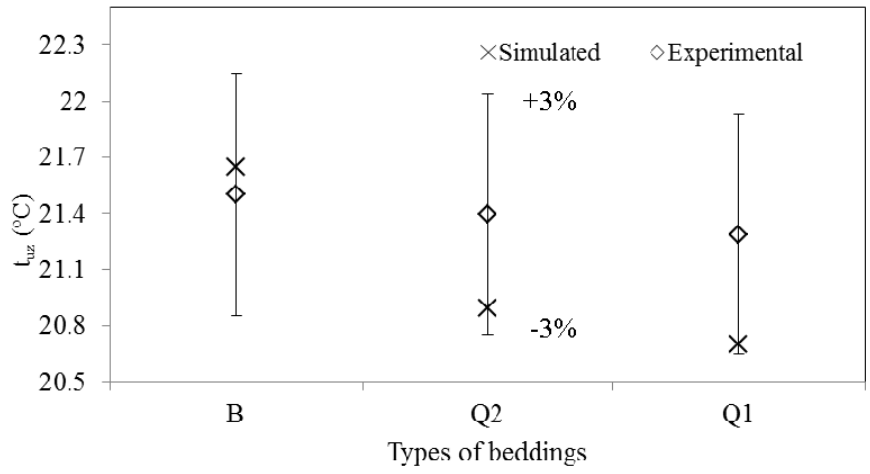

Fig. 7.13 Comparisons between simulated and experimental values of t_{uz} with different types of beddings

The above comparisons shown in Figs 7.2 to 7.13 suggested that the numerical model developed for the novel bed-based TAC system placed in the experimental bedroom could be used to predict the values of Q_{sk}, t_{uz} and t_{oz}, with an

acceptable accuracy.

7.4 Numerical study on the performance of the bed-based TAC system using the validated numerical model

In this section, the validated numerical model was used to evaluate the performance of the novel bed-based TAC system at the non-experimental operating conditions other than the experimental ones specified in Chapter 6.

From Section 7.3, it is known that all parameters to determine both PMV and EUC may be directly obtained using the numerical model except the total insulation value of a bedding system, R_t. Therefore, a naked SCTM was assumed, giving the value of R_t of 0.152 m^2·K/W [Lin and Deng 2008b].

7.4.1 Predicted PMVs in the occupied zone and predicted EUCs at different supply air flow rates

Fig. 7.14 shows the predicted values of EUC and PMV for Group 2 simulation cases. It can be seen that the predicted PMV values decreased with the increase in supply air flow rate, because the supply air flow rate mainly affected the thermal environment in the occupied zone. Therefore, a higher supply air flow rate would result in a reduction in the average air temperature in the occupied zone, leading to

an increase in sensible heat loss from the SCTM. Hence the predicted PMV values would be smaller according to Equation (6.1). These agreed well with the experimental results shown in Chapter 6.

However, the predicted EUC values increased firstly with the increase in supply air flow rate when the supply air flow rate increased to more than 75 L/s, but decreased thereafter. When the supply air flow rate was small, a higher supply air flow rate would result in a larger reduction in the average air temperature in the occupied zone than that in the unoccupied zone, leading to a higher EUC. However, at a large supply air flow rate, the air temperature in the unoccupied zone can also be significantly affected by the supply air. Therefore, the average air temperature in the unoccupied zone became close to that in the occupied zone, leading to a lower value of EUC. Figs. 7.15 and 7.16 show the simulated air temperature distributions inside the simulated experimental bedroom at the supply air flow rates 75 L/s and 100 L/s, respectively. Furthermore, Fig. 7.17 shows the simulated air velocity distribution inside the simulated experimental bedroom at the supply air flow rate of 75 L/s. As seen, the air velocity around SCTM was all smaller than 0.25 m/s, so that cold draft may be avoided.

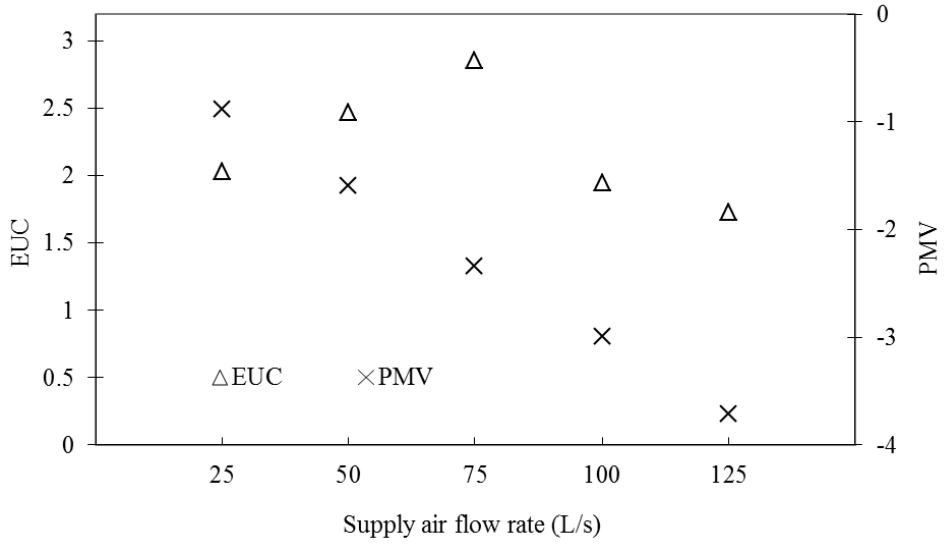

Fig. 7.14 Predicted EUCs and PMVs at different supply air flow rates

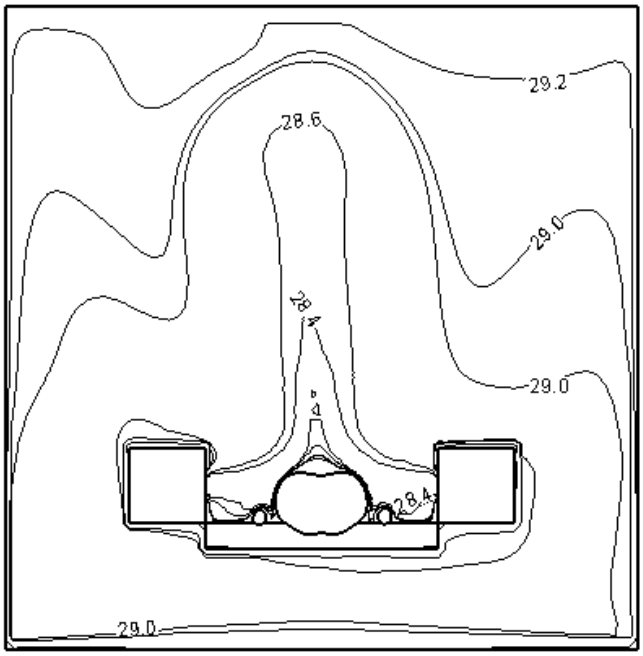

Fig. 7.15 Simulated air temperature distribution inside the simulated experimental bedroom at a supply air flow rate of 75 L/s (at y=0 plane)

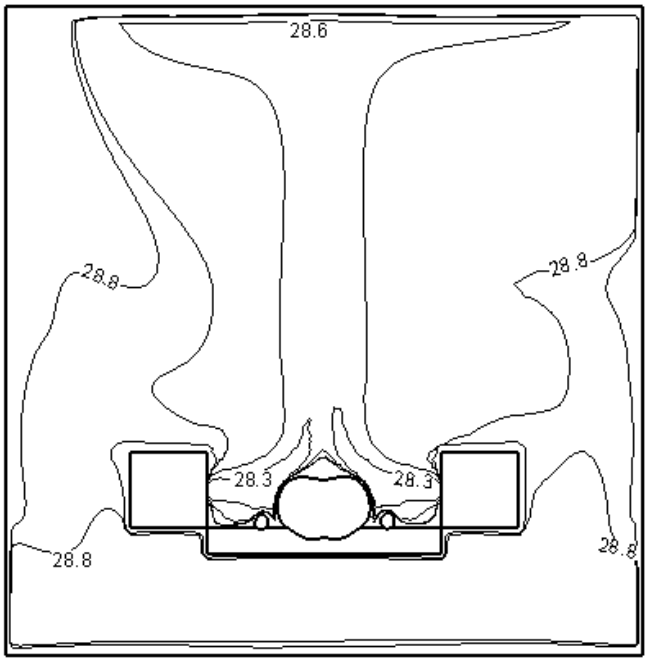

Fig. 7.16 Simulated air temperature distribution inside the simulated experimental bedroom at a supply air flow rate, 100 L/s (at y=0 plane)

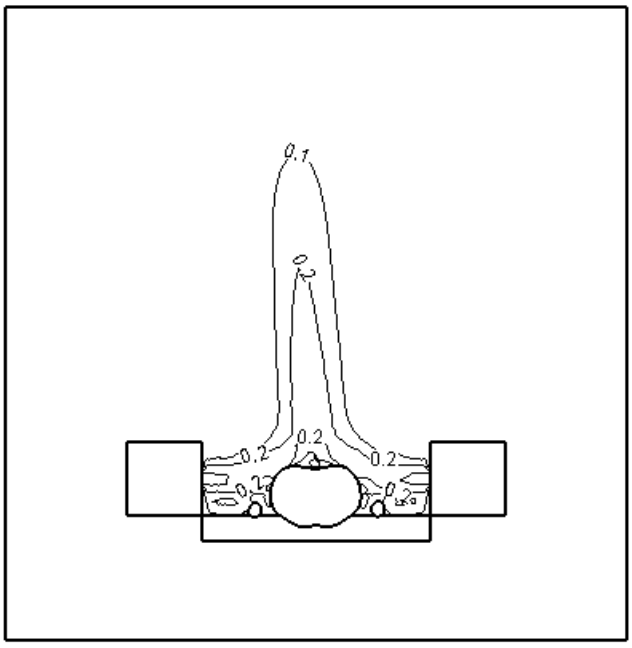

Fig. 7.17 Simulated air velocity distribution inside the simulated experimental bedroom at a supply air flow rate, 75 L/s (at y=0 plane)

From the above analysis, the supply air flow rate of 75 L/s might be regarded as an optimum one for the novel bed-based TAC system because of the largest saving energy potential without the risk of cold draft inside the occupied zone. Therefore, in the follow-up numerical study to be presented in the next two sections, a fixed supply air flow rate of 75 L/s was adopted.

7.4.2 Predicted PMVs in the occupied zone and predicted EUCs at different supply air flow temperatures

Fig. 7.18 shows the predicted values of EUC and PMV for Group 3 simulation cases. It can be seen that the predicted PMV values increased with the increase in supply air flow temperature, because at the supply flow rate of 75 L/s, the supply air mainly affected the thermal environment inside the occupied zone. Therefore, a higher supply air flow temperature would result in an increase in the average air temperature in the occupied zone, leading to a reduction in sensible heat loss from the SCTM. Hence the predicted PMV values would be larger according to Equation (6.1). These agreed well with the experimental results shown in Chapter 6.

However, the predicted values of EUC decreased with the increase in supply air flow temperature. Fig. 7.19 and Fig. 7.20 show the simulated air temperature distributions inside the simulated experimental bedroom at a supply air flow temperature of 26°C

and 30°C, respectively. It can be seen that with a higher supply air temperature, the average air temperature in the unoccupied zone would be close to that in the occupied zone, leading to a lower EUC value.

A lower supply air flow temperature would lead to more energy saving, but at the expense of reduced thermal comfort level, when the novel bed-based TAC system was used. For example, when the supply air temperature was at 26°C, the value of PMV was -3.9, which indicated that an acceptable level of thermal comfort was not resulted in.

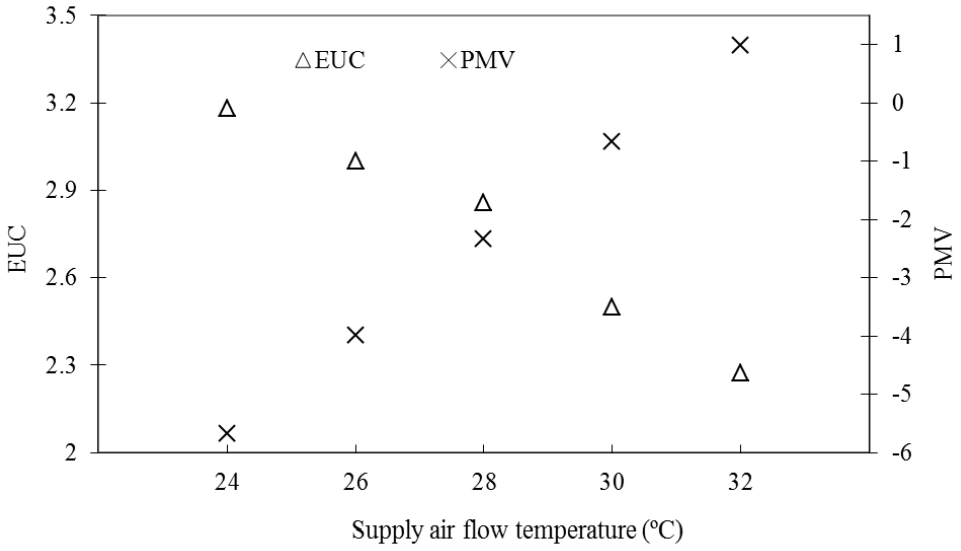

Fig. 7.18 Predicted EUCs and PMVs at different supply air flow temperatures

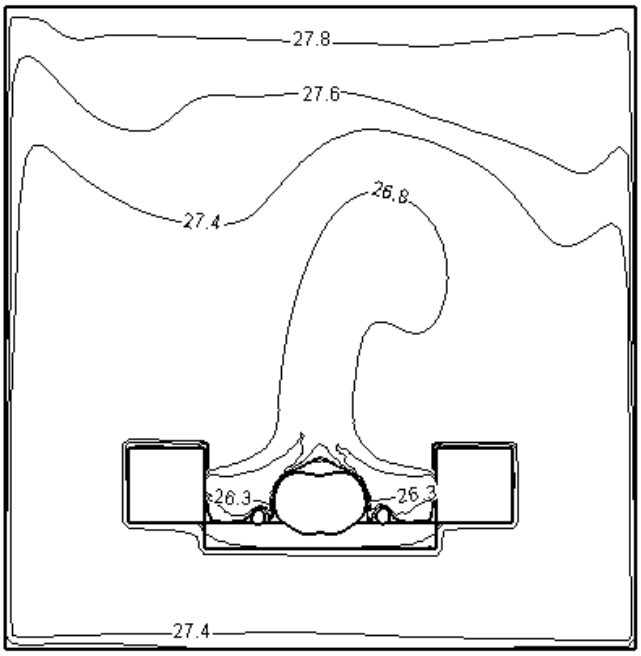

Fig. 7.19 Simulated air temperature distribution inside the simulated experimental bedroom at a supply air flow temperature of 26 °C (at y=0 plane)

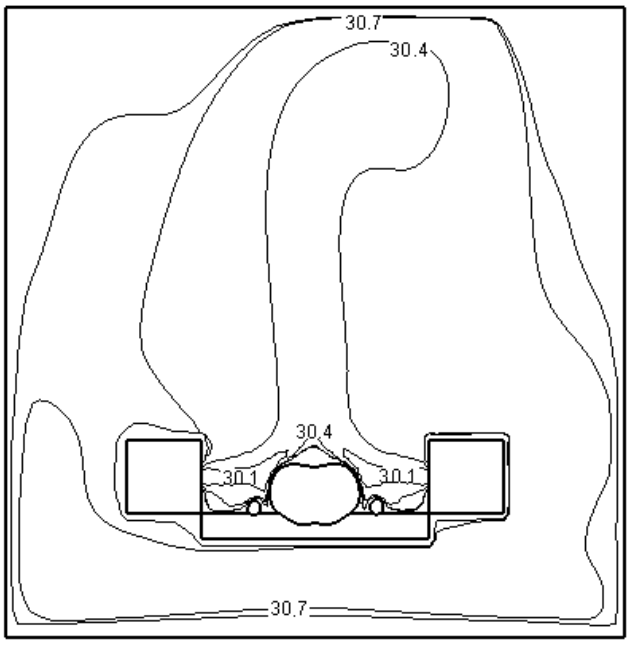

Fig. 7.20 Simulated air temperature distribution inside the simulated experimental bedroom at a supply air flow temperature of 30 °C (at y=0 plane)

7.4.3 Predicted PMVs in the occupied zone and predicted EUCs at different supply vane angles

Fig. 7.21 shows the predicted values of EUC and PMV for Group 4 simulation cases. As seen, at a supply vane angle of +60°, the predicted value of EUC was even smaller than 1. This was due to the fact that the air in the unoccupied zone was fully cooled down by the supply air, and the thermal plume around the SCTM became significant in the occupied zone. When the supply vane angle was set at +30°, the predicted EUC value was larger than 1. This was because part of the supply air was used to cool down the air in the unoccupied zone, and the thermal plume around the SCTM was partially depressed in the occupied zone. The predicted EUC values increased when supply vane angle was altered from -30° to 0°, and then to -60°. When the supply vane angle was at between 0°and -60°, the supply air was directed to the lower part of the occupied zone where the thermal plume around the SCTM was fully depressed, creating a lower average air temperature in the occupied zone, and resulting in a higher EUC value. Figs. 7.22 to 7.25 show the simulated air temperature distributions inside the simulated experimental bedroom at the supply vane angle of 60°, 45°, -45°and -60°, respectively. Therefore, when using the novel bed-based TAC system, the supply vane angle was an important parameter affecting the energy saving.

On the other hand, the value of PMV remained virtually unchanged when supply vane angle was altered from +60° to +45°, since the thermal plume around the SCTM dominated in the occupied zone at these two supply vane angles, as shown in Fig. 7.22. However, when supply vane angle was changed from +45° to +0°, the predicted values of PMV decreased significantly. Since the thermal plume around the SCTM was depressed by the supply air, as shown in Fig. 7.24, a lower average air temperature in the occupied zone temperature would lead to a higher sensible heat loss from the SCTM and hence a lower PMV value. Moreover, when supply vane angle was changed from +0° to -60°, the predicted values of PMV gradually decreased, since the average air temperature in the occupied temperature was around 28.2°at these supply vane angles, as shown in Figs. 7.24 and 7.25.

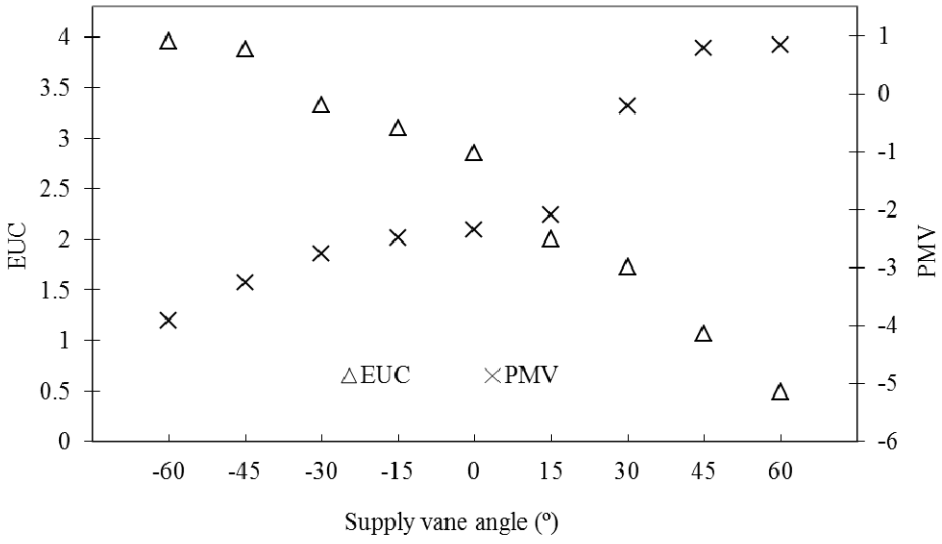

Fig. 7.21 Predicted EUCs and PMVs at different supply vane angles

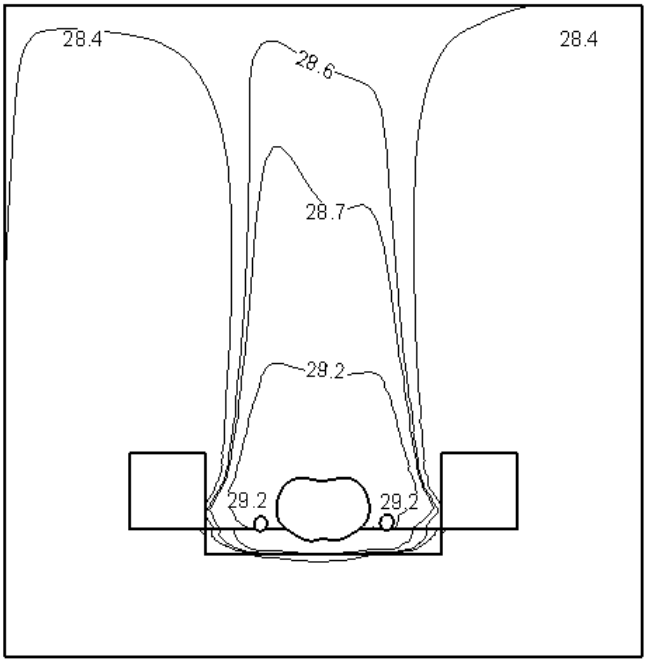

Fig. 7.22 Simulated air temperature distribution inside the simulated experimental bedroom at a supply vane angle of 60° (at y=0 plane)

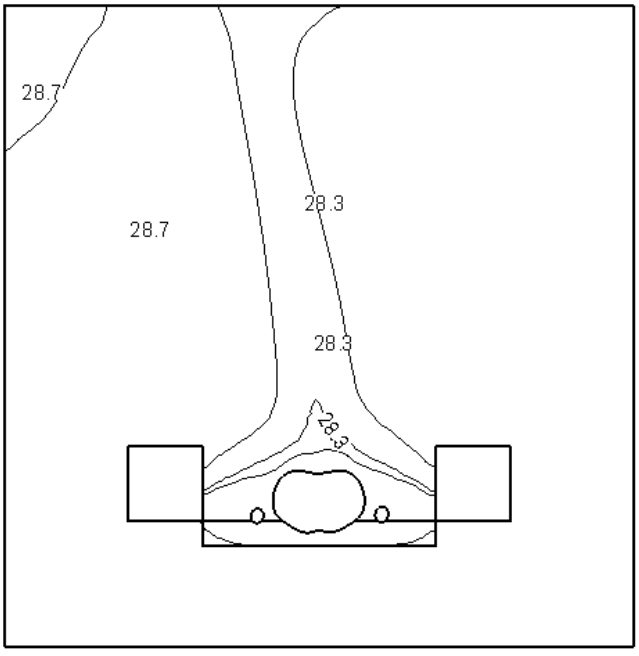

Fig. 7.23 Simulated air temperature distribution inside the simulated experimental bedroom at a supply vane angle of 30° (at y=0 plane)

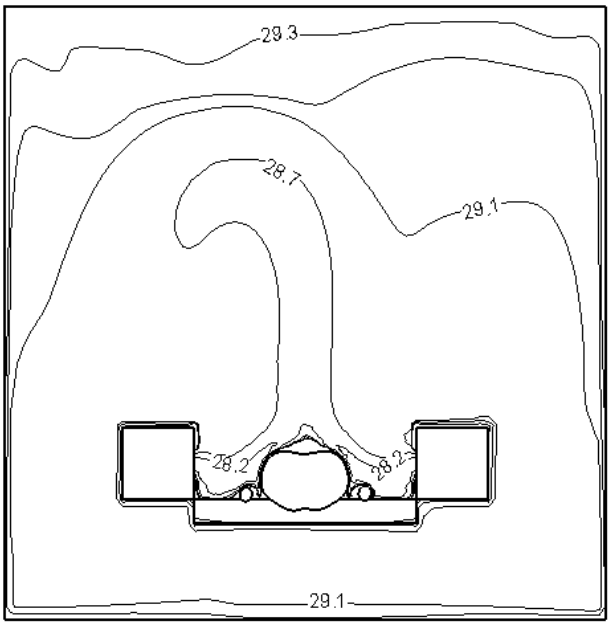

Fig. 7.24 Simulated air temperature distribution inside the simulated experimental bedroom at a supply vane angle of -30° (at y=0 plane)

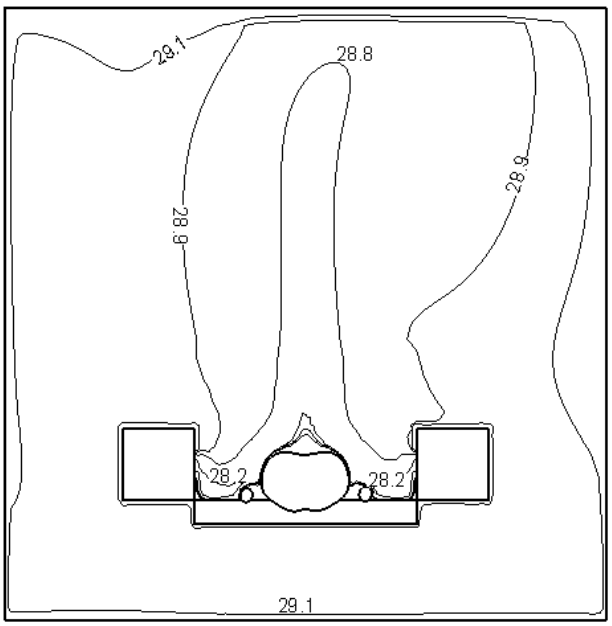

Fig. 7.25 Simulated air temperature distribution inside the simulated experimental bedroom at a supply vane angle of -60° (at y=0 plane)

7.5 Conclusions

A study on developing a novel bed-based TAC system has been carried out both experimentally and numerically. The experimental part and numerical part are reported in Chapter 6 and this Chapter, respectively. A numerical model for the novel bed-based TAC system placed in the experimental bedroom has been developed. The numerical model was validated using the experimental results presented in Chapter 6, proving that the numerical model could be used to predict the values of Q_{sk}, t_{uz} and t_{oz}, with an acceptable accuracy. Therefore, the operating performances of the novel bed-based TAC systems at non-experimental operating conditions were numerically studied using the validated numerical model, in terms of PMV and EUC, and the study results are reported. The numerical study results showed that by suitably controlling its supply air flow velocity and temperature, supply vane angles, the bed-based TAC system can be operated to maintain an acceptable level of thermal comfort without cold draft in an occupied zone at a low energy consumption.

It is believed that the validated numerical model can be used to predict the impacts of key operating parameters, such as supply air temperature and flow rate, on the operating performances of the novel bed-based TAC system. Therefore, similar numerical approach may also be applied to studying the operating performances of other bed-based TAC systems to save their development cost and time.

Chapter 8

Conclusions and Future Work

8.1 Conclusions

A programmed research work on studying the thermal environment in an air conditioned sleeping space has been successfully carried out and is reported in this thesis. The conclusions of the thesis are:

1) Two numerical studies on the micro-climate around, and the thermal neutrality of a sleeping person a sleeping person placed in a space with a displacement ventilation system have been carried out and are reported in Chapter 4. A sleeping computational thermal manikin (SCTM) was successfully developed and used in the two numerical studies. In the first numerical study, the micro-climate around the SCTM was, in terms of air temperature and velocity distributions and the heat transfer characteristics, numerically examined. The results of this numerical study were validated by comparing the simulated results with those obtained from previous related studies. In the second numerical study, the thermal neutrality for a naked sleeping person was investigated and the effects of the total insulation value of a bedding system on the thermal neutrality of a sleeping person placed in a space with a displacement ventilation system were also examined. The results showed that the thermal resistance of a bedding could significantly affect the thermal neutral temperature of a sleeping person, i.e., the higher the thermal resistance of the bedding, the lower the thermal neutral temperature. It was further suggested that the supply air velocity did not

significantly affect the thermal neutral temperature when people were covered with different beddings at 100% percentage coverage of body surface area by bedding and bed. The results of the second numerical study obtained were in good agreement with those from earlier related studies. People should be encouraged to use as less sleepwear and bedding (or cover as less body surface area by bedding) as possible to lower the total insulation of a bedding system so that the energy use for air conditioning for sleeping environments could be reduced to maintain a neutral sleeping environment.

2) Chapter 5 reports on the development of a four-node thermoregulation model to predict the thermoregulatory responses of a sleeping person. The model was validated by comparing the predicted values with the experimental data available in open literature. The comparison results demonstrated that the four-node thermoregulation model developed could be used to predict the thermoregulatory responses of a sleeping person with an acceptable accuracy. Therefore, the validated four-node thermoregulation model can be used to predict different indoor thermal parameters, such as air temperature and humidity, in a sleeping environment and different bedding systems on the thermoregulatory responses of a sleeping person. Consequently, the model is expected to be a powerful tool in the future studies on thermal comfort in sleeping environments and the related energy efficiency issues.

3) A study on evaluating the operational and energy saving performance of a novel bed-based TAC system is carried out using experimental and numerical approaches. The experimental part is firstly reported in Chapter 6, where the

development of the novel bed-based TAC system placed in an experimental bedroom and the related experimental performance evaluations are presented. The comparisons of EUCs between using a FAC system and the novel bed-based TAC system at different supply air temperatures were carried out. The EUC values when using the TAC system were all greater than 1.0. The experimental results and their analysis demonstrated that the use of the novel bed-based TAC system can help achieve energy saving, compared to the use of the FAC system. The results analysis further suggested that the operational and energy saving performances of the novel bed-based TAC system would be affected by a number of factors, such as supply air flow rates and temperatures, and supply vane angles, etc. For example, the EUC values slightly decreased when supply vane angles changed from -45° to 0°, and then to +45°, while however the PMV values increased. Furthermore, given the limitations of the current experimental bedroom, the energy saving potential using the novel bed-based TAC system in an actual bedroom was studied through a theoretical analysis. The results of theoretical analysis demonstrated that the energy saving potential when applying the novel bed-based TAC system to an actual bedroom can be significantly larger than that in the experimental bedroom. On the other hand, the numerical part is secondly reported in Chapter 7. A numerical model for the novel bed-based TAC system placed in the experimental bedroom has been developed. The numerical model was validated using the experimental results presented in Chapter 6, proving that the numerical model could be used to predict the values of Q_{sk}, t_{uz} and t_{oz}, with an acceptable accuracy. Then, the operating performances of the novel bed-based TAC systems at non-experimental operating conditions were numerically studied using the validated numerical model, in terms of PMV and

EUC. The numerical results showed that the supply air flow rate of 75 L/s might be regarded as an optimum one for the novel bed-based TAC system because of the largest energy saving potential without the risk of cold draft inside the occupied zone. At a supply vane angle of $+60^{\circ}$, the predicted value of EUC was even smaller than 1. When the supply vane angle was set at $+30^{\circ}$, the predicted EUC value was larger than 1. The predicted EUC values increased when the supply vane angle was altered from -30° to 0°, and then to -60°. Therefore, it was shown that by suitably controlling its supply air flow velocity and temperature, supply vane angles, the bed-based TAC system can be operated to maintain an acceptable level of thermal comfort without cold draft in an occupied zone at a low energy consumption. This novel bed-based TAC system may be applied to not only bedrooms in residences, but also hotel guest rooms and hospital wards during nighttime.

The outcomes of the programmed research work reported in this thesis have made significant contributions to studying the thermal environment in an air conditioned sleeping space. This would in turn help provide people with a thermally comfortable sleeping environment at a low energy consumption. The long-term significance of the work is its contribution to developing advanced air conditioning technology for sleeping environments to achieve a high level of indoor thermal comfort for sleepers at a low energy consumption.

8.2 Proposed future work

A number of future studies following on the successful completion of the project reported in this thesis are proposed:

1) Numerical approaches have been employed in the studies reported in Chapter 4 and Chapter 7. The mean indoor air relative humidity was however assumed at 50% in these studies and the air humidity distributions in a simulated space cannot be therefore predicted. At a moderate air temperature, air humidity did not significantly affect the thermal neutrality of a sleeping person. However, Okamoto-Mizuno et al. [1999] pointed out that at a high air temperature, a high humidity exposure for a sleeping person during night would increase the thermal load to suppress the decrease in rectal temperature, leading to an increased wakefulness. Moreover, indoor air humidity should be controlled within a suitable range to avoid bacterial growth in certain hospital wards. Therefore, it is highly desirable to incorporate simulating humidity distributions in a sleeping space in future numerical studies.

2) The experimental part and numerical part of a study to evaluate the operational and energy saving performance of a novel bed-based TAC system are presented in Chapter 6 and Chapter 7, respectively. However, the current novel bed-based TAC system has bulky supply air plenums. If a bed-based TAC system is to find a large-scale real-life applications, its design should be incorporated with the design of a bed so as to provide people with convenience when using the bed, and to save space. Therefore, other types of TAC systems should also be designed, and their operating performances experimentally and numerically investigated.

3) In the experimentally and numerically study reported in Chapter 6 and Chapter 7, only the level of thermal comfort was used to evaluate the operational performance of a novel bed-based TAC system. However, indoor air quality (IAQ) should also be considered. This is particularly important for places like hospital wards and guest rooms in prestigious hotels. Moreover, the level of IAQ is directly related to fresh air supply, which significantly affects energy consumption. Therefore, the level of IAQ should be considered when evaluating the operational and energy performance of any future novel bed-based TAC systems.

4) It is believed that the validated four-node thermoregulation model can be used to predict the impacts of different indoor thermal parameters, such as air temperature and humidity, in a sleeping environment and different bedding systems on the thermoregulatory responses of a sleeping person. This can however be studied in future.

5) The research reported in this thesis focused on the application of TAC systems in a single bed sleeping environment. The future potential application of the bed-based TAC system may include, but not limited to, multi-bed sleeping environments, such as a standard hotel guestroom having two beds, a multi-bed hospital ward, and in a sleeping berth compartment in a long-distance train. An investigation on the application of the bed-based TAC systems in a multiple-bed sleeping environment should be carried out in future.

References

1. Amai et al. 2007
Amai, H., Tanabe, S., Akimoto, T. and Genma, T.
Thermal sensation and comfort with different task conditioning system. *Building and Environment*, 2007, Vol. 42, No. 12, pp. 3955-3964 (2007)

2. ANSI/ASHRAE 2004
ASHRAE
ANSI/ASHRAE Standard 55-2004, Thermal Environment Conditions for Human Occupancy (2004)

3. Arens et al. 1991
Arens, E.A., Bauman, F.S., Johnston, L.P. and Zhang, H.
Testing of localized ventilation systems in a new controlled environment chamber. *Indoor Air*, 1991, Vol. 1, No. 3, pp. 263-281 (1991)

4. Argon 1994
Argon Corporation
The Argon system. Naples, FL: Argon Corporation, November (1994)

5. ASHRAE Handbook 2009
ASHRAE
Handbook of Fundamentals (2009)

6. Atkin 1963
Atkin, A.R.
An electrical analogue network of heat flow in the human body. *The South African Institution of Mechanical Engineer*, 1963, Vol. 13, No. 4, pp. 40-46 (1963)

7. Bach et al. 2002
Bach, V., Telliez, F. and Libert, J.P.
The interaction between sleep and thermoregulation in adults and neonates. *Sleep Medicine Reviews*, 2002, Vol. 6, No. 6, pp. 481-492 (2002)

8. Baldwin and Barth 1990
Baldwin, B.S. and Barth, T.J.
A one-equation turbulence transport model for high Reynolds number wall-bounded flows. NASA TM-102947, National Aeronautics and Space Administration, Ames Research Center, Moffett Field, CA. (1990)

9. Basner et al. 2011
Basner, M., Müller, U. and Elmenhorst, E.M.
Single and combined effects of air, road, and rail traffic noise on sleep and recuperation. *Sleep*, 2011, Vol. 34, No. 1, pp. 11-23 (2011)

10. Bauman and Arens 1996
Bauman, F.S. and Arens, E.A.
Task/ambient conditioning systems: engineering and application guidelines. Research Report. Center for Environment Design Research, University of California, Berkeley (1996)

11. Bauman et al. 1995
Bauman, F.S., Arens, E.A., Tanabe, S., Zhang, H. and Baharlo, A.
Testing and optimizing the performance of a floor-based task conditioning system. *Energy and Buildings*, 1995, Vol. 22, No. 3, pp. 173-186 (1995)

12. Bauman et al. 1998
Bauman, F.S., Carter, T.G., Baughman, A.V. and Arens, E.A.
Field study of the impact of a desktop Task/ambient conditioning system in office buildings. *ASHARE Transactions*, 1998, Vol. 104, Pt.1, pp. 1153-1171 (1998)

13. Bauman et al. 1991
Bauman, F.S., Johnston, L.P., Zhang, H. and Arens, E.A.
Performance testing of a floor-based, occupant controlled office ventilation system. *ASHARE Transactions*, 1991, Vol.97, Pt.1, pp. 553-565 (1991)

14. Bauman et al. 1993
Bauman, F.S., Zhang, H., Arens, E.A. and Benton, C.
Localized comfort control with a desktop task conditioning system: laboratory and field measurements. *ASHARE Transactions*, 1993, Vol. 99, Pt. 2, pp. 733-749 (1993)

15. Benzinger 1969
Benzinger, T.H.
Heat regulation: homeostasis of central temperature in man. *Physiological Reviews*, 1969, Vol. 49, No. 4, pp. 671-759 (1969)

16. BjØrn and Nielsen 1998
BjØrn, E. and Nielsen, P.V.
CFD simulation of contaminant transport between two breathing persons. *Proceedings of ROOMVENT'98*, 1998, Vol. 2, pp. 133-140 (1998)

17. Brebbia and Altshuler 1965
Brebbia, D.R. and Altshuler, K.Z.
Oxygen consumption rate and electroencephalographic stage of sleep. *Science*, 1965, Vol. 150, No. 703, pp. 1621-1623 (1965)

18. Brohus and Nielsen 1995
Brohus, H. and Nielsen, P.V.
Personal exposure to contaminant sources in uniform velocity field. *Proceedings of Healthy Buildings' 95*, 1995, No.3, pp. 1555-1560 (1995)

19. Candas et al. 1979a
Candas, V., Libert, J.P. and Vogt, J.J.
Influence of air velocity and heat acclimation on human skin wittedness and sweating efficiency. *Journal of Applied Physiology*, 1979a, Vol. 47, No. 6, pp.1194-1200 (1979a)

20. Candas et al. 1979b
Candas, V., Libert, J.P. and Vogt, J.J.
Human skin wittedness and evaporative efficiency of sweating. *Journal of Applied Physiology*, 1979b, Vol. 46, No. 3, pp.522-528 (1979b)

21. Candas et al. 1982
Candas, V., Libert, J.P. and Muzet, A.
Heating and cooling stimulations during SWS and REM sleep in man. *Journal of Thermal Biology*, 1982, Vol. 7, No. 3, pp.155-158 (1982)

22. Chen 1995
Chen, Q.
Comparison of different k-ε models for indoor airflow computations. *Numerical Heat Transfer, Part B: Fundamentals*, 1995, Vol. 28, No. 3, pp. 353-369 (1995)

23. Chen 1996
Chen, Q.
Prediction of room air motion by Reynolds-stress models. *Building and Environment*, 1996, Vol. 31, No. 3, pp. 233-244 (1996)

24. Chen and Srebric 2002
Chen, Q. and Srebric, J.
A procedure for verification, validation, and reporting of indoor environment CFD analysis. *HAVC&R Research*, 2002, Vol. 8, No. 2, pp. 201-216 (2002)

25. Chen and Xu 1998
Chen, Q. and Xu, W.
A zero-equation turbulence model for indoor airflow simulation. *Energy and buildings*, 1998, Vol. 28, No. 2, pp. 137-144 (1998)

26. Chen and Zhai 2004
Chen, Q. and Zhai, Z.
The use of CFD tools for indoor environmental design. *Advanced Building Simulation*, eds. Malkawi, A. and Augenbroe, G. New York: Spon Press, pp. 119-140 (2004)

27. Chinese Standard JGJ
Ministry of Construction P.R. China
Design standard for energy efficiency of residential buildings in hot summer and warm winter zone (2003)

28. Colin and Houdas 1967
Colin, J. and Houdas, Y.
Experimental determination of coefficient of heat exchanges by convection of human body. *Journal of Applied Physiology*, 1967, Vol. 22, No. 1, pp. 31-38(1967)

29. Crosbie et al. 1961
Crosbie, R.J., Hardy, J.D. and Fessenden, E.
Electrical analog simulation of temperature regulation in man. *IRE Transactions on Bio-Medical Electronics*, 1961, Vol. 8, No. 4, pp. 245-252 (1961)

30. Davidson et al. 2003
Davidson, L., Nielsen, P.V. and Sveningsson, A.
Modification of the V2F model for computing the flow in a 3d wall jet. *Turbulence Heat and Mass Transfer*, 2003, Vol. 4, pp. 577-584 (2003)

31. de Dear et al.1997
de Dear, R.J., Arens, E., Zhang, H. and Oguro, M.
Convective and radiative heat transfer coefficients for individual human body segments. *International Journal of Biometeorology*, 1997, Vol. 40, No. 3, pp. 141-156 (1997)

32. de Dear and Brager 1998
de Dear, R.J. and Brager, G.S.
Developing an adaptive model of thermal comfort and preference. *ASHRAE Transactions*, 1998, Vol. 104, Pt. 1, pp. 145-167 (1998)

33. de Dear and Brager 2002
de Dear, R.J. and Brager, G.S.
Thermal comfort in naturally ventilated buildings: revisions to ASHRAE Standard 55. *Energy and Buildings*, 2002, Vol. 34, No. 6, pp. 549-561 (2002)

34. Deardorff 1970
Deardorff, J.W.
A numerical study of three-dimensional turbulent channel flow at large Reynolds numbers. *Journal of Fluid Mechanics*, 1970, Vol. 41, No. 2, pp. 453-480 (1970)

35. Dewasmes et al. 2003
Dewasmes, G., Loos, N., Candas,V. and Muzet, A.
Effects of a moderate nocturnal cold stress on daytime sleep in humans. *European Journal of Applied Physiology*, 2003, Vol. 89, No. 5, pp. 483-488 (2003)

36. Di Nisi et al. 1989
Di Nisi, J., Ehrhart, J., Galeou, M. and Libert, J.P.
Influence of repeated passive body heating on subsequent night sleep in humans. *European Journal of Applied Physiology and Occupational Physiology*, 1989, Vol. 59, No. 1-2, pp. 138-145 (1989)

37. Dijk et al. 2000
Dijk, D.J., Duffy, J.F. and Czeisler, C.A.
Contribution of circadian physiology and sleep homeostasis to age-related changes in human sleep. *Chronobiology International*, 2000, Vol. 17, No. 3, pp. 285-311 (2000)

38. Doherty and Arens 1988
Doherty, T.J. and Arens, E.A.
Evaluation of the physiological bases of thermal comfort models. *ASHRAE Transactions*, 1988, Vol. 94, Pt. 1, pp. 1371-1385 (1988)

39. DuBois and DuBois 1916
DuBois, D. and DuBois, E.F.
A formula to estimate the approximate surface area if height and weight be known. *Archives of Internal Medicine*, 1916, Vol. 17, pp. 863-871 (1916)

40. Durmer and Dinges 2005
Durmer, J.S. and Dinges, D.F.
Neurocognitive consequences of sleep deprivation. *Seminars in Neurology*, 2005, Vol. 25, No. 1, pp. 117-129 (2005)

41. Emmerich 1997
Emmerich, S.J.
Use of computational fluid dynamics to analyze indoor air quality issues. Report NIS-TIR 5997, National Institute of Standards and Technology, Gaithersburg, MD (1997)

42. Evin and Siekierski 2002
Evin, F. and Siekierski, E.
Sensory evaluation of heating and air conditioning systems. *Energy and Buildings*, 2002, Vol. 34, No. 6, pp. 647-651 (2002)

43. Fanger 1970
Fanger, P.O.
Thermal Comfort. Danish Technical Press. Copenhagen (1970)

44. Fanger et al. 1980
Fanger, P.O., Banhidi, L., Olesen, B.W. and Langkilde, G.
Comfort limits for heated ceiling. *ASHARE Transactions*, 1980, Vol. 86, Pt. 2, pp. 141-156 (1980)

45. Fanger et al. 1986
Fanger, P.O. and Christensen, N.K.
Perception of draught in ventilated spaces. *Ergonomics*, 1986, Vol. 29, No. 2, pp. 215-235 (1986)

46. Faulkner et al. 1993
Faulkner, D., Fisk, W.J. and Sullivan, D.P.
Indoor air flow and pollutant removal in a room with desktop ventilation. *ASHARE Transactions*, 1993, Vol. 99, Pt. 2, pp. 750-758 (1993)

47. Faulkner et al. 1995
Faulkner, D., Fisk, W.J. and Sullivan, D.P.
Indoor airflow and pollutant removal in a room with floor-based task ventilation: results of additional experiments. *Building and Environment*, 1995, Vol. 30, No. 3, pp. 323-332 (1995)

48. Faulkner et al. 1999
Faulkner, D., Fisk, W.J., Sullivan, D.P. and Wyon, D.P.
Ventilation efficiencies of desk-mounted Task/Ambient Conditioning systems. *Indoor air*, 1999, Vol. 9, No. 4, pp. 273-281 (1999)

49. Fiala 1998
Fiala, D.
Dynamic simulation of human heat transfer and thermal comfort. PhD dissertation, Institute of Energy and Sustainable Development, De Montfort University, Leicester (1998)

50. Fletcher, et al. 1999
Fletcher, A., Heuvel, C.V.D. and Dawson, D.
Sleeping with an electric blanket: Effects on core body temperature, sleep and melatonin in young adults. *Sleep*, 1999, Vol. 22, pp. 313-318 (1999)

51. Fu 1995
Fu, G.
A transient three-dimensional mathematical thermal model for the clothed human. PhD dissertation, Kansas State University, Manhattan, Kansas (1995)

52. Gagge 1973
Gagge, A.P.
A two-node model of human temperature regulation in FORTRN. *In Bioastronautics Data Book*, 2nd., eds. Washington, D.C. (1973)

53. Gagge et al. 1986
Gagge, A.P., Fobelets, A.P. and Berglund, L.G.
A standard predictive index of human response to the thermal environment. *ASHRAE Transactions*, 1986, Vol. 92, Pt. 2B, pp. 709-731 (1986)

54. Gagge et al. 1971
Gagge, A.P., Stolwijk, J.A.J. and Nishi, Y.
An effective temperature scale based on a simple model of human physiological regulatory response. *ASHRAE Transactions*, 1971, Vol. 77, Pt. 1, pp. 247-262 (1971)

55. Gan 1995
Gan, G.
Evaluation of room air distribution systems using computational fluid dynamics. *Energy and Buildings*, 1995, Vol. 23, No. 2, pp. 83-93 (1995)

56. Gao and Niu 2004
Gao, N.P. and Niu, J.L.
CFD study on micro-environment around human body and personalized ventilation. *Building and Environment*, 2004, Vol. 39, No. 7, pp. 795-805 (2004)

57. Gao and Niu 2005a
Gao, N.P. and Niu, J.L.
CFD study of the thermal environment around a human body: a review. *Indoor and Built Environment*, 2005, Vol. 14, No. 1, pp. 5-16 (2005)

58. Gao and Niu 2005b
Gao, N.P. and Niu, J.L.
Modeling the performance of personalized ventilation under different conditions of room air and personalized air. *HVAC&R Research*, 2005b, Vol. 11, No. 4, pp. 587-602 (2005b)

59. Gao et al. 2006
Gao, N.P., Niu, J.L. and Zhang, H.
Coupling CFD and human person thermoregulation model for the Assessment of personalized ventilation. *HVAC&R Research*, 2006, Vol. 12, No. 3, pp. 497-518 (2006)

60. Germano et al. 1991
Germano, M., Piomelli, U., Moin, P. and Cabot, W.H.
A dynamic subgrid-scale eddy viscosity model. *Physics of Fluids*, 1991, Vol. 3, No. 7, pp. 1760-1765 (1991)

61. Gibsaon and Launder 1978
Gibson, M.M. and Launder, B.E.
Ground effects on pressure fluctuations in the atmospheric boundary layer. *Journal of Fluid Mechanics*, 1978, Vol. 86, Pt. 3, pp. 491-511 (1978)

62. Glotzbach and Heller 1976
Glotzbach, S.F. and Heller, H.C.
Central nervous regulation of body temperature during sleep. *Science*, 1976, Vol. 194, No. 4264, pp. 537-539 (1976)

63. Gong et al. 2005
Gong, N., Tham, K.W. and Melikov, A.K.
Human perception of local air movement and the acceptable air velocity range for local air movement. *Proceedings of Indoor Air*, 2005, pp. 452-457 (2005)

64. Gong et al. 2006
Gong, N., Tham, K.W., Melikov, A.K., Wyon, D.P., Sekhar, S.C. and Cheong, K.W.
The acceptable air velocity range for local air movement in the tropics. *HVAC&R Research*, 2006, Vol. 12, No. 4, pp. 1065-1076 (2006)

65. Gooley et al. 2011
Gooley, J.J., Chamberlain, K., Smith, K.A., Khalsa, S.B.S., Rajaratnam, S.M.W., Reen, E.V., Zeiter, J.M., Czeisler, C.A. and Lockley, S.W.
Exposure to room light before bedtime suppresses melatonin onset and shortens melatonin duration in humans. *The Journal of Clinical Endocrinology & Metabolism*, 2011, Vol. 96, No. 3, pp. E463-472 (2011)

66. Guyton and Hall 2005
Guyton, A.C. and Hall, J.E.
Textbook of Medical Physiology. Saunders/Elsevier Press. (2005)

67. Hammel et al. 1963
Hammel, H.T., Jackson, D.C., Stolwijk, J.A.J., Hardy, J.D. and StrØmme, S.B.
Temperature regulation by hypothalamic proportional control with an adjustable set point. *Journal of Applied Physiology*, 1963, Vol. 18, No. 6, pp. 1146-1154 (1963)

68. Harbison 2002
Harbison, J.
Sleep disorders in older people. *Age and Ageing*, 2002, Vol. 31, pp. 6-9 (2002)

69. Haskell 1978
Haskell, E.H.
Effects of sleep at altered ambient temperatures on electrophysiological sleep and thermoregulatory mechanisms/in human subjects and in ground squirrel. PhD dissertation, University of California Stanta Cruz (1978)

70. Haskell et al. 1981a
Haskell, E.H., Palca, J.W., Walker, J.M., Berger, R.J. and Heller, H.C.
The effects of high and low ambient temperatures on human sleep stages. *Electroencephalography and Clinical Neurophysiology*, 1981a, Vol. 51, No. 5, pp. 494-501 (1981a)

71. Haskell et al. 1981b
Haskell, E.H., Palca, J.W., Walker, J.M., Berger, R.J. and Heller, H.C.
Metabolism and thermoregulation during stages of sleep in humans exposed to heat and cold. *Journal of Applied Physiology*, 1981b, Vol. 51, No. 4, pp. 948-954 (1981b)

72. Hayashi et al. 2002a
Hayashi, T., Ishizu, Y., Kato, S. and Murakami, S.
CFD analysis on characteristics of contaminated indoor air ventilation and

its application in the evaluation of the effects of contaminant inhalation by a human occupant. *Building and Environment*, 2002a, Vol. 37, No. 3, pp. 219-230 (2002a)

73. Hayashi et al. 2002b
Hayashi, T., Murakami, S., Kato, S. and Yang, J.H.
CFD analysis on rising stream around a human body and its effect on inhalation air quality. *ASHARE Transactions*, 2002b, Vol. 108, Pt. 2, pp. 1173-1178 (2002b)

74. Heiselberg et al. 1998
Heiselberg, P., Murakami, S. and Roulet, C.A.
Ventilation of large spaces in buildings: analysis and prediction techniques. *Annex 26: Energy efficient ventilation of large enclosures*, Aalborg University, Aalborg, Demark (1998)

75. Henane et al. 1977
Henane, R., Buguet, A., Roussel, B. and Bittel, J.
Variations in evaporation and body temperature during sleep in man. *Journal of Applied Physiology*, 1977, Vol. 42, No. 1, pp. 50-55 (1977)

76. Hensel 1973
Hensel, H.
Neural processes in thermoregulation. *Physiological Reviews*, 1973, Vol. 53, No. 4, pp. 948-1017 (1973)

77. Hobson 1989
Hobson, J.A.
Sleep. Scientific American Library, A Division of HPHLP, New York, ISSN 1040-3213 (1989)

78. Holman 2010
Holman, J.P.
Heat transfer.10th ed. New York: McGraw Hill (2010)

79. Holmér 2004
Holmér, I.
Thermal manikin history and application. *European Journal of Applied Physiology*, 2004, Vol. 92, No. 6, pp. 614-618 (2004)

80. Höppe 2002
Höppe, P.
Different aspects of assessing indoor and outdoor thermal comfort. *Energy and Buildings*, 2002, Vol. 34, No. 6, pp. 661-665 (2002)

81. Hui et al. 2002
Hui, D.S., Wong, T.Y., Li, T.S., Ko, F.W., Choy, D.K., Szeto, C.C., Lui, S.F. and Li, P.K.
Prevalence of sleep disturbances in Chinese patients with end stage renal failure on maintenance hemodialysis. *Medical Science Monitor*, 2002, Vol. 8, No. 5, pp. CR331-336 (2002)

82. Huizenga et al. 2001
Huizenga, C., Zhang, H. and Arens, E.
A model of human physiology and comfort for assessing complex thermal environments. *Building and Environment*, 2001, Vol. 36, No. 6, pp. 691-699 (2001)

83. ISO 9920 2007
International Standard Organization
ISO 9920 2007: Ergonomics of the thermal environment – Estimation of the thermal insulation and evaporative resistance of a clothing ensemble. (2007)

84. Jeong et al. 2006
Jeong, K., Krarti, M. and Zhai, Z.
CFD-based parametric analysis on the performance of personalized partition air distribution system. *Proceedings of ISEC 2006: ASME International Solar Energy Conference*, July 8-13, Denver, CO (2006)

85. Jones and Whittle 1992
Jones, P.J. and Whittle, G.E.
Computational fluid dynamics for building air flow prediction- Current status and capacities. *Building and Environment*, 1992, Vol. 27, No. 3, pp. 321-338 (1992)

86. Karacan et al. 1978
Karacan, I., Thornby, J.I., Anch, A.M., Williams, R.L. and Perkins, H.M.
Effects of high ambient temperature on sleep in young men. *Aviation, Space, and Environment Medicine*, 1978, Vol. 49, No. 7, pp. 855-860 (1978)

87. Kim and Chen 1989
Kim, S.W. and Chen, C.P.
A multi-time-scale turbulence model based on variable partitioning of the turbulent kinetic energy spectrum. *Numerical Heat Transfer, Part B: Fundamentals*, 1989, Vol. 16, pp. 193-211 (1989)

88. Kreider et al. 1958
Kreider, M.B., Buskirk, E.R. and Bass, D.E.
Oxygen consumption and body temperatures during the night. *Journal of Applied Physiology*, 1958, Vol. 12, No. 3, pp. 361-366 (1958)

89. Kubo et al. 1999
Kubo, H., Yanase, T. and Akagi, H.
Sleep stage and skin temperature regulation during night-sleep in winter. *Psychiatry and Clinical Neurosciences*, 1999, Vol. 53, No. 2, pp. 121-123 (1999)

90. Kurazumi et al. 2008
Kurazumi, Y., Tsuchikawa, T., Ishii, J., Fukagawa, K., Yamato, Y. and Matsubara, N.
Radiative and convective heat transfer coefficients of the human body in natural convection. *Building and Environment*, 2008, Vol. 43, No. 12, pp. 2142-2153 (2008)

91. Ladeinde and Nearon 1997
Ladeinde, F. and Nearon, M.D.
CFD applications in the HVAC&R industry. *ASHRAE Journal*, 1997, Vol. 39, No. 1, pp. 44-48 (1997)

92. Lai and Yang 1997
Lai, J.C.S. and Yang, C.Y.
Numerical simulation of turbulence suppression: Comparison of the performance of four k-ε turbulence models. *International Journal of Heat and Fluid Flow*, 1997, Vol. 18, No. 6, pp. 575-584 (1997)

93. Lang 1979
Lang, V.P.
Principles of air conditioning. 3th edition, Delmar Publishers, Albany, New York (1979)

94. Lam and Bremhorst 1981
Lam, C.K.G. and Bremhorst, K.
A modified form of the k-ε model for predicting wall turbulence. *Journal of Fluids Engineering*, 1981, Vol. 103, No. 3, pp. 456-460 (1981)

95. Launder and Sharma 1974
Launder, B.E. and Sharma, B.I.
Application of the energy-dissipation model of turbulence to the calculation of flow near a spinning disc. *Letters in Heat and Mass Transfer*, 1974, Vol. 1, No. 2, pp. 131-138 (1974)

96. Launder and Spalding 1974
Launder, B.E. and Spalding, D.B.
The numerical computation of turbulent flows. *Computer Methods in Applied Mechanics and Engineering*, 1974, Vol. 3, No. 2, pp. 269-289 (1974)

97. Lavie 1996
Lavie, P.
The Enchanted World of Sleep. Yale University Press, New Haven and London, ISBN 0-300-06602-3 (1996)

98. Liddament 1991
Liddament, M.W.
A review of building air flow simulation. AIVC Technical Note 33, UK (1991)

99. Lilly 1992
Lilly, D.K.
A proposed modification of the Germano subgrid-scale closure method. *Physics of Fluids*, 1992, Vol. 4, No. 2, pp. 633-635 (1992)

100. Lin and Deng 2004
Lin, Z.P. and Deng, S.M.
A study on the characteristic of nighttime bedroom cooling load in tropics and subtropics. *Building and Environment*, 2004, Vol. 39, No. 9, pp. 1101-1114 (2004)

101. Lin and Deng 2006
Lin, Z.P. and Deng, S.M.
A questionnaire survey on sleeping thermal environment and bedroom air conditioning in high-rise residences in Hong Kong. *Energy and Buildings*, 2006, Vol. 38, No. 11, pp. 1302-1307 (2006)

102. Lin and Deng 2008a
Lin, Z.P. and Deng, S.M.
A study on the thermal comfort in sleeping environments in the subtropics – Developing a thermal comfort model for sleeping environments. *Building and Environment*, 2008a, Vol. 43, No. 1, pp. 70-81 (2008a)

103. Lin and Deng 2008b
Lin, Z.P. and Deng, S.M.
A study on the thermal comfort in sleeping environments in the subtropics

–Measuring the total insulation values for bedding systems commonly used in the subtropics. *Building and Environment*, 2008b, Vol. 43, No. 5, pp. 905-916 (2008b)

104. Liu et al. 2008
Liu, W.W., Lian, Z.W. and Yao, Y.
Optimization on indoor air diffusion of floor-standing type room air-conditioners. *Energy and Buildings*, 2008, Vol. 40, No. 2, pp. 59-70 (2008)

105. Macpherson 1973
Macpherson, R.K.
Thermal stress and thermal comfort. *Ergonomics*, 1973, Vol. 16, No. 5, pp. 611-622 (1973)

106. Matsunawa et al. 1995
Matsunawa, K., Lizuka, H. and Tababe, S.
Development and application of an underfloor air-conditioning system with improved outlets for a 'smart' building in Tokyo. *ASHARE Transactions*, 1995, Vol. 101, Pt. 2, pp. 887-901 (1995)

107. McCullough et al. 1987
McCullough, E.A., Zbikowski, P.J. and Jones, B.W.
Measurement and prediction of the insulation provided by bedding systems. *ASHRAE Transactions*, 1987, Vol. 93, Pt. 1, pp. 1055-1068 (1987)

108. Menter 1994
Menter, F.R.
Two equation eddy-viscosity turbulence models for engineering applications. *AIAA Journal*, 1994, Vol.32, No. 8, pp. 1598-1605 (1994)

109. Mihira et al. 1977
Mihira, K., Toda, H. and Arai, H.,
Study on thermal manikin. *Japanese Journal of Human Factor*, 1977, Vol. 13, No. 2, pp. 47-53 (1977)

110. Miyazawa 1994
Miyazawa, M.
Seasonal changes of sleep environment at bedtime and on arising. *The proceeding of the 18th symposium on human-environment system* (1994) [In Japanese]

111. Morin et al. 1998
Morin, C.M., Gibson, D. and Wade, J.

Self-reported sleep and mood disturbance in chronic pain patients. *Clin J Pain*, 1998, Vol. 14, No. 4, pp. 311- 314 (1998)

112. Moser 1992
Moser, A.
Numerical simulation of room thermal convection-Review of IEA Annex 20 results. *Proceeding of International Symposium on Room Air Convection and Ventilation Effectiveness*, Tokyo, Japan, pp. 76- 96 (1992)

113. Murakami 1998
Murakami, S.
Overview of turbulence models applied in CWE-1997. *Journal of Wind Engineering and Industrial Aerodynamics*, 1998, Vol. 74-76, pp. 1-24 (1998)

114. Murakami et al. 1997
Murakami, S., Kato, S. and Zeng, J.
Flow and temperature fields around human body with various room air distribution: CFD study on computational thermal manikin – Part I. *ASHRAE transactions*, 1997, Vol. 10. Pt. 1, pp. 3- 15 (1997)

115. Murakami et al. 2000
Murakami, S., Kato, S. and Zeng, J.
Combined simulation of airflow, radiation and moisture transport for heat release from a human person. *Building and Environment*, 2000, Vol. 35, No. 6, pp. 489-500 (2000)

116. Muzet 2007
Muzet, A.
Environmental noise, sleep and health. *Sleep medicine review*, 2007, Vol. 11, No. 2, pp. 135-142 (2007)

117. Muzet et al. 1983
Muzet, A., Ehrhart, J., Candas,V., Libert, J.P. and Vogt, J.J.
REM sleep and ambient temperature in man. *International Journal of Neuroscience*, 1983, Vol. 18, No. 1-2, pp. 117-126 (1983)

118. Muzet et al. 1984
Muzet, A., Libert, J.P. and Candas,V.
Ambient temperature and human sleep. *Cellular and Molecular Life Sciences*, 1984, Vol. 40, No. 5, pp. 425-429(1984)

119. Nakano et al. 2002
Nakano, J, Tanabe, S.I. and Kimura, K.I.

Differences in perception of indoor environment between Japanese and non-Japanese workers. *Energy and Buildings*, 2002, Vol. 34, No. 6, pp. 615-621 (2002)

120. National Institute of Mental Health 2001
National Institute of Mental Health
The invisible disease: Depression. (2001)

121. Nelson et al. 1947
Nelson, N., Eichna, L.W., Horvath, S.M., Shelley, W.B. and Hatch, T.F.
Thermal exchanges of man at high temperature. *American Journal of Physiology*, 1947, Vol. 151, No. 2, pp.626-652 (1947)

122. Newsham and Tiller 1997
Newsham, G.R. and Tiller, D.K.
Field study of office thermal comfort using questionnaire software. *ASHRAE Transactions*, 1997, Vol. 103, Pt. 2, pp.3-17 (1997)

123. Nielsen 1974
Nielsen, P.V.
Flow in air-conditioned rooms: model experiments and numerical solution of the flow equation. PhD thesis, Technical University of Denmark, Copenhagen, Denmark (1974)

124. Nielsen 1998
Nielsen, P.V.
The selection of turbulence models for prediction of room airflow. *ASHRAE Transactions*, 1998, Vol. 104, Pt. 1B, pp. 1119-1127 (1998)

125. Nishi et al. 1970
Nishi, Y. and Gagge, A.P.
Direct evaluation of convective heat transfer coefficient by naphthalene sublimation. *Journal of Applied Physiology*, 1970, Vol. 29, No. 6, pp. 830-838 (1970)

126. Niu and Kooi 1992
Niu, J.L. and Kooi, J.V.D.
Grid-optimization for k-ε turbulence model simulation of natural convection in rooms. *Proceedings ROOMVENT-92: Air Distribution in Rooms-Third International Conference*, 1992, Vol. 1, pp. 207-223 (1992)

127. Obal 1984
Obal, F.
Thermoregulation and sleep. In: Sleep mechanisms, Borbely, A., Valatx,

J.L., eds. Berlin, Springer-Verlag, 1984, pp.157-172 (1984)

128. Okamoto-Mizuno et al. 1993
Okamoto-Mizuno, K., Fukami, Y., Iizuka, S. and Okudaira, N.
Effects of electric blankets upon bed climate and human physiology. *Journal of Sleep Environment*, 1993, Vol. 1, pp. 55-62 (1993)

129. Okamoto-Mizuno et al. 1999
Okamoto-Mizuno, K., Mizuno, K., Michie, S., Maeda, A. and Lizuka, S.
Effects of humid heat exposure on human sleep stages and body temperature. *Sleep*, 1999, Vol. 22, No. 6, pp. 767-773 (1999)

130. Okamoto-Mizuno et al. 2005
Okamoto-Mizuno, K., Tsuzuki, K., Ohshiro, Y. and Mizuno, K.
Effects of an electric blanket on sleep stages and body temperature in young men. *Ergonomics*, 2005, Vol. 48, No. 7, pp. 749-757 (2005)

131. Olesen and Parsons 2002
Olesen, B.W. and Parsons, K.C.
Introduction to thermal comfort standards and to the proposed new version of EN ISO 7730. *Energy and Buildings*, 2002, Vol. 34, No. 6, pp. 537-548 (2002)

132. Ogawa et al. 1967
Ogawa, T., Satoh, T. and Takagi, K.
Sweating during night sleep. *The Japanese Journal of Physiology*, 1967, Vol. 17, No. 2, pp. 135-148 (1967)

133. Öhrström 1993
Öhrström, E.
Research on noise since 1988: present state. *Noise as a Public Health Problem: Sixth international congress on Noise as a Public Health Problem*, 1993, pp. 331-338 (1993)

134. Parmeggiani 2003
Parmeggiani, P.L.
Thermoregulation and sleep. *Frontiers in Bioscience*, 2003, Vol. 34, pp. s557-567 (2003)

135. Palca 1986
Palca, J.W.
Thermoregulation, metabolism, and stages of sleep in cold-exposed men. *Journal of Applied Physiology*, 1986, Vol. 61, No. 3, pp. 940-947 (1986)

136. Pan et al. 2005
Pan, C.S., Chiang, H.C., Yen, M.C. and Wang, C.C.
Thermal comfort and energy saving of a personalized PFCU air-conditioning system. *Energy and Buildings*, 2005, Vol. 37, No. 5, pp. 443-449 (2005)

137. Pan et al. 2010
Pan, D.M., Lin, Z.P. and Deng, S.M.
A mathematical model for predicting the total insulation value of a bedding system. *Building and Environment*, 2010, Vol. 45, No. 8, pp.1866-1872 (2010)

138. Pauken 1999
Pauken, M.
Sleeping soundly on summer nights: a history of air conditioning in the home. *ASHRAE Journal*, 1999, Vol. 41, No. 5, pp. 40-47 (1999)

139. Pilowsky et al. 1985
Pilowsky, I., Crettenden, I. and Townley, M.
Sleep disturbance in pain clinic patients. *Pain*, 1985, Vol. 23, pp. 27-33 (1985)

140. Peirce and Rees 1946
Peirce, F.T. and Rees, W.H.
The transmission of heat through textile fabrics – part II. *Journal of the Textile Institute*, 1946, Vol. 37, No. 9, pp. 181-204 (1946)

141. Raymann et al. 2008
Raymann, R.J.E.M., Swaab, D.F. and Van Someren, E.J.W.
Skin deep: enhanced sleep depth by cutaneous temperature manipulation. *Brain*, 2008, Vol. 131, No. 2, pp. 500-513 (2008)

142. Rechtschaffen and Kales, 1968
Rechtschaffen, A. and Kales, A.
A manual of standardized terminology, techniques and scorning system for sleep stages of human subjects. Bethesad: United States Department of Health, Education and Welfare (1968)

143. Rodi 1991
Rodi, W.
Experience with two-layer models combining the k-ε model with a one-equation model near the wall. *29th Aerospace Sciences Meeting*, Reno, NV (1991)

144. Roehrs and Roth 2005
Roehrs, T. and Roth, T.
Sleep and pain: interaction of two vital functions. *Seminars in Neurology*, 2005, Vol. 25, No. 1, pp. 106-116 (2005)

145. Sagot et al. 1987
Sagot, J.C., Amoros, C., Candas, V. and Libert, J.P.
Sweating responses and body temperatures during nocturnal sleep in humans. *America Journal of Physiology*, 1987, Vol. 252, pp. R462-R470 (1987)

146. Sakaguchi et al. 1979
Sakaguchi, S., Glotzbach, S.F. and Heller, H.C.
Influence of hypothalamic and ambient temperatures on sleep in Kangaroo rats. *America Journal of Physiology*, 1979, Vol. 237, No. 1, pp. R80-R88 (1979)

147. Sakoi et al. 2005
Sakoi, T., Tsuzuki, K., Kato, S., Ooka, R., Song, D. and Zhu, S.W.
Development of a three-dimensional human thermal model accounting for direction of blood flow. *Proceedings of the 3rd International Conference on Human-Environment-System*, pp. 337-342 (2005)

148. Sakoi et al. 2006
Sakoi, T., Tsuzuki, K., Kato, S., Ooka, R., Song, D. and Zhu, S.W.
A three-dimensional human thermal model for non-uniform thermal environment. *Proceedings of the 6th International Thermal Manikin and Modeling Meeting*, pp. 77-88 (2006)

149. Sayar et al. 2002
Sayar, K., Arikan, M. and Yontem, T.
Sleep quality in chronic pain patients. *Canadian Journal Psychiatry*, 2002, Vol. 47, No. 9, pp. 844-848 (2002)

150. Schiller 1990
Schiller, G.E.
A comparison of measured and predicted comfort in office buildings. *ASHRAE Transactions*, 1990, Vol. 96, Pt. 1, pp. 609-622 (1990)

151. Sewitch et al. 1986
Sewitch, D.E., Kittrell, E.M.W., Kupfer, D.J. and Reynolds, C.F.
Body temperature and sleep architecture in response to a mild cold stress in women. *Physiology & Behavior*, 1986, Vol. 36, No. 5, pp. 951-957 (1986)

152. Shapiro et al. 1974
Shapiro, C.M., Moore, A.T., Mitchell, D. and Yodaiken, M.L.
How well does man thermoregulate during sleep? *Cellular and Molecular Life Sciences*, 1974, Vol. 30, No. 11, pp. 1279-1281 (1974)

153. SHASE 1991
The Society of Heating, Air-conditioning, and Sanitary Engineers of Japan
Special edition: personal air conditioning. *SHASE Journal*, 1992, Vol. 65, No. 7 (1991)

154. Shih et al. 1995
Shih, T., Liou, W., Shabbir, A., Yang, Z. and Zhu, J.
A new k-ε eddy viscosity model for high Reynolds number turbulent flows. *Computers and Fluids*, 1995, Vol. 24, No. 3, pp. 227-238 (1995)

155. Shochat et al. 2001
Shochat, T., Loredo, J. and Ancoli-Israel, S.
Sleep disorders in the elderly. *Current Treatment Options in Neurology*, 2001, Vol. 3, No. 1, pp. 19-36 (2001)

156. Shur et al. 1999
Shur, M., Spalart, P.R., Strelets, M. and Travin, A.
Detached-eddy simulation of an airfoil at high angle of attack. *Proceedings of the 4th International Symposium on Engineering Turbulence Modeling and Experiments*, France, pp. 669-678 (1999)

157. Shute 1992
Shute, R.W.
Integrating access floor plenums for HVAC air distribution. *ASHRAE Journal*, 1992, Vol. 34, No. 10, pp. 46-51 (1992)

158. Shute 1995
Shute, R.W.
Integrated access floor HVAC: lessons learned. *ASHRAE Transactions*, 1995, Vol. 101, Pt. 2, pp. 877-886 (1995)

159. Silva and Coelho 2002
Silva, M.C.G. and Coelho, J.A.
Convection coefficients for the human body parts determined with a thermal mannequin. *Proceedings of ROOMVENT 2002*, Copenhagen, Denmark, pp. 277-280 (2002)

160. Smagorinsky 1963
Smagorinsky, J.

General circulation experiments with the primitive equations I: The basic experiment. *Monthly Weather Review*, 1963, Vol. 91, No. 3, pp. 99-164 (1963)

161. Smith 1962
Smith, P.E.
Analog simulation of the physiological responses of men working in hot environments. In proceedings of the 2nd symposium for biomedical engineering in San Diego, 1962, pp. 117-125 (1962)

162. Smith 1991
Smith, C.E.
A transient three-dimensional model of human thermal system. PhD dissertation, Kansas State University, Manhattan, Kansas (1991)

163. Smith et al. 2000
Smith, M.T., Perlis, M.L., Smith, M.S., Giles, D.E. and Carmody, T.P.
Sleep quality and presleep arousal in chronic pain. *International Journal of Behavioral Medicine*, 2000, Vol. 23, No. 1, pp. 1-13 (2000)

164. Sodec 1984
Sodec, F.
Air distribution systems. Report No. 3554A, Aachen, West Germany: Krantz GmbH & Co., September (1984)

165. Sodec and Craig 1990
Sodec, F. and Craig, R.
The underfloor air supply system-the European experience. *ASHARE Transactions*, 1990, Vol. 96, Pt. 2, pp. 690-695 (1990)

166. Sodec and Craig 1991
Sodec, F. and Craig, R.
Underfloor air supply system: guidelines for the mechanical engineer. Report No. 3787A, Aachen, West Germany: Krantz GmbH & Co., January (1991)

167. SØrensen and Voigt 2003
SØrensen, D.N. and Voigt, L.K.
Modeling flow and heat transfer around a seated human body by computational dynamics. *Building and Environment*, 2003, Vol. 38, No. 6, pp. 753-762 (2003)

168. Spalart and Allmaras 1992
Spalart, P.R. and Allmaras, S.R.

A one-equation turbulence model for aerodynamic flows. Technical Report AIAA-92-0439, Reston, VA. (1992)

169. Spengler and Chen 2000
Spengler, J.D. and Chen, Q.
Indoor air quality factors in designing a healthy building. Annual Review of *Energy and the Environment*, 2000, Vol. 25, pp. 567-600 (2000)

170. Spoormaker 1990
Spoormaker, H.J.
Low-pressure underfloor HVAC system. *ASHRAE Transactions*, 1990, Vol. 96, Pt. 2, pp. 670-677 (1990)

171. Stamou and Katsiris 2006
Stamou, A. and Katsiris, I.
Verification of a CFD model for indoor airflow and heat transfer. *Building and Environment*, 2006, Vol. 41, No. 9, pp. 1171-1181 (2006)

172. Stolwijk 1971
Stolwijk, J.A.J.
A mathematical model of physiological temperature regulation in man. NASA Technical Report, No. NASA CR-1855 (1971)

173. Stolwijk 1980
Stolwijk, J.A.J.
Mathematical models of thermal regulation. *Annals of the New York Academy of Sciences*, 1980, Vol. 335, No. 1, pp. 98-106 (1980)

174. Takagi 1970
Takagi, K
Sweating during sleep. *In: Physiological and behavioral temperature regulation*. Eds: Hardy, J.D., Gagge, A.P. and Stolwijk, J.A.J., Thoms, Springfiled IL, pp. 669-675 (1970)

175. Tamblyn 1995
Tamblyn, R.T.
Toward zero complaint for office conditioning system. *Heating, Piping and Air Conditioning*, 1995, Vol. 120, pp. 67-72 (1995)

176. Tham et al. 2004
Tham, K.W., Sekhar, S.C., Cheong, D.K.W. and Gong, N.
A case study of quantitative energy efficiency of personalized ventilation in the tropics. *Proceedings of ROOMVENT 2004*, Portugal, pp. 5-8 (2004)

177. Tanabe 1995
Tanabe, S.
Task/ambient conditioning systems in Japan. *Proceedings: Workshop on task/ambient conditioning systems in commercial buildings*, San Francisco, CA (1995)

178. Tanabe et al. 1989
Tanabe, S., Kimura, K. and Inoue, U.
Proposal of evaluation method with thermal manikin. *Annual meeting of Architecture of Japan*, 1989, Vol. 1, pp. 875-876 (1989)

179. Tanabe et al. 2002
Tanabe, S., Kobayashi. K., Nakano, J., Ozeki, Y. and Konishi, M.
Evaluation of thermal comfort using combined multi-node thermoregulation (65MN) and radiation models and computational fluid dynamics. *Energy and Buildings*, 2002, Vol. 34, No. 6, pp. 637-646 (2002)

180. Topp et al. 2002
Topp, C., Nielsen, P.V. and SØrensen, D.N.
Application of computer simulated persons in indoor environmental modeling. *ASHRAE Transactions*, 2002, Vol. 108, Pt. 2, pp.1084-1089 (2002)

181. Tsuzuki et al. 2008
Tsuzuki, K., Okamoto-Mizuno. K., Mizuno, K. and Iwaki, T.
Effects of airflow on body temperatures and sleep stages in a warm humid climate. *International Journal of Biometeorology*, 2008, Vol. 52, No. 4, pp. 261-70 (2008)

182. Walsh and Leong 2004
Walsh, P.C. and Leong, W.H.
Effectiveness of several turbulence models in natural convection. *International Journal of Numerical Methods for Heat & Fluid Flow*, 2004, Vol. 14, No. 5, pp. 633-648 (2004)

183. Wang 1994
Wang, S.K.
Handbook of air conditioning and refrigeration. McGraw-Hill Inc. (1994)

184. Website_1 2011
http://www.chinanews.com/ga/2011/06-23/3131234.shtml

185. Website_2 2011
http://news.sohu.com/20110322/n279935652.shtml

186. Winslow et al. 1939
Winslow, C.E.A., Gagge, A.P. and Herrington, L.P.
The influence of air movement upon heat losses from the clothed human body. *American Journal of Physiology*, 1939, Vol. 127, No. 3, pp. 505–518 (1939)

187. Wissler 1964
Wissler, E.H.
A mathematical model of the human thermal system. *Bulletin of mathematical biophysics*, 1964, Vol. 26, No. 2, pp. 147-166 (1964)

188. Woodcock and Breckenridge 1965
Woodcock, A.H. and Breckenridge, J.R.
A model description of thermal exchange for the nude man in hot environments. *Ergonomics*, 1965, Vol. 8, No. 2, pp. 223–235(1965)

189. World Health Organization 2007
World Health Organization
Guidelines for Community Noise (2007)

190. Wringt and Eason 1999
Wringt, N.G. and Eason, G.J.
Comparison of several computational turbulence models with full-scale measurements of flow around a building. *Wind and Structures*, 1999, Vol. 2, No. 4, pp. 305-323 (1999)

191. Wyon 1995
Wyon, D.
Thermal manikin experiments on Climadesk. *Proceedings: Workshop on task/ambient conditioning systems in commercial buildings*, San Francisco, CA (1995)

192. Xing et al. 2001
Xing, H., Hatton, A. and Awbi, H.B.
A study of the air quality in the breathing zone in a room with displacement ventilation. *Building and Environment*, 2001, Vol. 36, No. 7, pp. 809-820 (2001)

193. Yakhot and Orszag 1986
Yakhot, V. and Orszag, S.A.
Renormalization group analysis of turbulence. *Journal of Scientific Computing*, 1986, Vol. 1, No. 1, pp. 3-51 (1986)

194. Yakhot et al. 1992
Yakhot, V., Orszag, S.A., Thangam, S., Gatski, T.B. and Speziale, C.G.
Development of turbulence models for shear flows by a double expansion technique. *Physics of Fluids*, 1992, Vol. 4, No. 7, pp. 1510-1520 (1992)

195. Yang et al. 2002
Yang, J.H., Kato, S., Hayashi, T. and Murakami, S.
Measurement of local convective heat transfer coefficients of the human body in outdoor and indoor environments. *Proceedings of ROOMVENT 2002*, Copenhagen, Denmark, pp. 281-284 (2002)

196. Yang et al. 2007
Yang, B. and Sekhar, S.C.
Numerical study of circular jet diffuser for task ventilation of under-floor air supply system in tropics. *Proceedings of Building Simulation 2007*, Beijing, China, pp. 1021-1026 (2007)

197. Yang et al. 2008
Yang, B., Sekhar, S.C. and Melikov, A.K.
Cooling effect of ceiling mounted personalized ventilation system. *In Proceedings of Indoor Air 2008*, Copenhagen, Denmark, August (2008)

198. Yang et al. 2009
Yang, B., Sekhar, S.C. and Melikov, A.K.
Performance evaluation of ceiling mounted personalized ventilation system. *ASHARE Transactions*, 2009, Vol. 115, Pt. 2, pp. 395-406 (2009)

199. Yang et al. 2010
Yang, B., Sekhar, S.C. and Melikov, A.K.
Ceiling-mounted personalized ventilation system integrated with a secondary air distribution system - a human response study in hot and humid climate. *Indoor air*, 2010, Vol. 20, No. 4, pp. 309-319 (2010)

200. Zhai 2006
Zhai, Z.
Applications of CFD in building designing: Aspects and trends. *Indoor and Built Environment*, 2006, Vol. 15, No. 4, pp. 305-313 (2006)

201. Zhai et al. 2007
Zhai, Z., Zhang, Z., Zhang, W. and Chen, Q
Evaluation of various turbulence models in predicting airflow and turbulence in enclosed environments by CFD: Part 1- Summary of prevalent

turbulence models. *HVAC&R Research*, 2007, Vol. 13, No. 6, pp. 853-870 (2007)

202. Zhang 2003
Zhang, H.
Human thermal sensation and comfort in transient and nonuniform thermal environments, PhD thesis, CEDR, University of California at Berkeley (2003)

203. Zhang et al. 2007
Zhang, Z., Zhang, W., Zhai, Z. and Chen, Q
Evaluation of various turbulence models in predicting airflow and turbulence in enclosed environments by CFD: Part 2- Comparison with experimental data from literature. *HVAC&R Research*, 2007, Vol. 13, No. 6, pp. 871-886 (2007)

204. Zhu et al. 2007
Zhu, S., Kato, S., Ooka, R. and Sakoi, T.
Development of a Computational Thermal Manikin applicable in a nonuinform thermal environment. Part 1: Coupled simulation of convection, radiation, and Smith's human thermal physiological model for sensible heat transfer from a seated human person in radiant environment. *HVAC&R Research*, 2007, Vol. 13, No. 4, pp. 661-679 (2007)

205. Zhu et al. 2008
Zhu, S., Kato, S., Ooka, R., Sakoi, T. and Tsuzuki, K.
Development of a Computational Thermal Manikin applicable in a nonuinform thermal environment. Part II: Coupled simulation using Sakoi's human thermal physiological. *HVAC&R Research*, 2008, Vol. 14, No. 4, pp. 545-564 (2008)